Welcome to Today's Webinar!

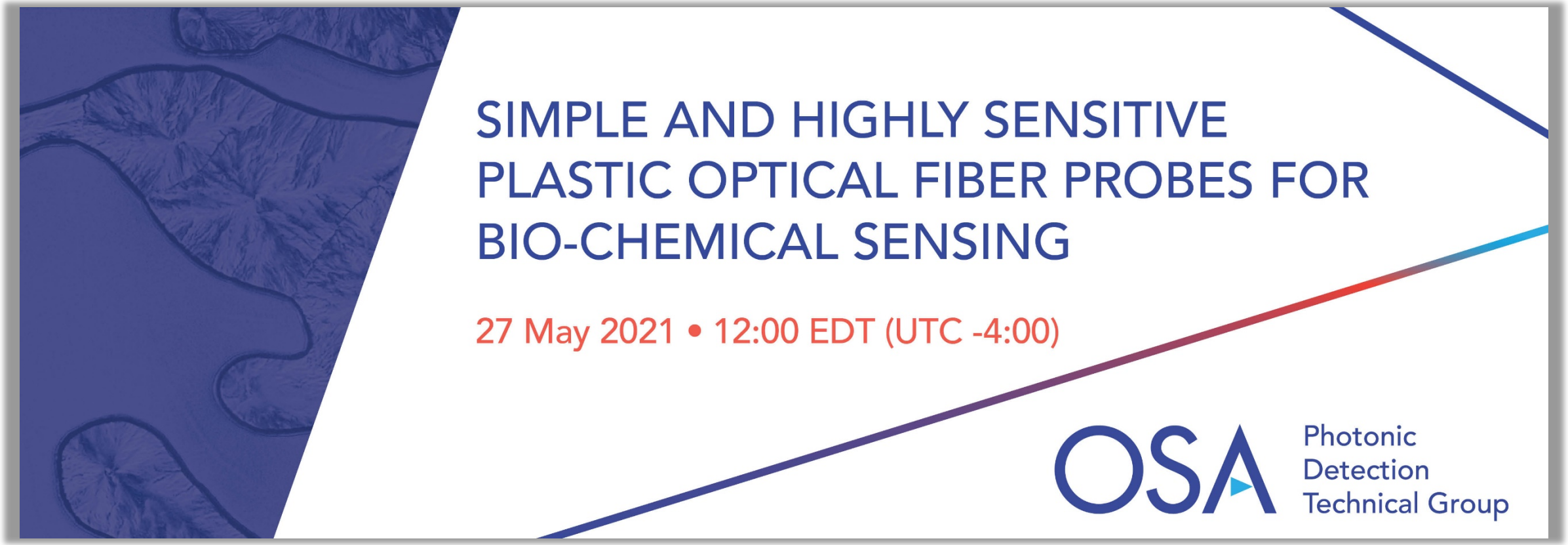

Technical Group Executive Committee

Giuseppe D'Aguanno
Chair
Johns Hopkins University, Applied Physics Laboratory

Achyut Dutta
Vice Chair
Founder Banpil Photonics

Shuren Hu
Events Officer
SiLC Technology

Kimberly Reichel
Webinar Officer
3DEO, Inc.

Vivek Nagal
Social Media Officer
Johns Hopkins University

About the Photonic Detection Technical Group

Our technical group focuses on detection of photons as received from images, data links, and experimental spectroscopic studies to mention a few. Within its scope, it is involved in the design, fabrication, testing of single and arrayed detectors. Detector materials, structures, and readout circuitry needed to translate photons into electrical signals.

Our mission is to connect the 2000+ members of our community through technical events, webinars, networking events, and social media.

Our past activities have included:

- Special sessions at CLEO and OFC, including a panel discussion on *Silicon Photonics for LiDAR and Other Applications*
- 10 previous webinars

Connect with our Technical Group

Join our online community to stay up to date on our group's activities. You also can share your ideas for technical group events or let us know if you're interested in presenting your research.

Ways to connect with us:

- Our website at www.osa.org/pd
- On LinkedIn at https://www.linkedin.com/groups/8297763/
- Email us at TGactivities@osa.org

Today's Speaker

Nunzio Cennamo

University of Campania Luigi Vanvitelli

Short Bio:

- Professor of Electronics, University of Campania Luigi Vanvitelli (Naples) Italy
- Research Interests: design and fabrication of optical fiber sensors, chemical sensors, biosensors and optoelectronic devices
- Cofounder of the Spin Off "MORESENSE srl" in Milan (Fondazione Filarete, Milan-Italy)

OSA The Optical Society | 100 Since 1916

Università degli Studi della Campania *Luigi Vanvitelli*

Department of Engineering

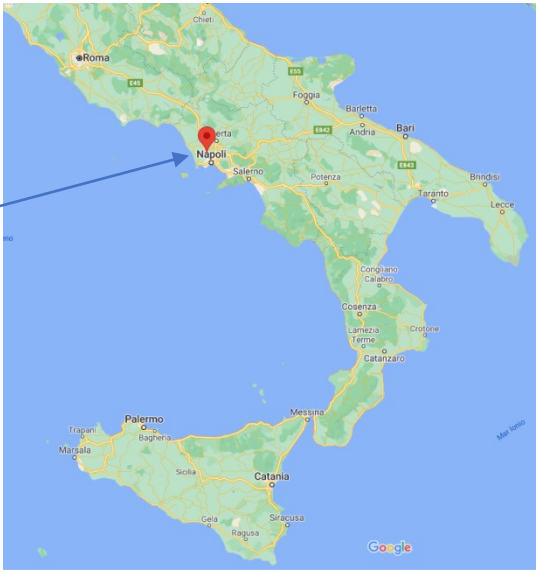

Photonics & Electronics Group

Leader Prof. Luigi Zeni

Research lines in Optoelectronics & Photonics:

- ✓ Distributed optical fiber sensors
  (Coordinators Aldo Minardo & Luigi Zeni)

opto sensing

Spin-Off

- ✓ Optical bio-chemical sensors
  (Coordinators Nunzio Cennamo & Luigi Zeni)

MORE SENSE S.R.L.

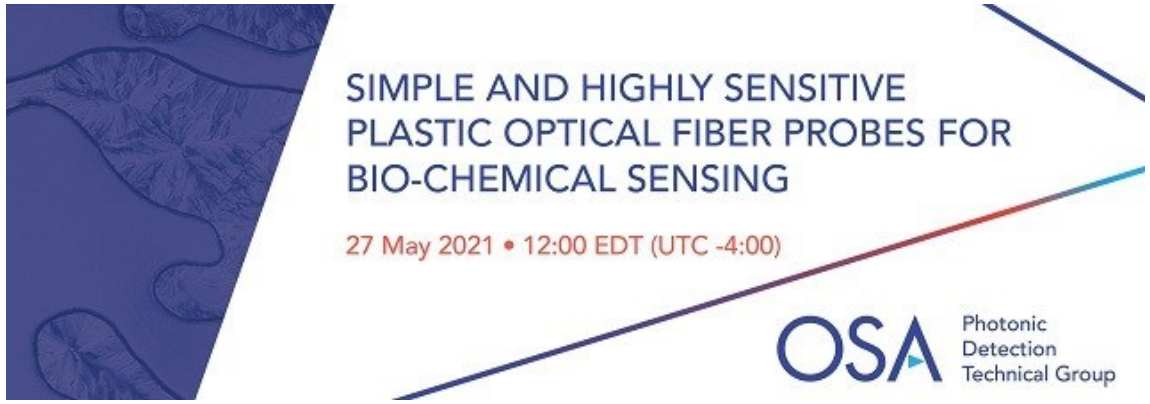

Outline

- Selective Sensors or Electronic nose?
- *Optical* Biosensors and Chemical Sensors
- Plasmonic Intrinsic Plastic Optical Fibers (POFs) Biosensors
- Plasmonic Extrinsic POFs-based Biosensors
- Conclusions

Electronic nose

The electronic nose is a device intended to detect "*odors*", in a similar way as the human nose

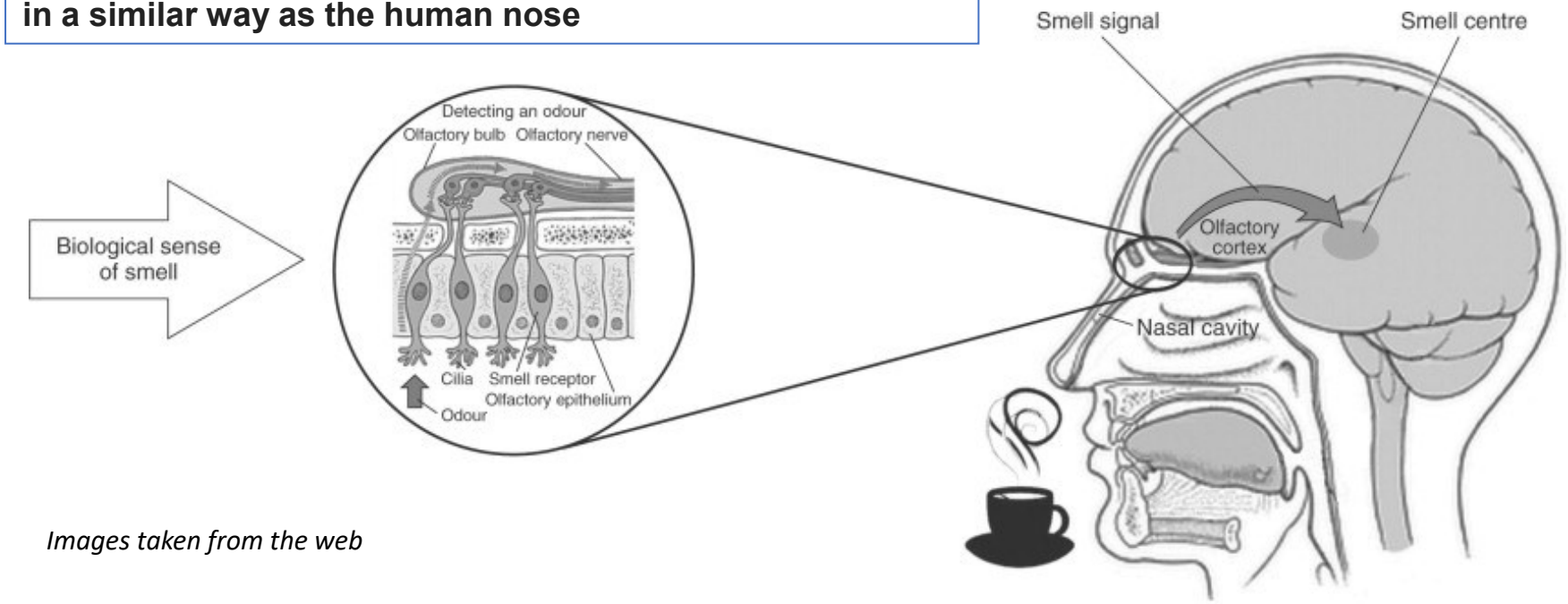

Images taken from the web

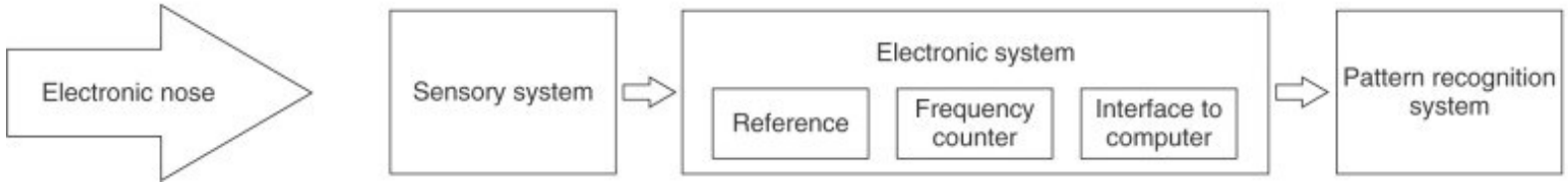

The most commonly used **(aspecific) sensors** for electronic noses include:

1) **metal–oxide–semiconductor** (**MOSFET**) devices – (transistor) a way of measuring the change in resistivity caused by a mass variation.
2) **quartz crystal microbalance (QCM)** - a way of measuring mass per unit area by measuring the change in frequency of a quartz crystal resonator
3) **microelectromechanical systems (MEMS)** - a way of measuring physical phenomenon variation caused by a different mass.

Selective Sensors

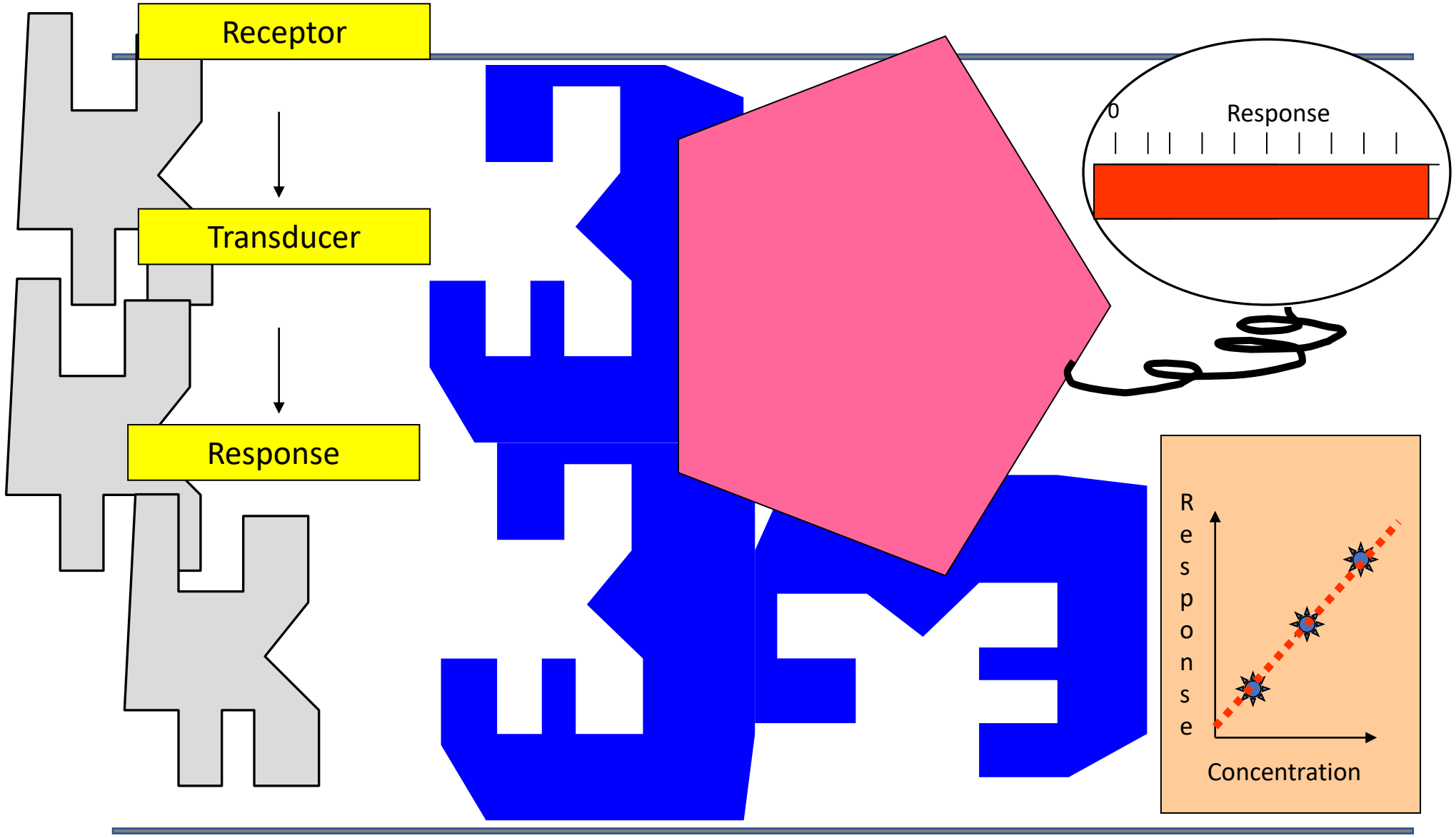

Images taken from the web

Selective Sensors or Electronic nose?

Selective Sensors

Advantage

- High Selectivity
- No starting training phase
- Reproducibility on an industrial scale
- Easy maintenance
- Low starting and maintenance costs
- Small size
- High integrability
- Real-time Monitoring

Disadvantage

- Fair flexibility
- Some probes are selective but not reversible
- Impossibility of use in the classification of “odors”
- High interdisciplinarity in the design and development phases

Electronic nose

Advantage

- Good Selectivity
- Capability to define and quantify “odors"
- Replacement of man in several production and/or cataloging processes

Disadvantage

- High training times
- Maintenance problems related to the replacement of a single sensor. In this case it is necessary to train the sensor again
- Poor reproducibility on an industrial scale (due to the training phase)
- Performance instability on long periods (new training phases are required)
- High costs (due to the training phases)

Selective Sensors

"Conventional" *Chemical Sensors*

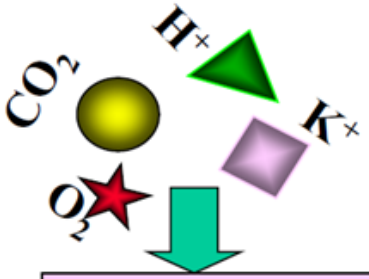

Simple molecules

Non-Biological Molecular Recognition → Transduction

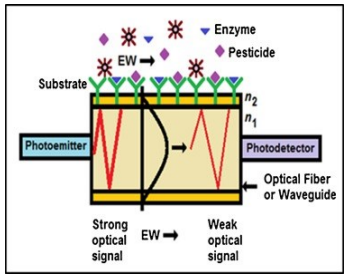

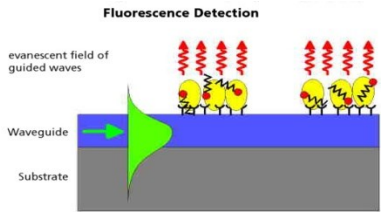

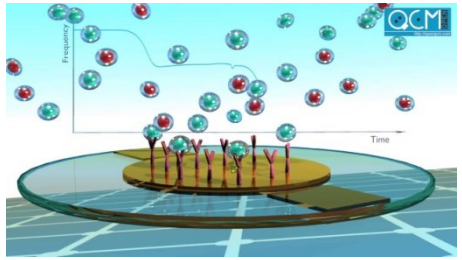

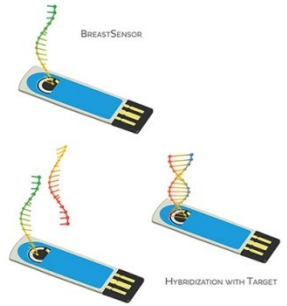

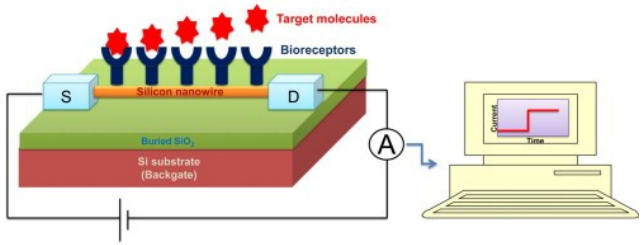

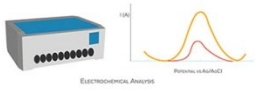

Images taken from the web

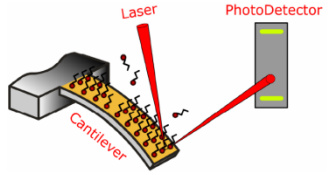

Signal Processing

Measurable Signal (Response):

Current (I)
Voltage (V)
Photon (h v)
Frequency (f)
Wavelength (λ)
……etc

Transducers

Selective Sensors

"Conventional" *Biosensors*

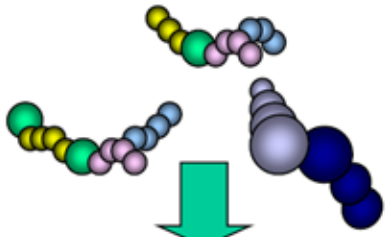

Complex molecules

Biological Molecular Recognition → Transduction

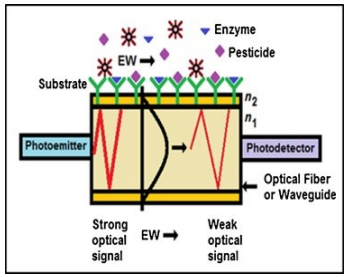

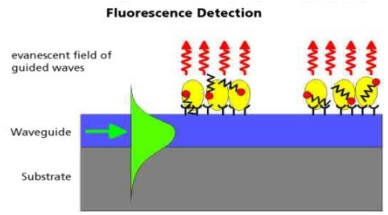

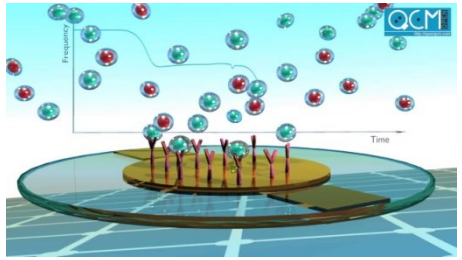

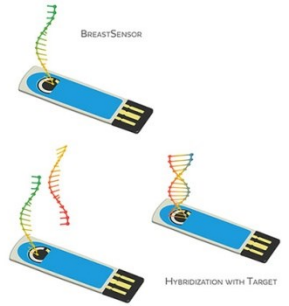

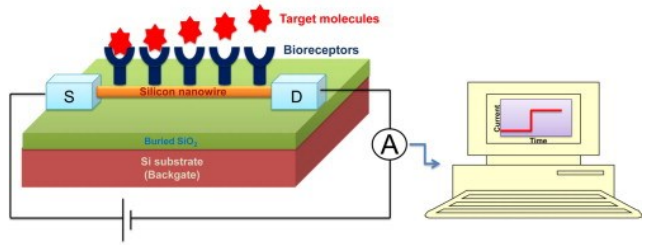

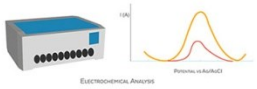

Images taken from the web

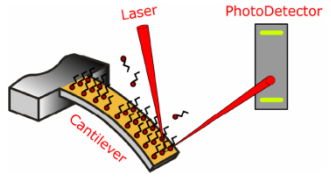

Measurable Signal (Response):

Current (I)
Voltage (V)
Photon (h v)
Frequency (f)
Wavelength (λ)
……etc

Transducers

Signal Processing

Selective Sensors

Biosensors "*in a general sense*"

…can be based on molecular recognition elements (**MREs**), which can be **biological** (bio-receptors such as proteins, nucleic acids, enzymes, antibodies, etc) *or* ***bio-mimetic*** (artificial polymers with special selective properties), such as Molecularly Imprinted Polymers (**MIPs**).

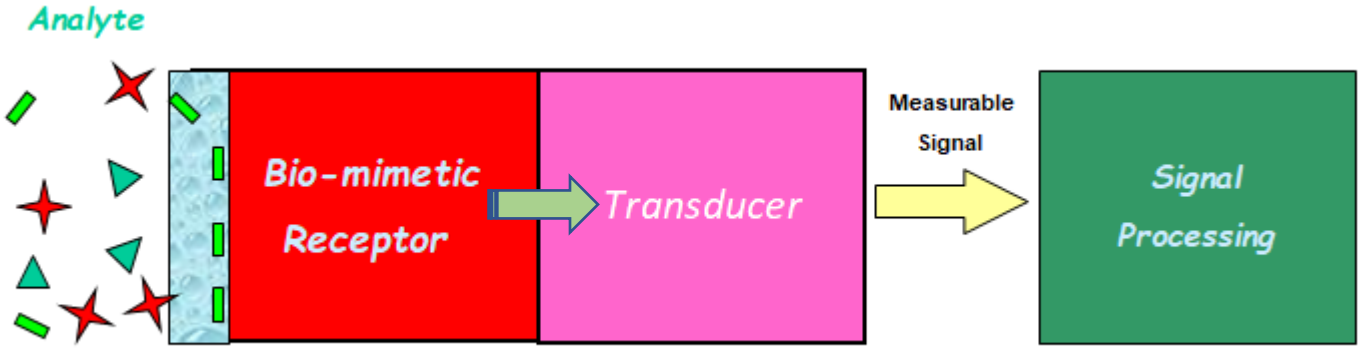

Optical Biosensors

High Sensitivity; Real time monitoring; Immunity to electromagnetic interferences; Remote sensing capability and Low-cost approaches (by optical fibers); small size; No sparking problems

Optical transduction

- Refractive index (RI) sensing
- Fluorescence emission
- Absorbance or Chemiluminescence
- Intensity or phase sensing

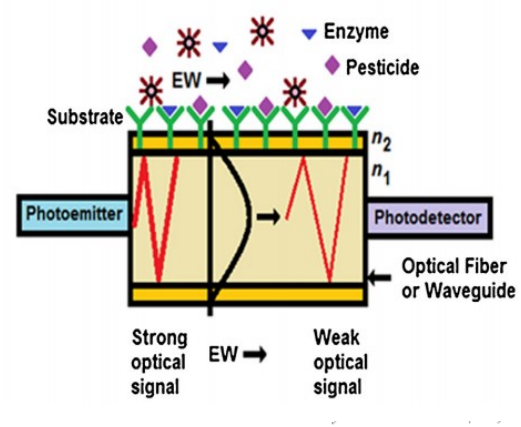

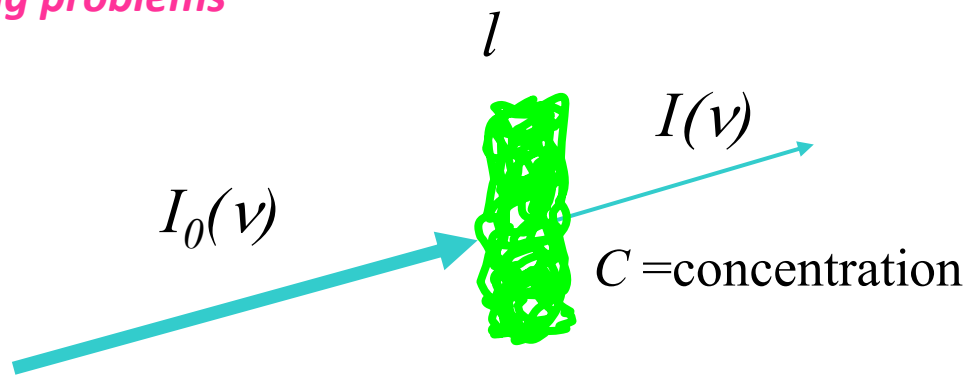

Images taken from the web

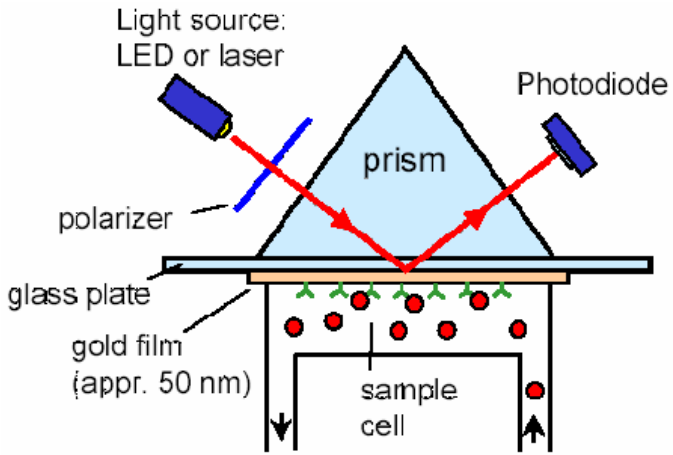

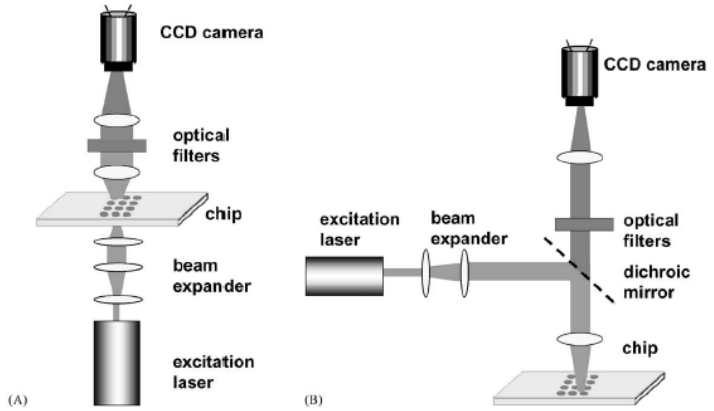

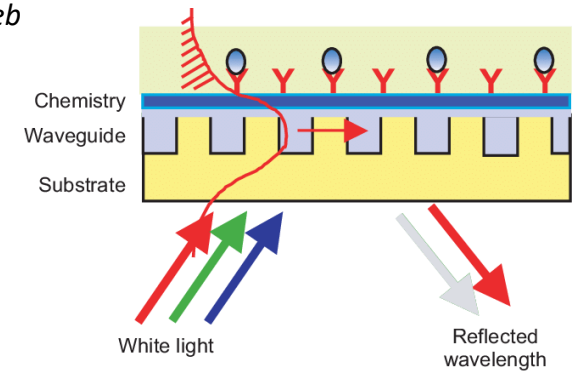

There are several transduction mechanisms that can be employed, including sensors based on variations of the evanescent field or on spectroscopic methods (absorption, fluorescence and refractive index).

Biosensors in Planar Waveguides

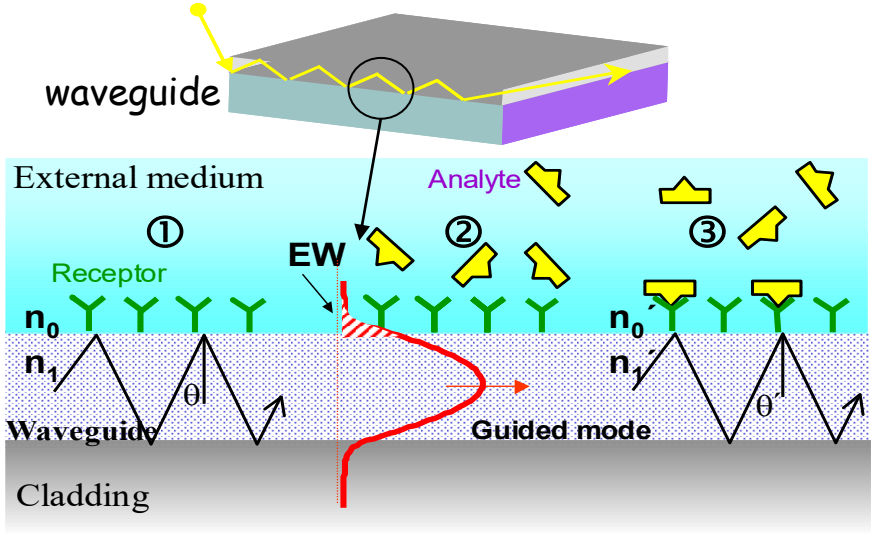

Optical Evanescent-Wave Sensor

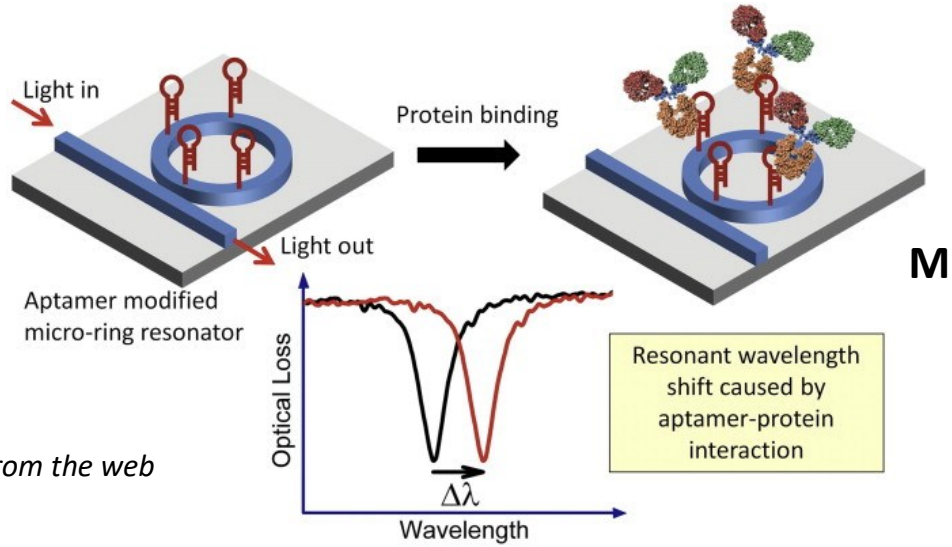

Micro-ring Resonator

Images taken from the web

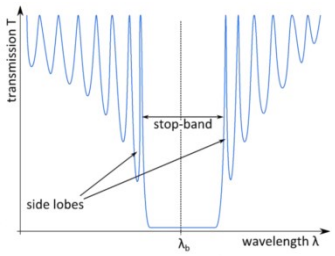

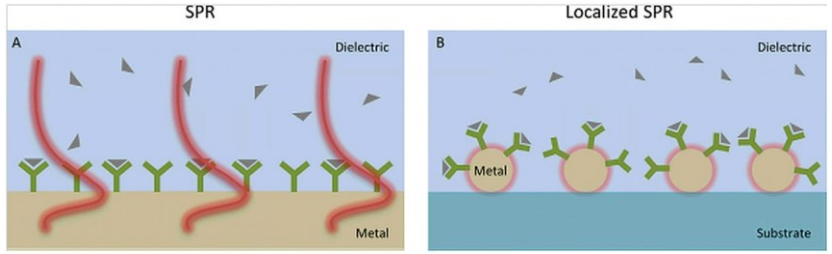

Plasmonic Sensors

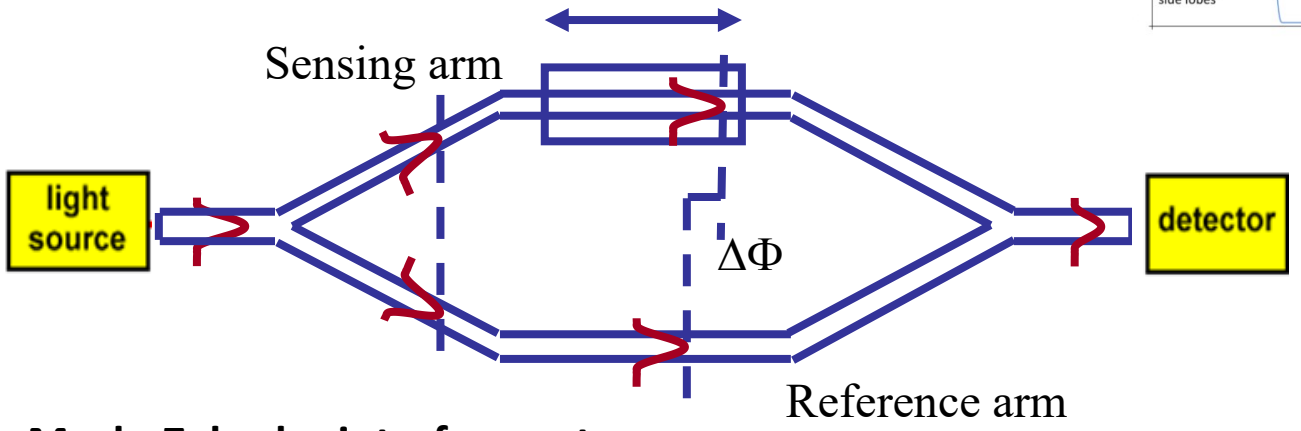

Mach–Zehnder interferometer

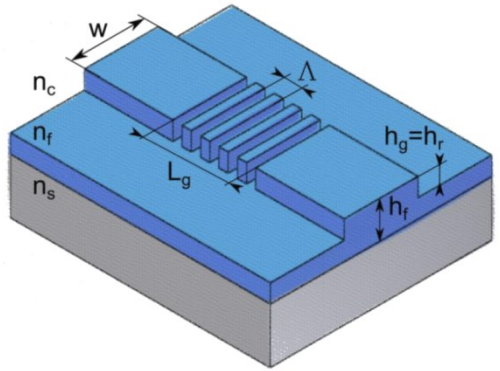

Bragg Grating Resonator

Biosensors in Optical Fibers

Reflection mode

The light source and the detector are placed on the same side of the fiber.

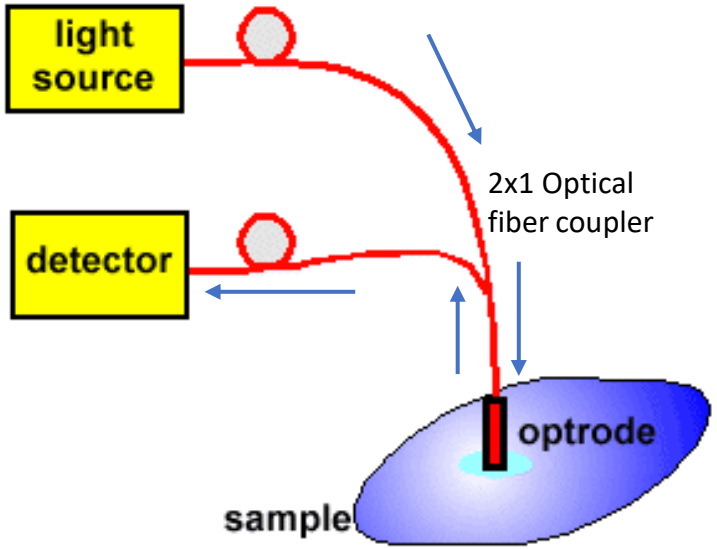

Images taken from the web

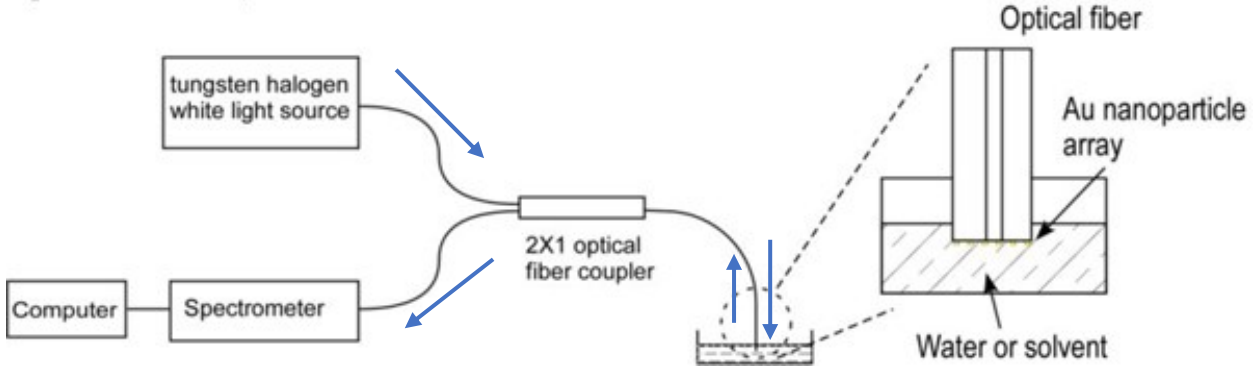

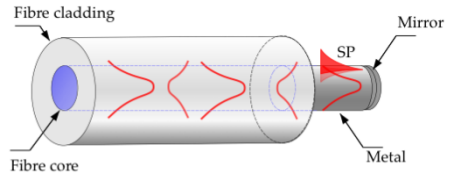

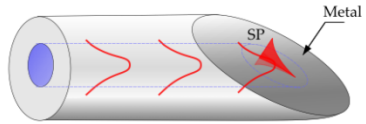

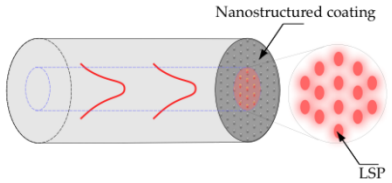

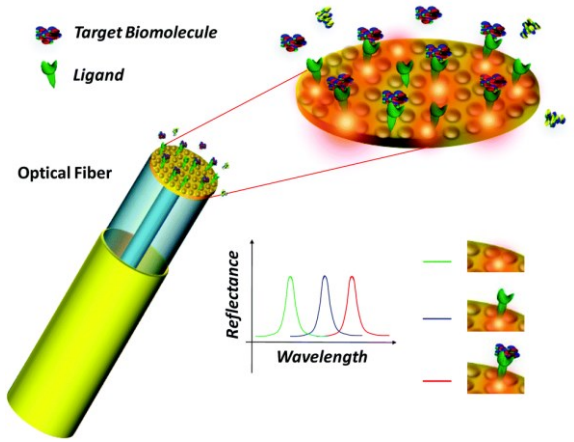

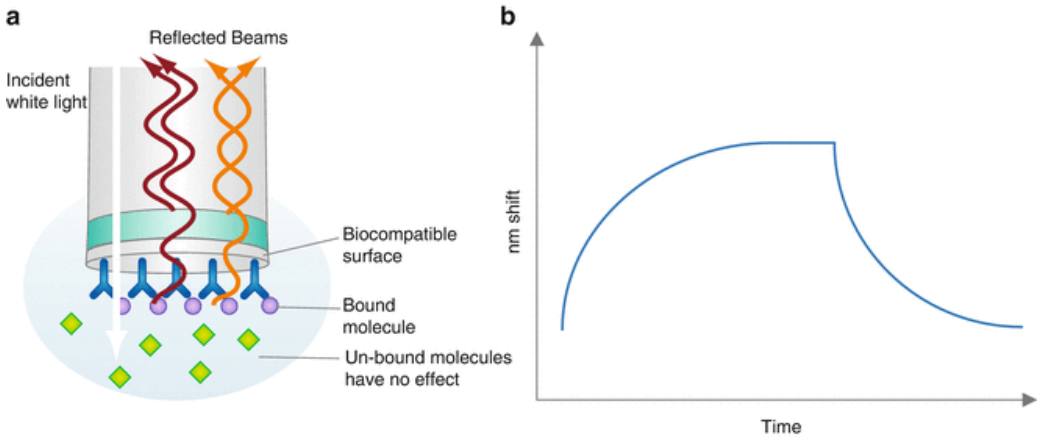

Biosensors in Optical Fibers

Transmission mode

The light source and the detector are placed on opposite sides.

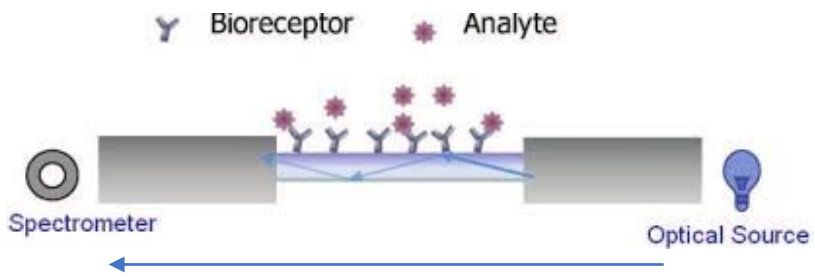

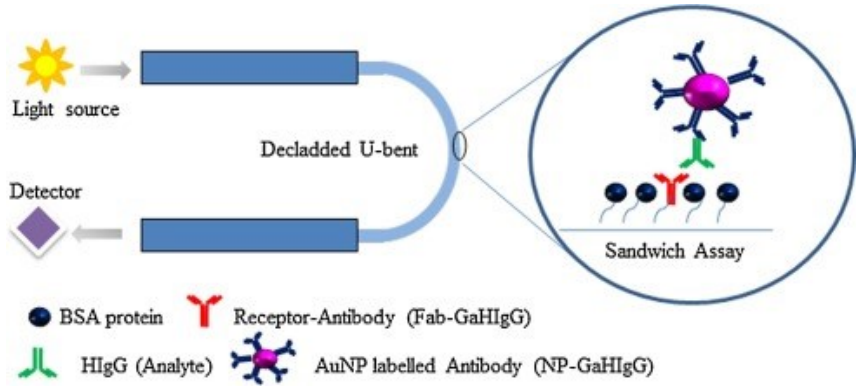

Images taken from the web

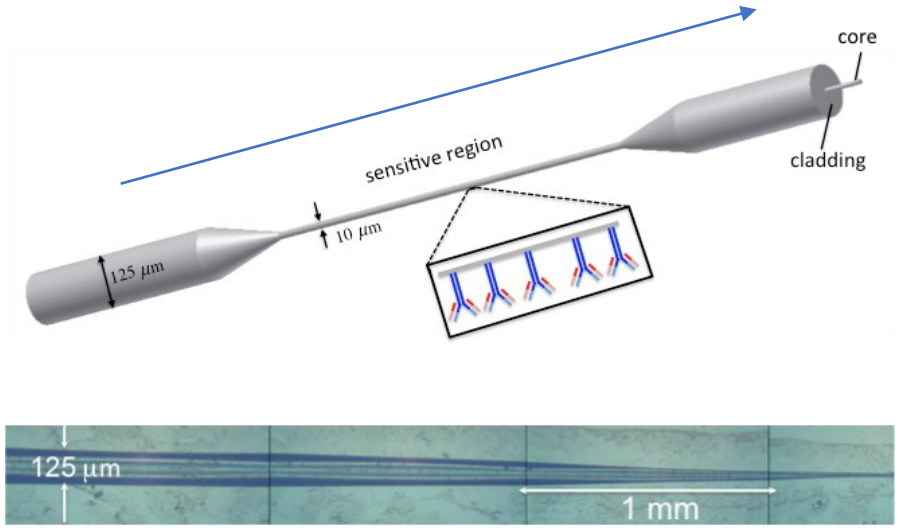

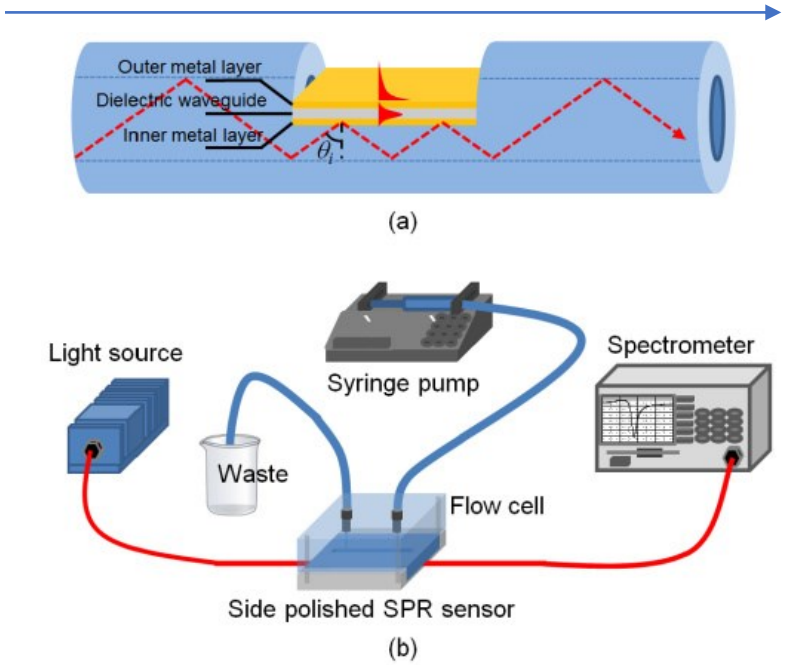

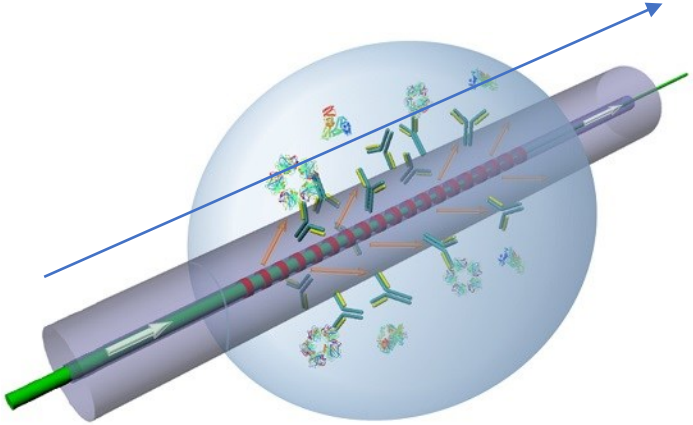

Schematic diagram of an Extrinsic and Intrinsic optical fiber sensor

a)

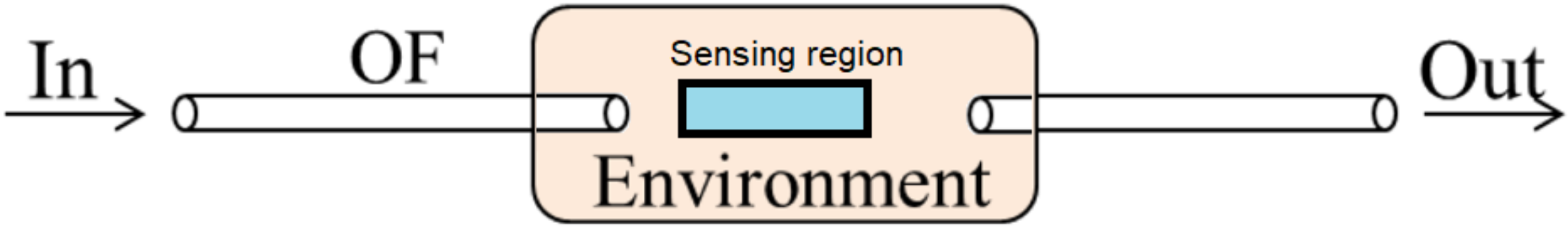

Extrinsic optical fiber sensor

The **optical fiber sensors** can be classified as **intrinsic and extrinsic**, depending on whether the fiber is interacting with the analysed medium or it is used only as a waveguide that allows the propagation of the light to the sensing region and its collection, respectively.

b)

Intrinsic optical fiber sensor

Surface Plasmon Resonance (SPR) Sensors

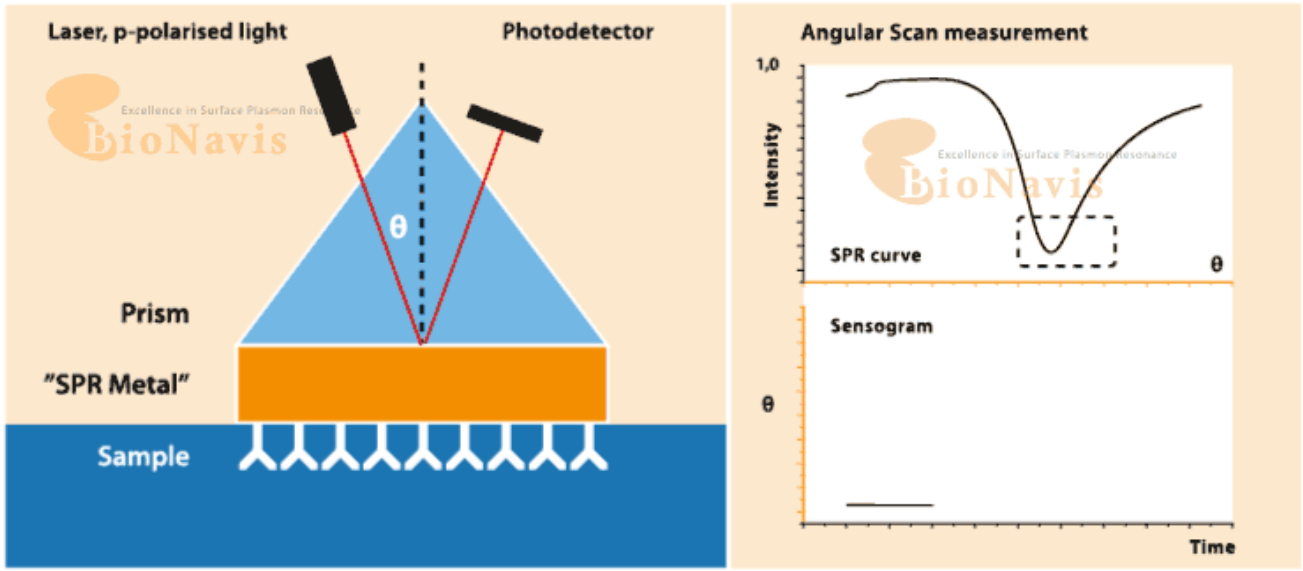

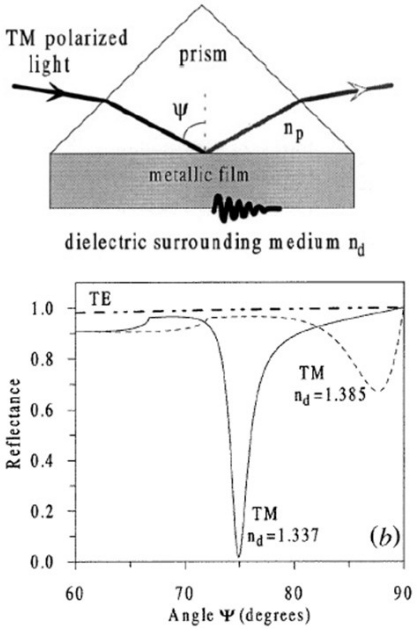

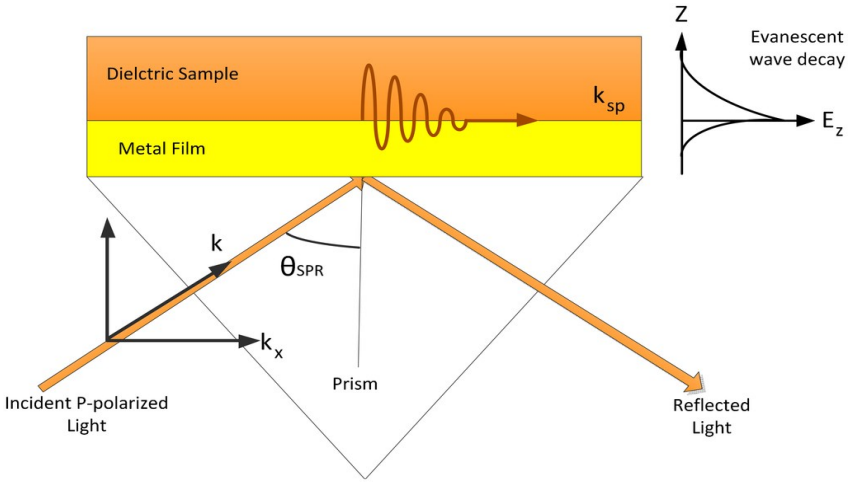

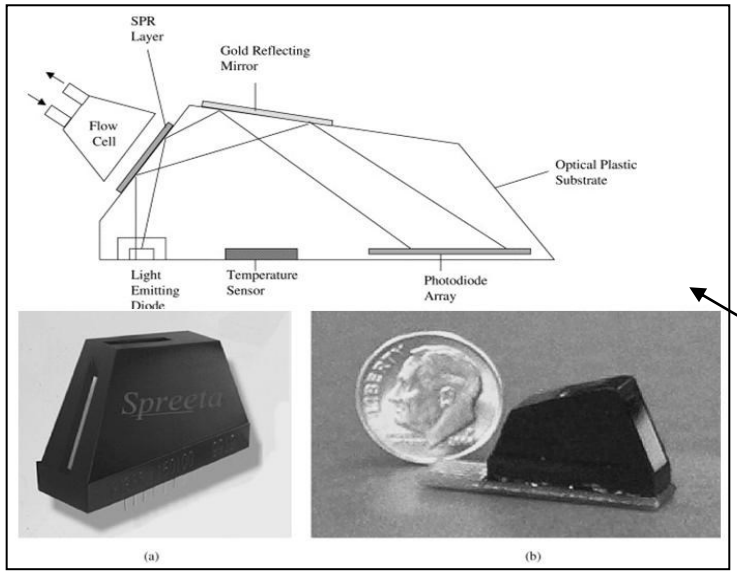

Images taken from the web

Spreeta, U.S. Patent Number 5912456 - Filed Mar 19, 1997 - Texas Instruments Incorporated

SPR Sensors in Optical Fibers

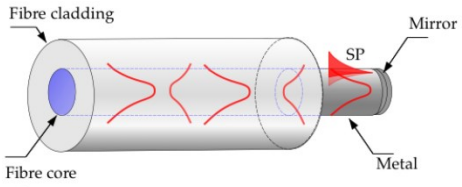

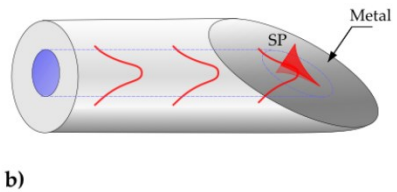

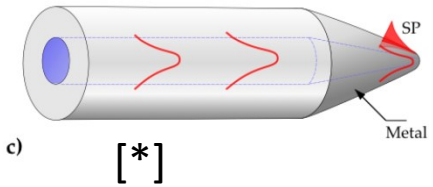

[*]

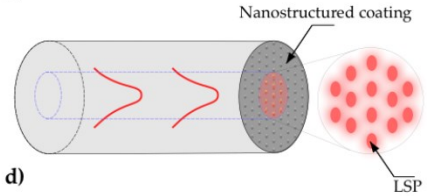

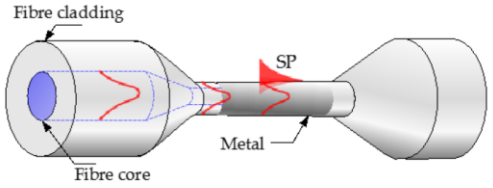

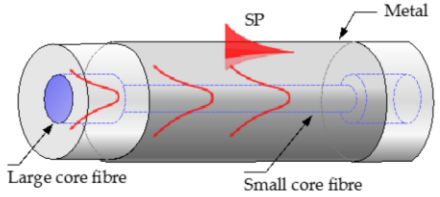

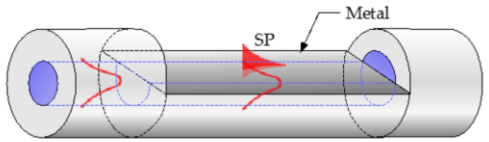

[*]

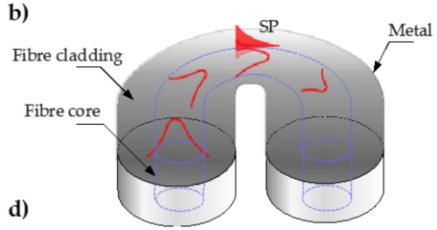

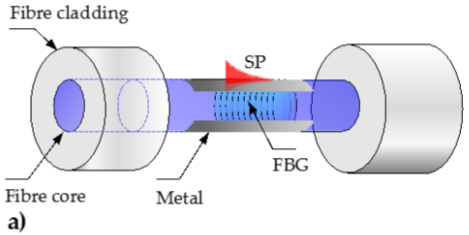

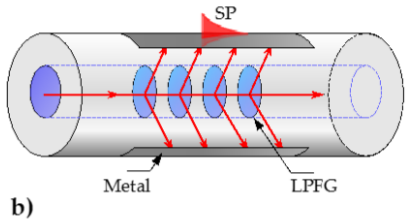

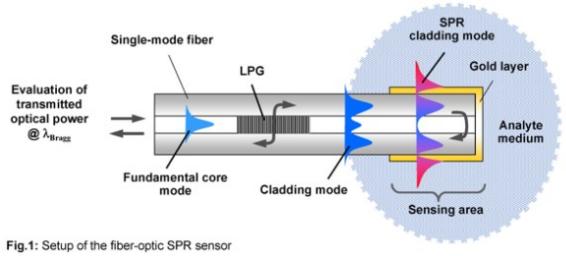

Fig.1: Setup of the fiber-optic SPR sensor

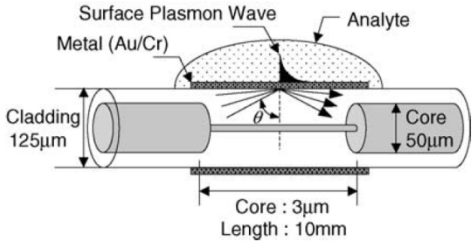

Hetero-core structured optical fiber sensor

Iga, M.; Seki, A.; Watanabe, K. Gold Thickness Dependence of SPR-Based Hetero-Core Structured Optical Fiber Sensor. **Sens. Actuat. B Chem 2005**, 106, 363–368

[*]

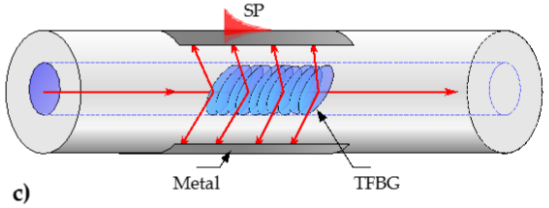

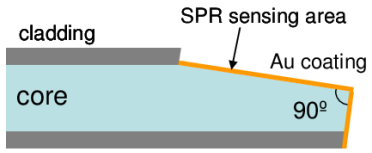

[*] Elizaveta Klantsataya, Peipei Jia, Heike Ebendorff-Heidepriem, Tanya M. Monro, and Alexandre François, *Plasmonic Fiber Optic Refractometric Sensors: From Conventional Architectures to Recent Design Trends*, **Sensors 2017**, 17(1), 12

A simple optical platform: SPR in D-shaped POF

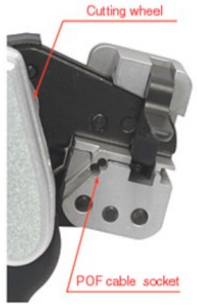

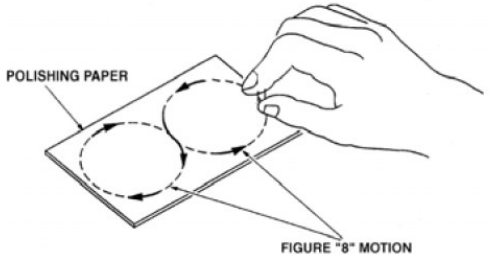

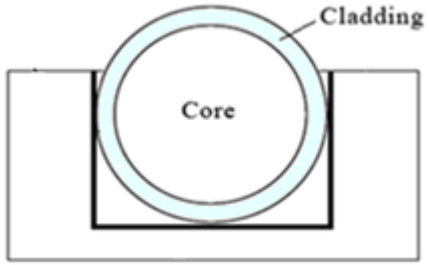

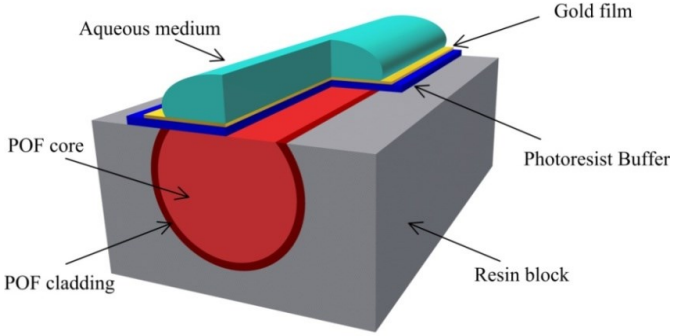

Spin coater

Sputter coater

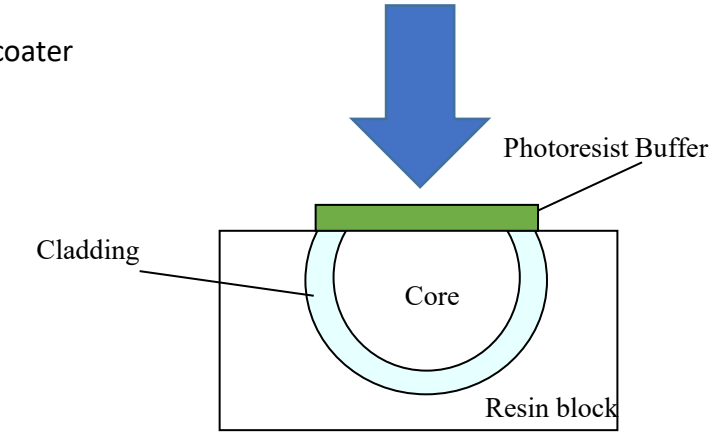

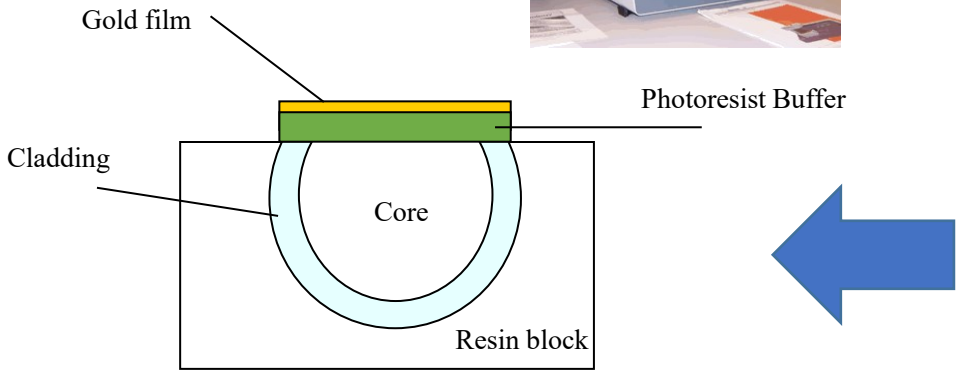

N. Cennamo, D. Massarotti, L. Conte, L. Zeni, Low cost sensors based on SPR in a plastic optical fiber for biosensor implementation, **Sensors**, 11, 11752–11760 (**2011**)

A simple highly sensitive and general-purpose platform: SPR in D-shaped POFs

- Core (PMMA) 980 µm ; RI=1.49
- Fluorinated cladding 10 µm; RI=1.41
- Microposit S1813 Photoresist 1.5 µm; RI=1.61
- Gold film 60 nm

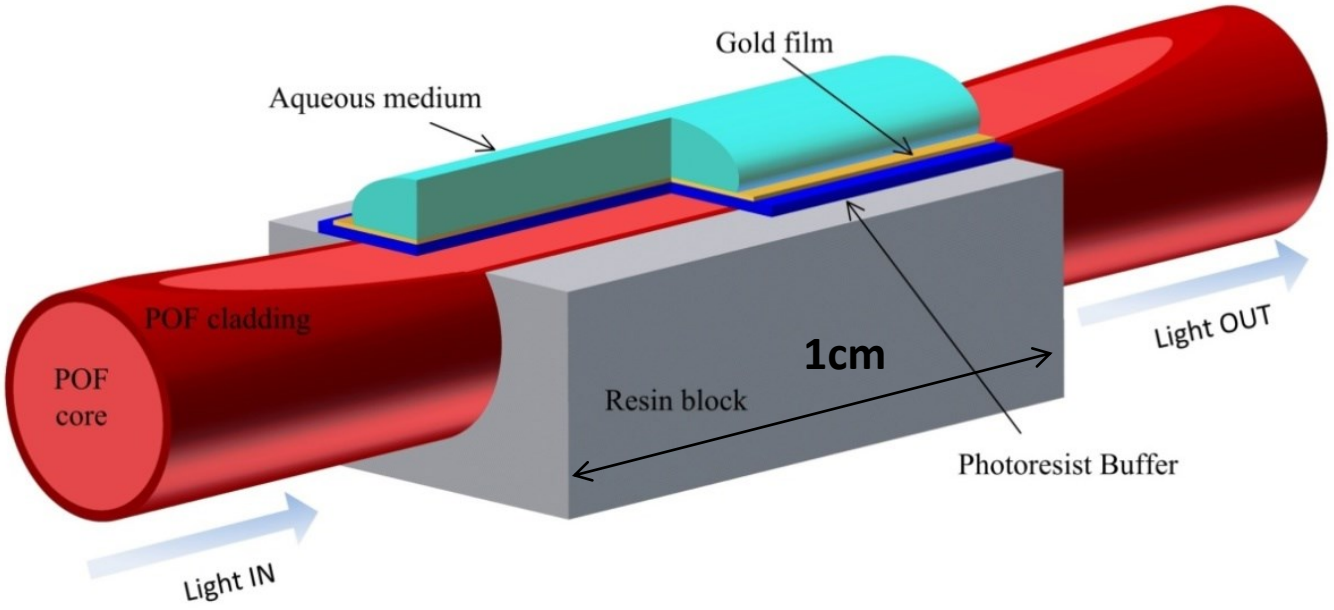

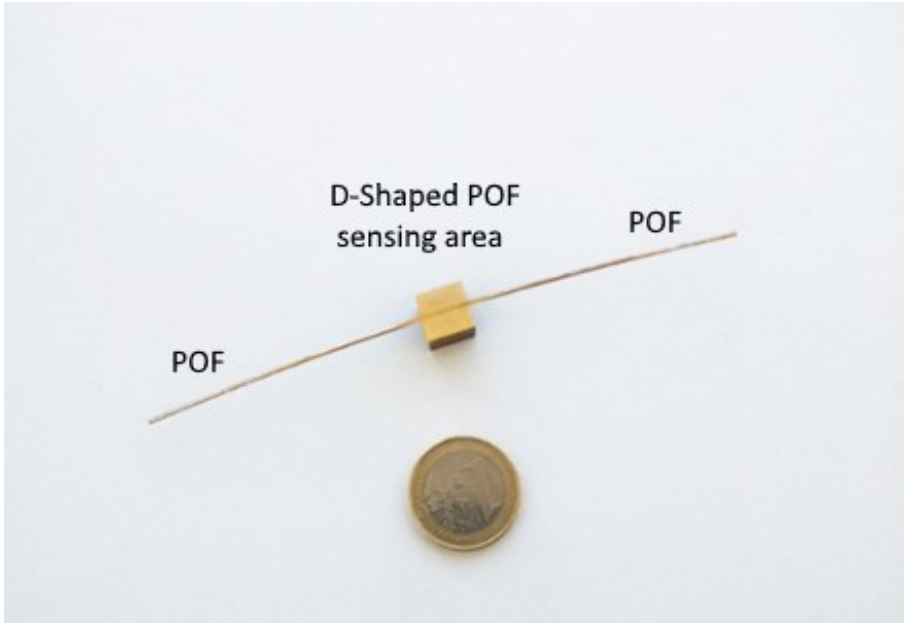

Price of the optical sensor:
about 3 $

POFs are especially advantageous due to their excellent flexibility, easy manipulation, great numerical aperture, large diameter, and the fact that plastic is able to withstand smaller bend radii than glass!

N. Cennamo, D. Massarotti, L. Conte, L. Zeni, Low cost sensors based on SPR in a plastic optical fiber for biosensor implementation, **Sensors**, 11, 11752–11760 (**2011**)

Experimental Configurations

Experimental Setup

based on Raspberry Pi

N. Cennamo et al. International Conference IEEE SAS (**2016)**

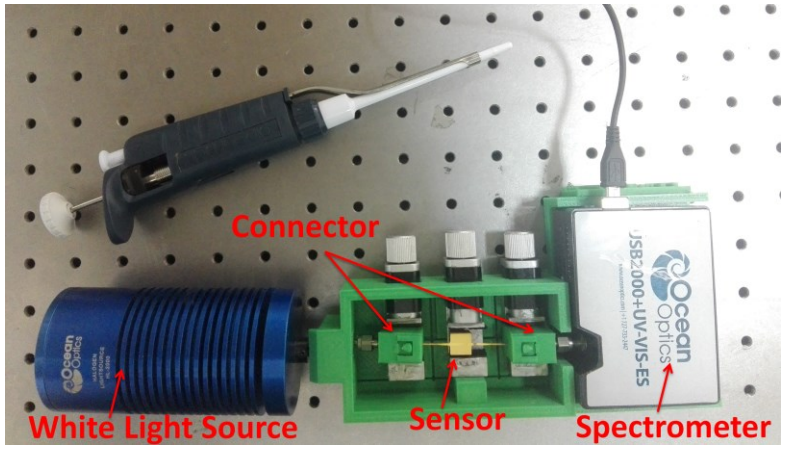

N. Cennamo et al. **Sensors**, (**2011**)

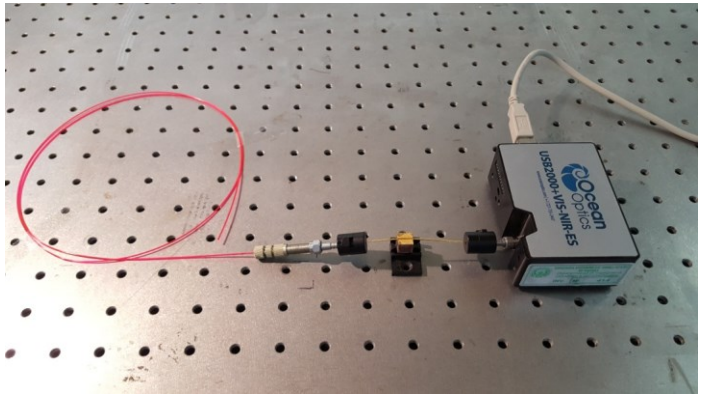

Red fluorescent optical fibers as light source

N. Cennamo et al. **TIM IEEE**, (**2017)**

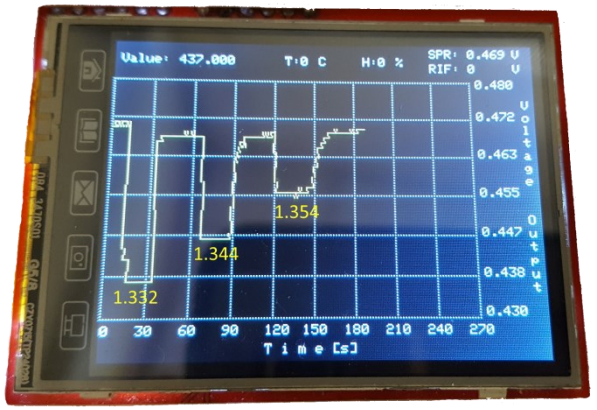

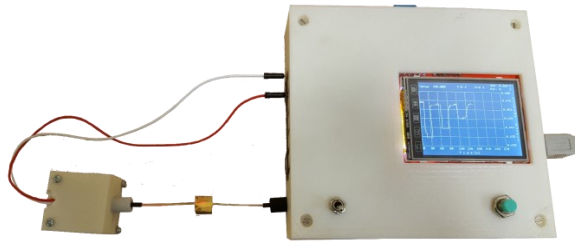

ARDUINO-BASED CONFIGURATION

(LED-Photodetector)

N. Cennamo et al. Italian Conference on Photonics Technology (**2015)**

Experimental setup

White Light Source
(360 ÷ 2000 nm)

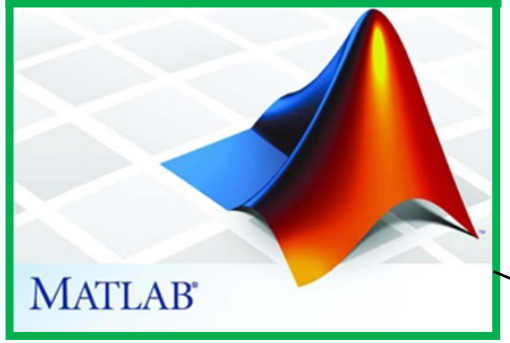

Software

Spectrometer
(200 ÷ 850 nm or 300 ÷ 1050 nm)

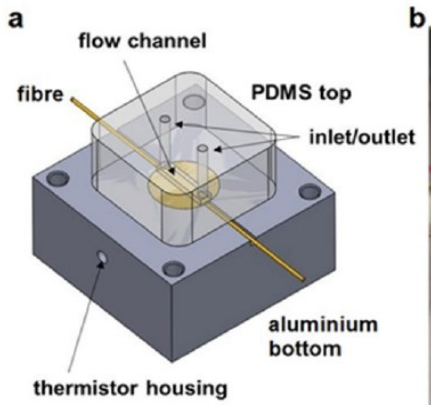

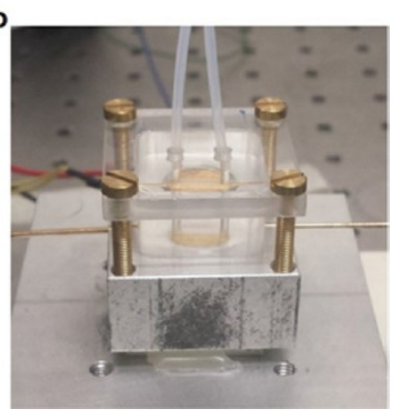

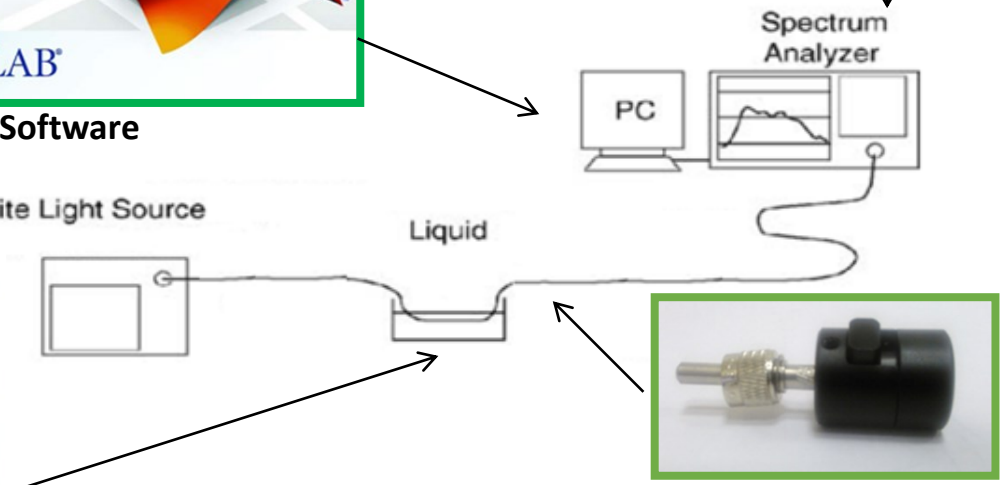

SMA connectors

Cennamo, N.; Chiavaioli, F.; Trono, C.; Tombelli, S.; Giannetti, A.; Baldini, F.; Zeni, L. A Complete Optical Sensor System Based on a POF-SPR Platform and a Thermo-Stabilized Flow Cell for Biochemical Applications. *Sensors* **2016**, *16*, 196

Receptors on SPR D-shaped POF platforms

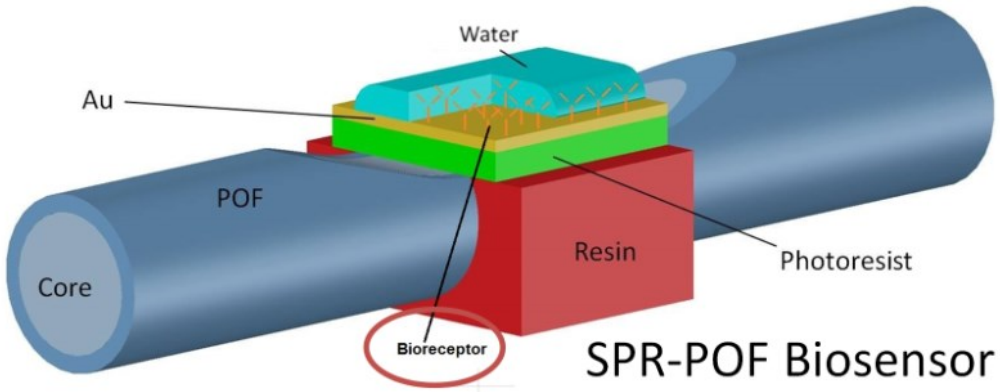

SPR-POF Biosensor

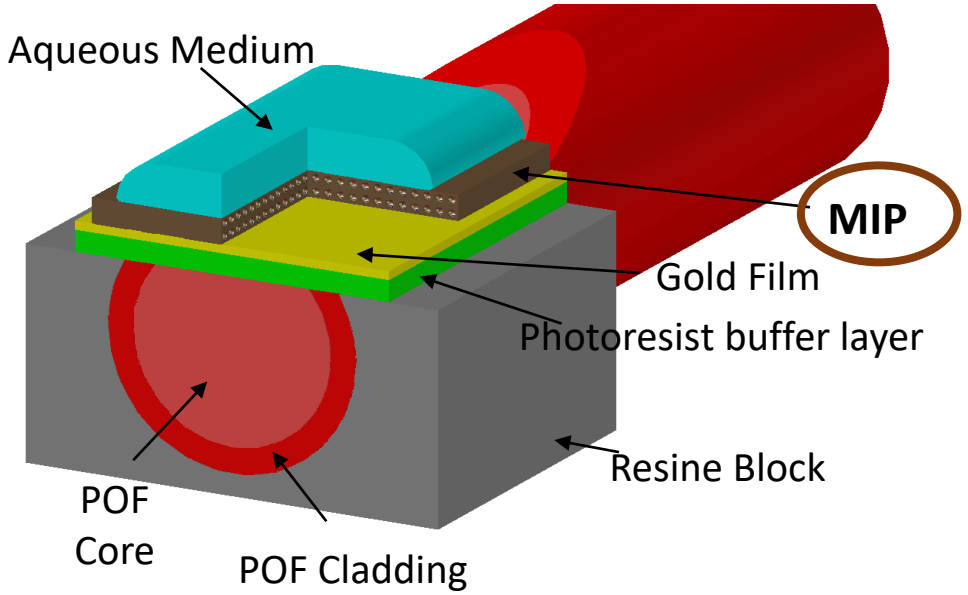

- **MIPs:** detection of **trinitrotoluene (TNT**), important in security applications, of **furfural (furan-2-carbaldehyde)** in transformer oil and in beverages, very significant in industrial and food applications, of **PFAs** in water in environmental monitoring applications and health, and **L-nicotine, human transferrin (HTR),** and **SARS-CoV-2** in clinical applications.
- **Bio-receptors:** detection of **transglutaminase/anti-transglutaminase** antibodies useful in the diagnosis and/or follow-up of celiac disease and the detection of Vascular endothelial growth factor (**VEGF**), selected as a circulating protein potentially associated with cancer, such as **SARS-CoV-2** virus, **Pancreatic Amylase** in Surgically-Placed Drain Effluentvery, **thrombin** and **therapeutic antibodies** in human serum, important in clinical applications, and of **PFAs and naphthalene** in environmental monitoring applications.
- **Chemical-receptors**: detection of **Fe(III) and Cu(II)** in clinical applications.

N. Cennamo, M. Pesavento, and L. Zeni, “A review on simple and highly sensitive plastic optical fiber probes for bio-chemical sensing”, Sensors & Actuators: B. Chemical, Volume 331, **2021**, 129393

A potential Advanced Material for Specific Sensing is the MIP (Molecularly Imprinted Polymer)

MIPs are porous solids or nano-particles containing specific sites interacting with the molecule of interest (analyte), according to a "**key and lock**" model.

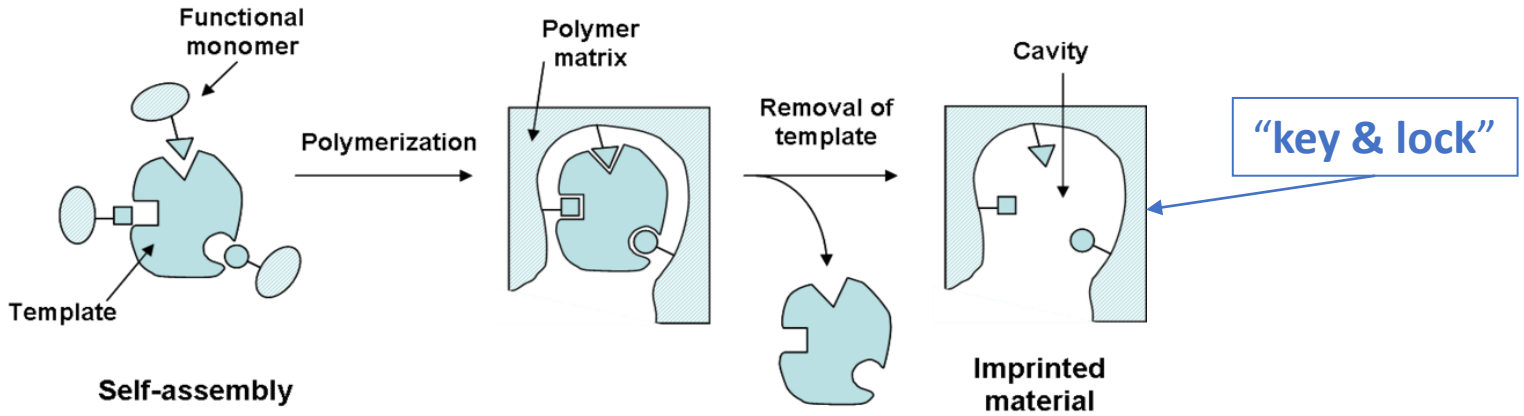

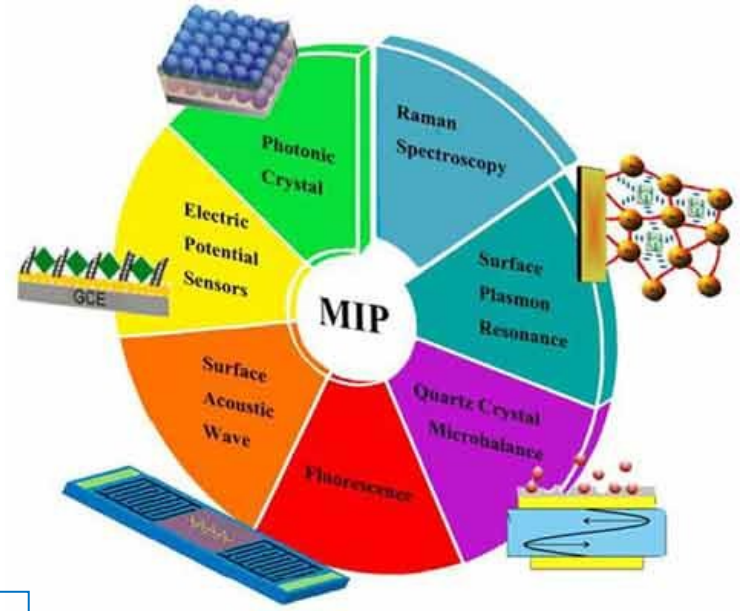

Images taken from the web

The cavity in the porous solid is obtained by polymerization of the aggregate substrate-coordinating monomers after extraction of the template from the selective site.

MIPs are synthetical receptors obtained by the molecular imprinting methods, *presenting a number of favourable aspects for sensing in comparison to bioreceptors*, as for example antibodies, including a **better stability out of the native environment, reproducibility on an industrial scale and low-cost.**

MIPs on SPR-POF platform

Schematic view

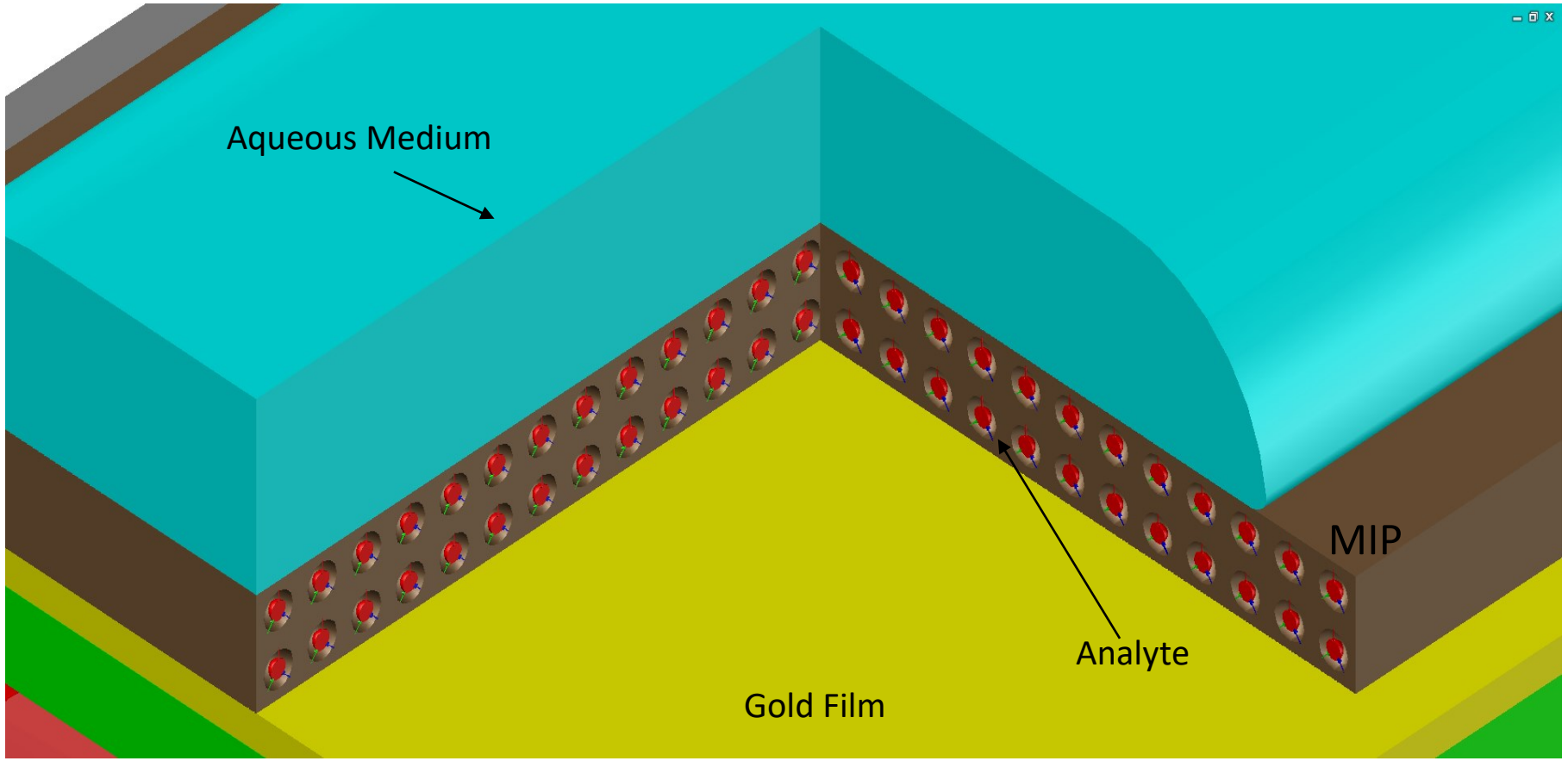

The advantage of MIPs is that they can be directly formed on a flat gold surface by depositing a drop of prepolymeric mixture directly over gold, spinning in a spin coater machine, and in situ polymerization without modifying the surface (functionalization and passivation), as needed for the bio-receptors

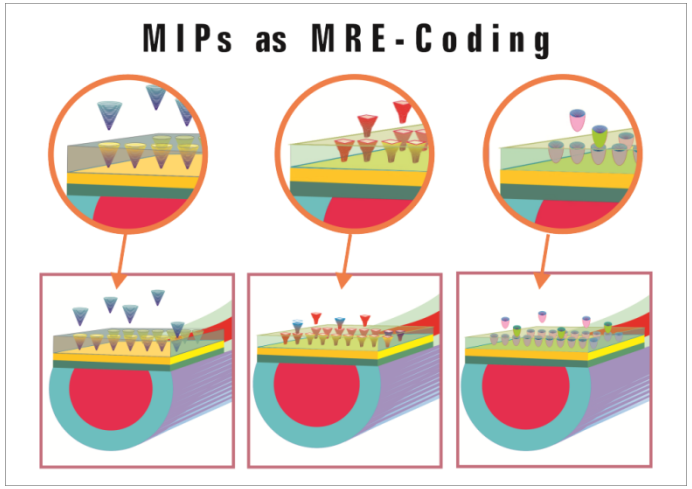

Moreover, the polymer layer may contain a relatively **high density of recognition elements**, included in a three-dimensional matrix, which should help the recognition by SPR/LSPR even for relatively **low molecular mass molecules**.

2-FAL detection in transformer oil (Industrial applications)

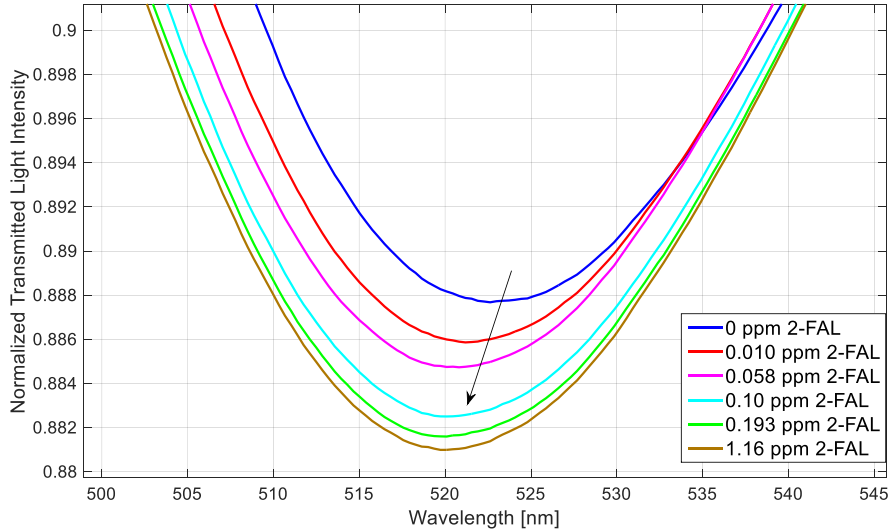

Sensing layer (MIP) for the selective detection of furfural (2-FAL) in transformer oil

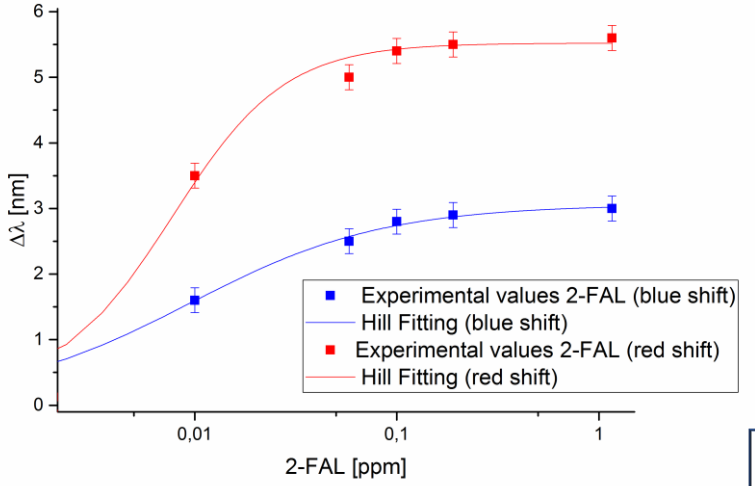

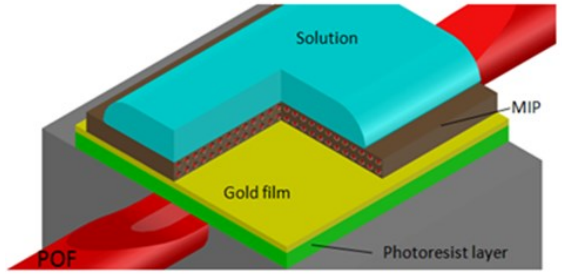

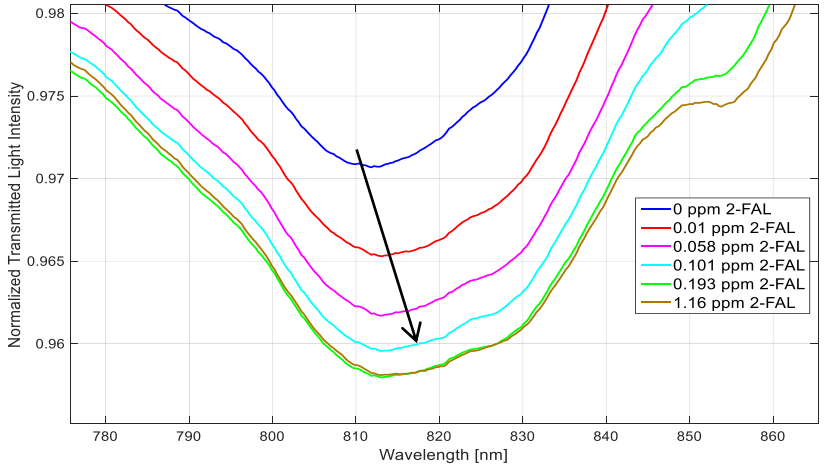

Analyte	Shift Type	K_{aff} (M^{-1})	Sens. at low conc. (nm· M^{-1})	LOD (M) from error of intercept (2*s)
2-FAL	Blue	$6.44 \cdot 10^{6}$	$2.04 \cdot 10^{7}$	$3.46 \cdot 10^{-7}$
2-FAL	Red	$1.06 \cdot 10^{7}$	$6.15 \cdot 10^{7}$	$4.08 \cdot 10^{-7}$

Current Research Partners

University of Pavia Italy

RSE Spa - Milan Italy

N. Cennamo, L. De Maria, C. Chemelli, A. Profumo, L. Zeni and M. Pesavento, Markers detection in transformer oil by plasmonic chemical sensor system based on POF and MIPs, IEEE Sensors Journal, VOL. 16, NO. 21, **2016**, 7663-7670

SPR Biosensor based on MIPs and tapered POFs

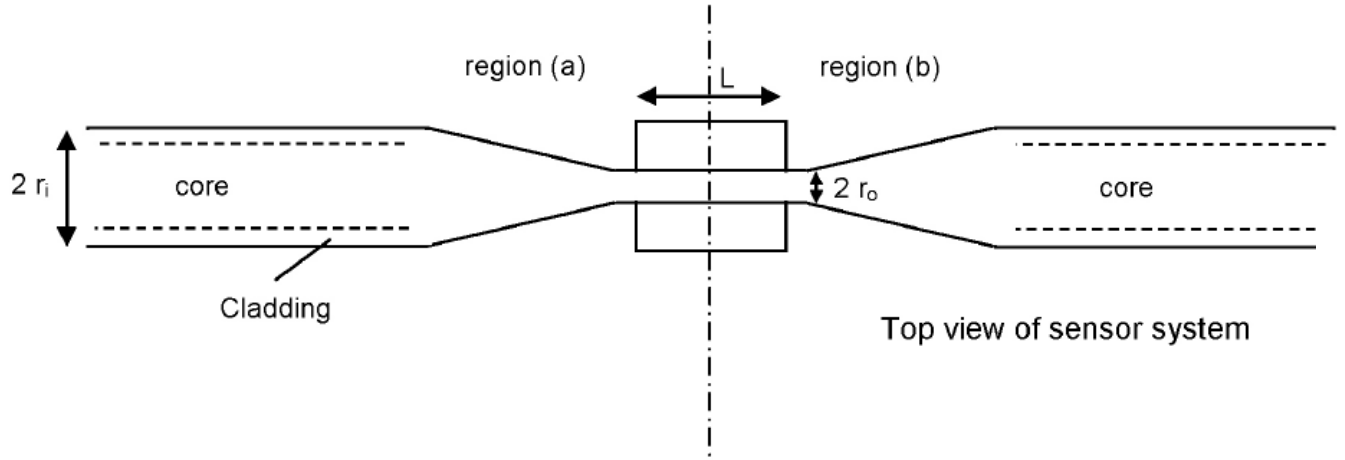

Top view of sensor system

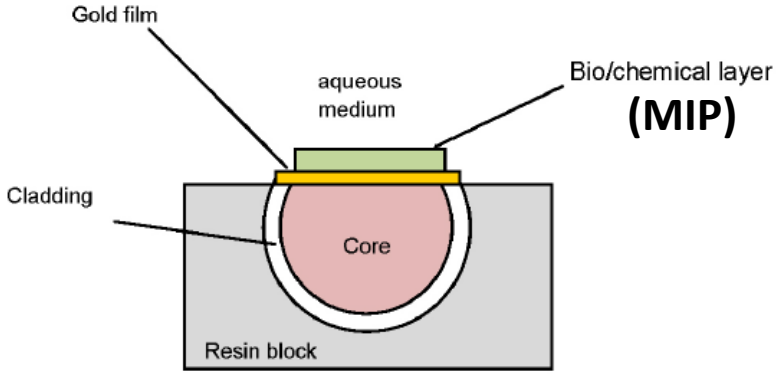

Section view of sensor system

Chemical sensor system based on SPR in tapered POF.

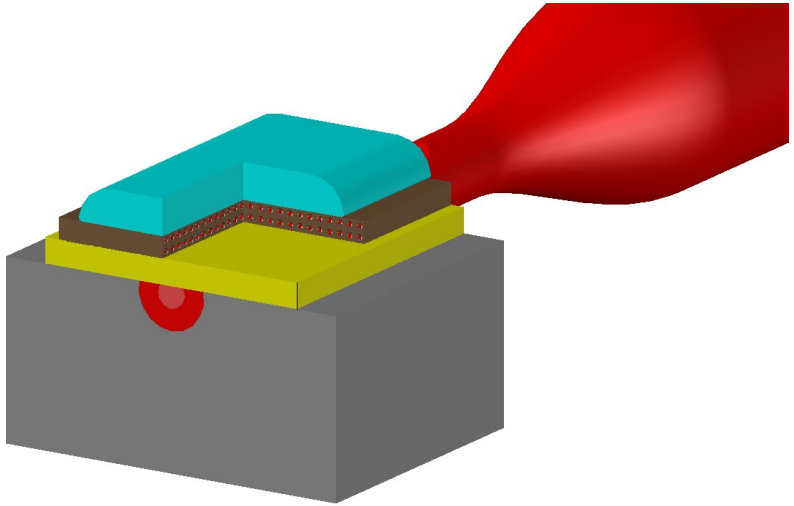

Specific MIP for the detection of **L-nicotine** in water solution

Current Research Partners

University of Pavia Italy

N. Cennamo, G. D'Agostino, M. Pesavento and L. Zeni, "High selectivity and sensitivity sensor based on MIP and SPR in tapered plastic optical fibers for the detection of l-nicotine" **Sensors and Actuators: B. Chemical**, 191, 529–536 (**2013**)

Experimental results: detection of L-nicotine

SPR transmission spectra obtained on tapered fiber sensor, normalized to the spectrum in air before spin coating the MIP layer, for different concentrations of **L-nicotine in water**, 0 - 10^{-2} M.

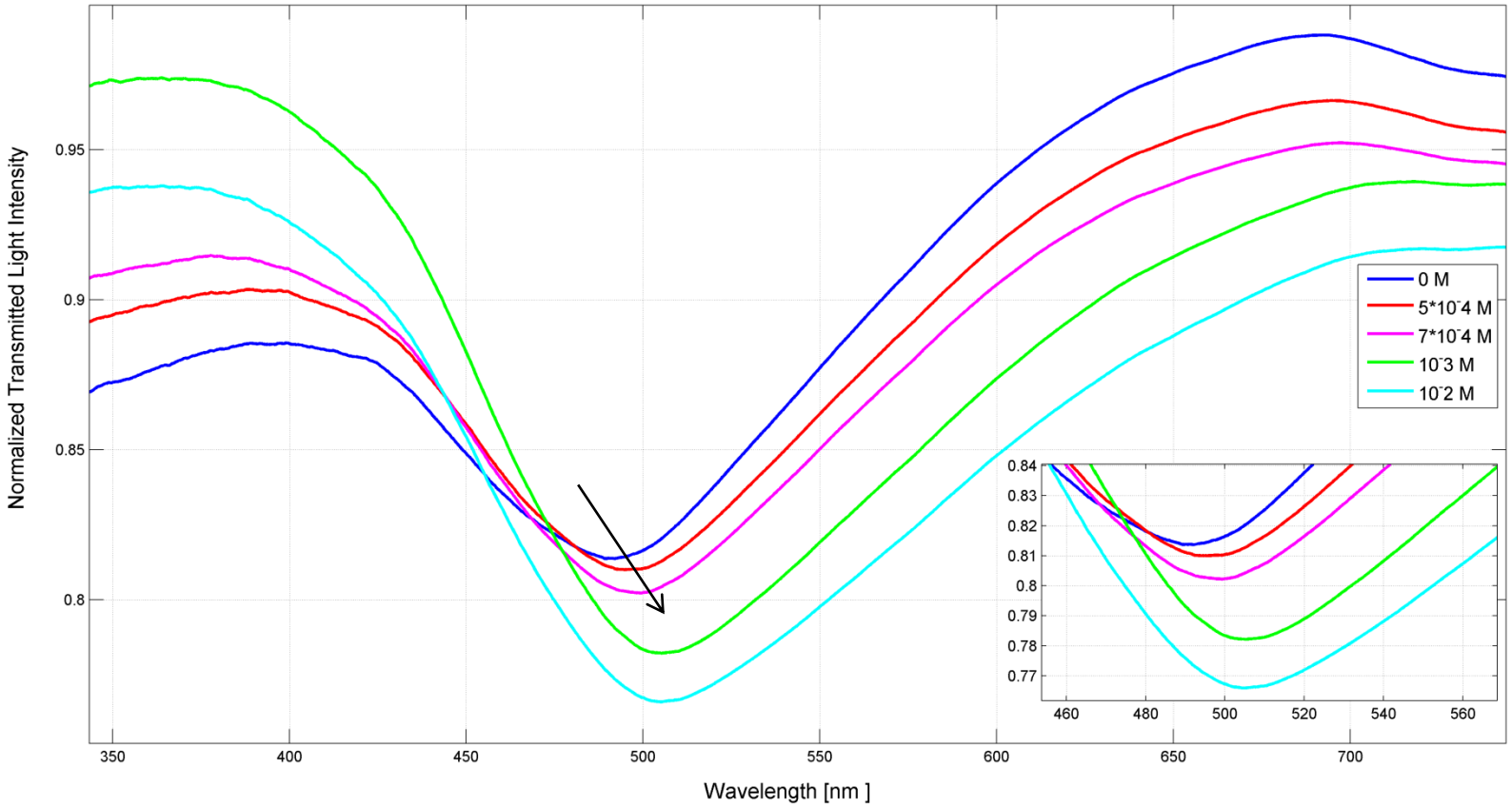

N. Cennamo, G. D'Agostino, M. Pesavento and L. Zeni, "High selectivity and sensitivity sensor based on MIP and SPR in tapered plastic optical fibers for the detection of l-nicotine" **Sensors and Actuators: B. Chemical**, 191, 529–536 **(2013)**

SPR transmission spectra obtained on tapered fiber sensor, normalized to the reference (spectrum in air before spin coating the MIP layer), for different analytes: **L-nicotine, caffeine and dopamine.**
For comparison, the spectrum of **pure water** is reported

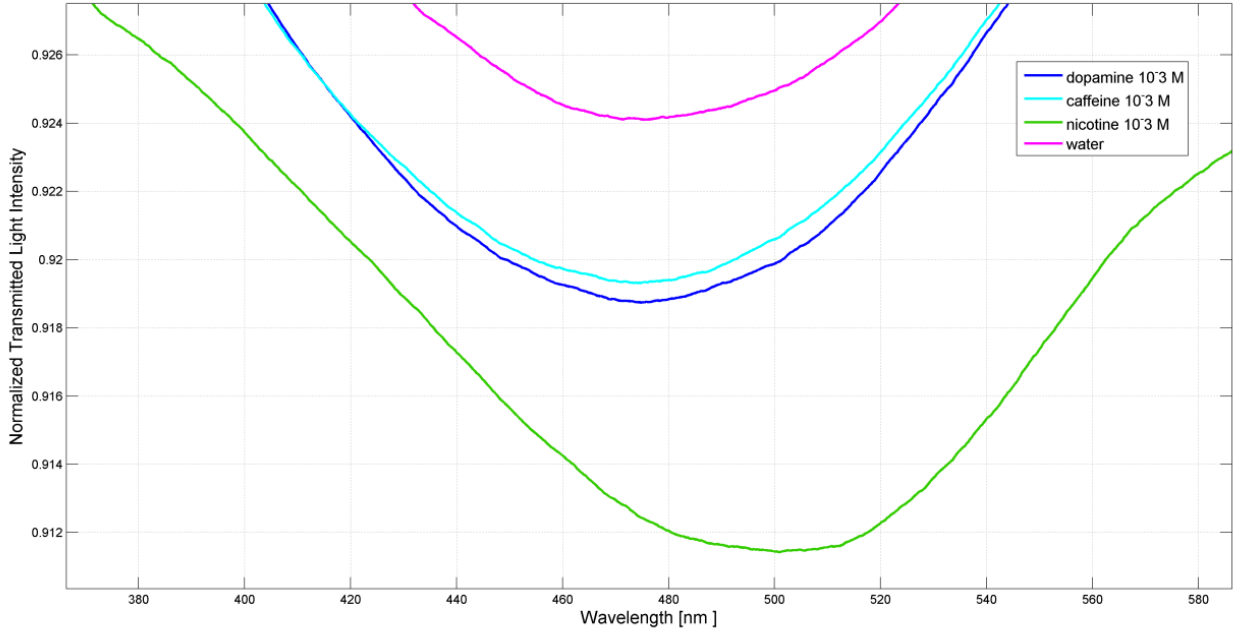

Experimental results
L-nicotine detection

Selectivity analysis

SPR transmission spectra obtained on tapered fiber sensor, **without MIP layer**, normalized to the reference (spectrum in air), for different concentrations of L-nicotine

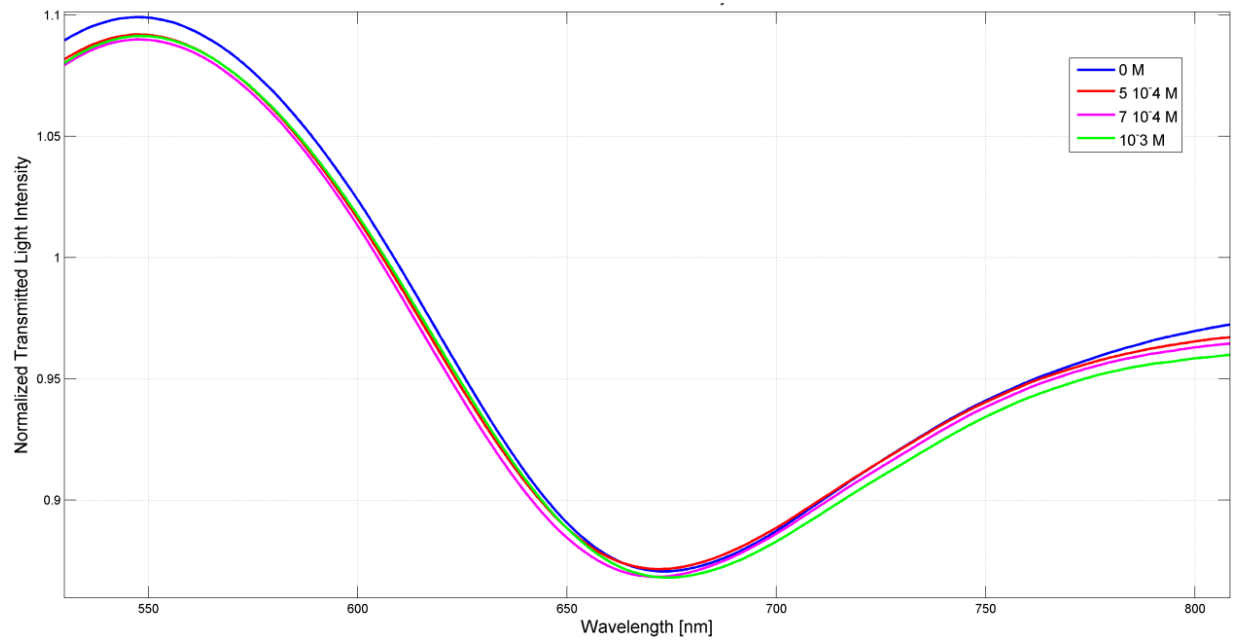

N. Cennamo, G. D'Agostino, M. Pesavento and L. Zeni, "High selectivity and sensitivity sensor based on MIP and SPR in tapered plastic optical fibers for the detection of l-nicotine" **Sensors and Actuators: B. Chemical**, 191, 529–536 **(2013)**

Dose-response curve for L-nicotine

N. Cennamo et al. / Sensors and Actuators B 191 (2014) 529–536

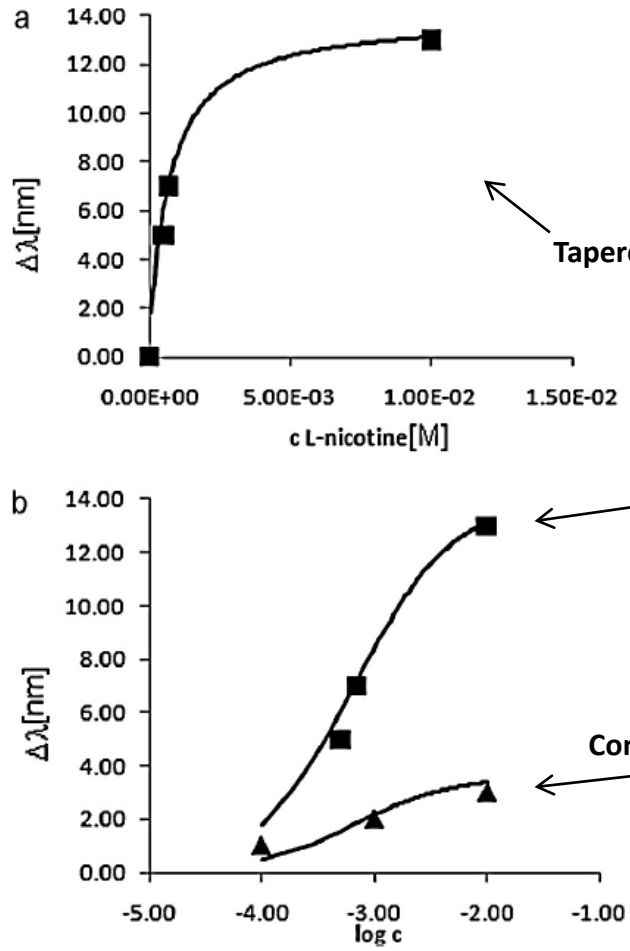

Fig. (a) Plasmon resonance wavelength variation as a function of L-nicotine concentration in the range 0–10^{-3} M at sensor with tapered fiber. Continuous line: calculated Hill function with $K_a = 1.5 \times 10^3\ M^{-1}$, $\gamma = 1$, $\Delta\lambda_\infty = 14$ nm; (b) lin–log relation at sensor with tapered fiber (black squares) and not tapered fiber (black triangles). Continuous lines: calculated with $K_a = 1.5 \times 10^3\ M^{-1}$ and $\gamma = 1$, $\Delta\lambda_\infty = 14$ nm for tapered fiber and $\Delta\lambda_\infty = 3.6$ nm for not tapered fiber, respectively.

Detection Limit (LOD) 1.86 × 10^{-4}M, calculated from twice the standard deviation of the ordinate at the origin of the standardization curve (the blank) divided by the slope (the sensitivity)

Tapered fiber configuration

The sensitivity at low concentration is about 7.6 times higher than that of the sensor without tapered fiber

Configuration without tapered fiber

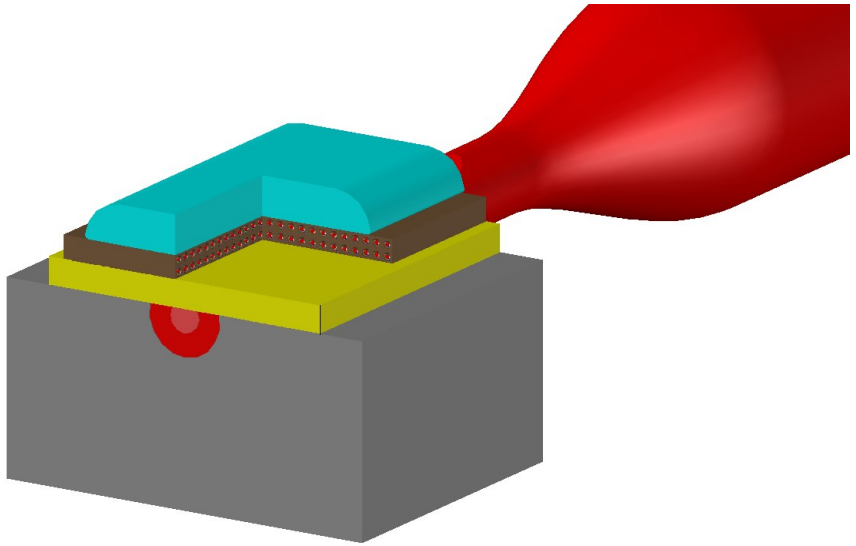

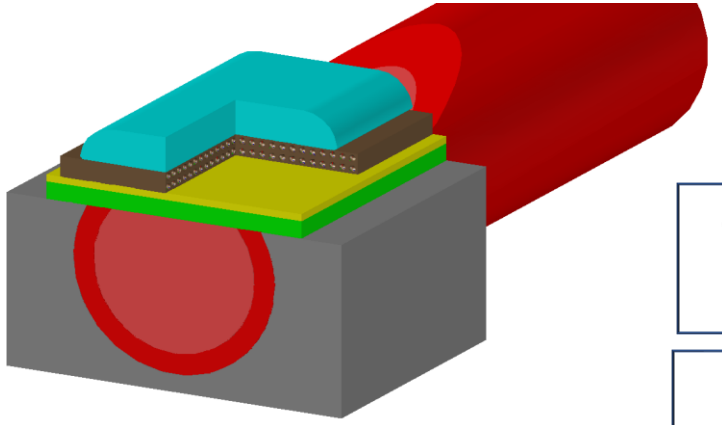

Current Research Partners

University of Pavia Italy

Curves are reported for a sensor based on **tapered and not tapered POF**.
In the not tapered POF configuration the sensitivity is much smaller.
In both cases the calculated Hill functions are shown for comparison. The affinity constant and the Hill factor are similar for the two sensors.

High Sensor performances. The case of a security application

Sensing layer (MIP with GNS) for the selective detection and analysis of **2,4,6-trinitrotoluene (TNT)** in aqueous solution

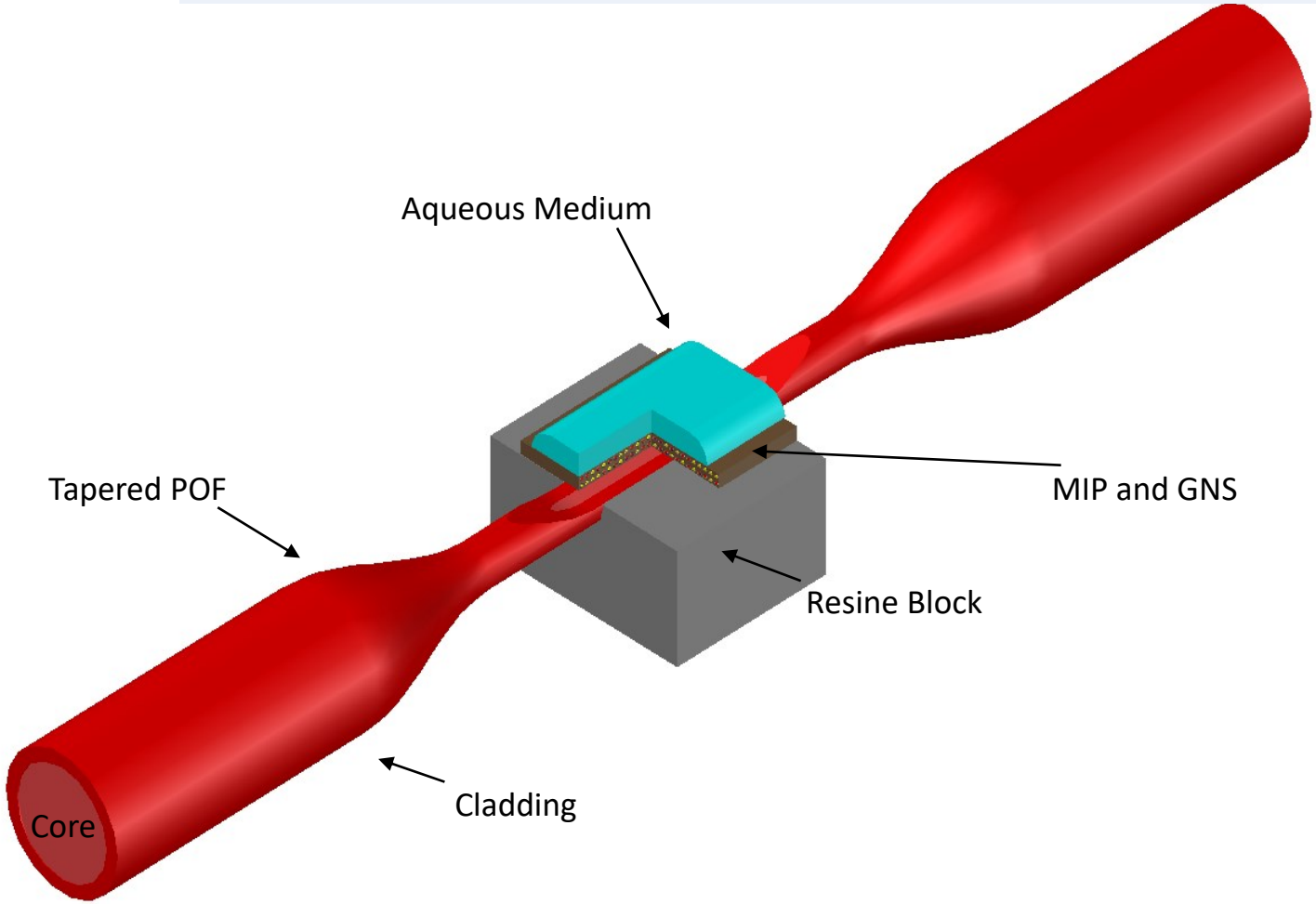

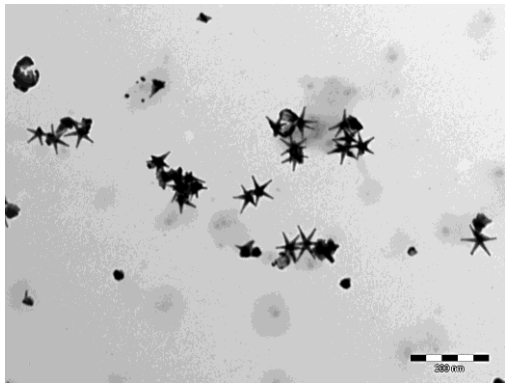

TEM image of GNS

Current Research Partners

University of Pavia Italy

Nunzio Cennamo, Donà A., Pallavicini P., D'Agostino G., Dacarro G., Zeni L., Pesavento M., Sensitive detection of 2,4,6-trinitrotoluene by tridimensional monitoring of molecularly imprinted polymer with optical fiber and five-branched gold nanostars, **Sensors and Actuators, B: Chemical**, 208, 291-298, **2015**

Different chemical sensing layer

Sensing layer (MIP with GNS)

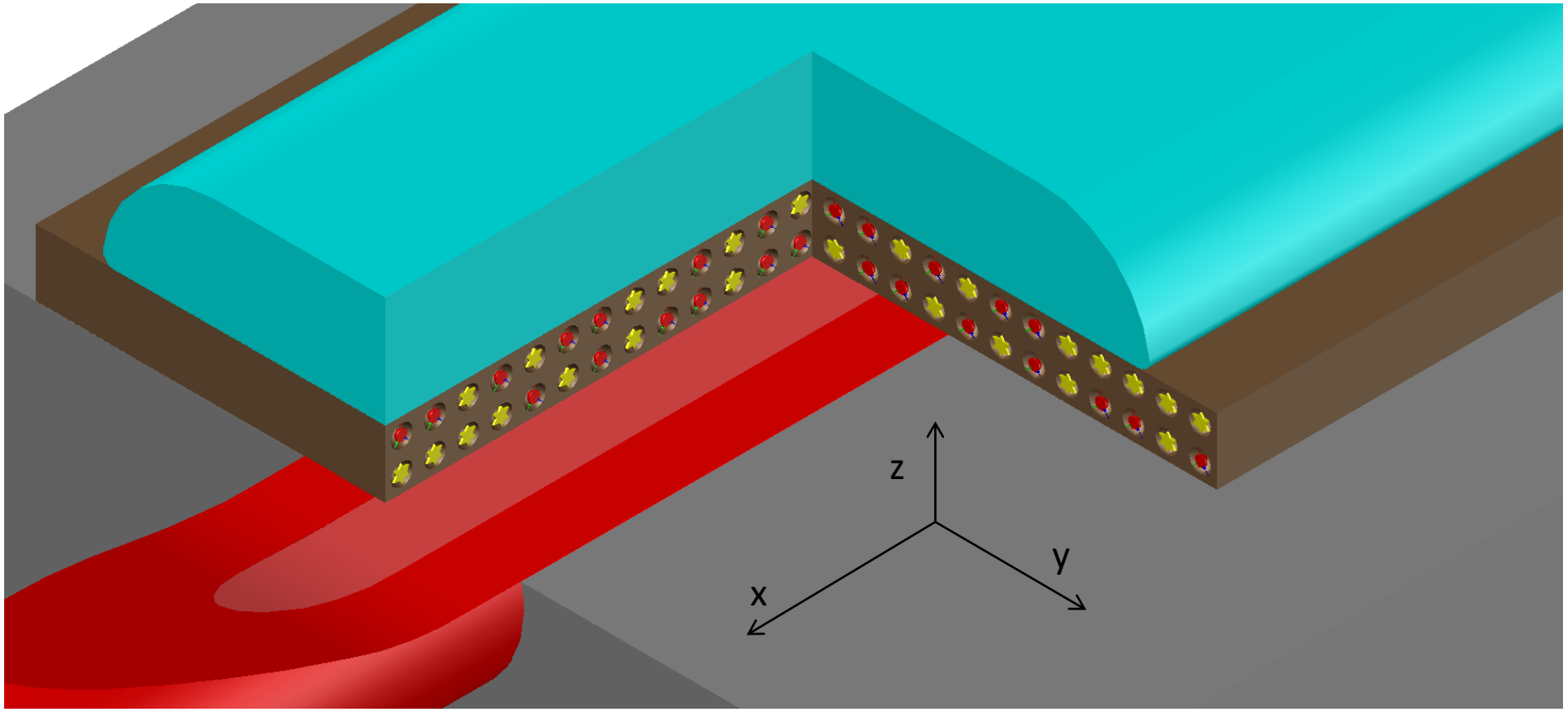

"3-D *Sensing*"

Nunzio Cennamo, Donà A., Pallavicini P., D'Agostino G., Dacarro G., Zeni L., Pesavento M., Sensitive detection of 2,4,6-trinitrotoluene by tridimensional monitoring of molecularly imprinted polymer with optical fiber and five-branched gold nanostars, **Sensors and Actuators, B: Chemical**, 208, 291-298, **2015**

Security applications

MIP with GNS for the selective Detection of TNT

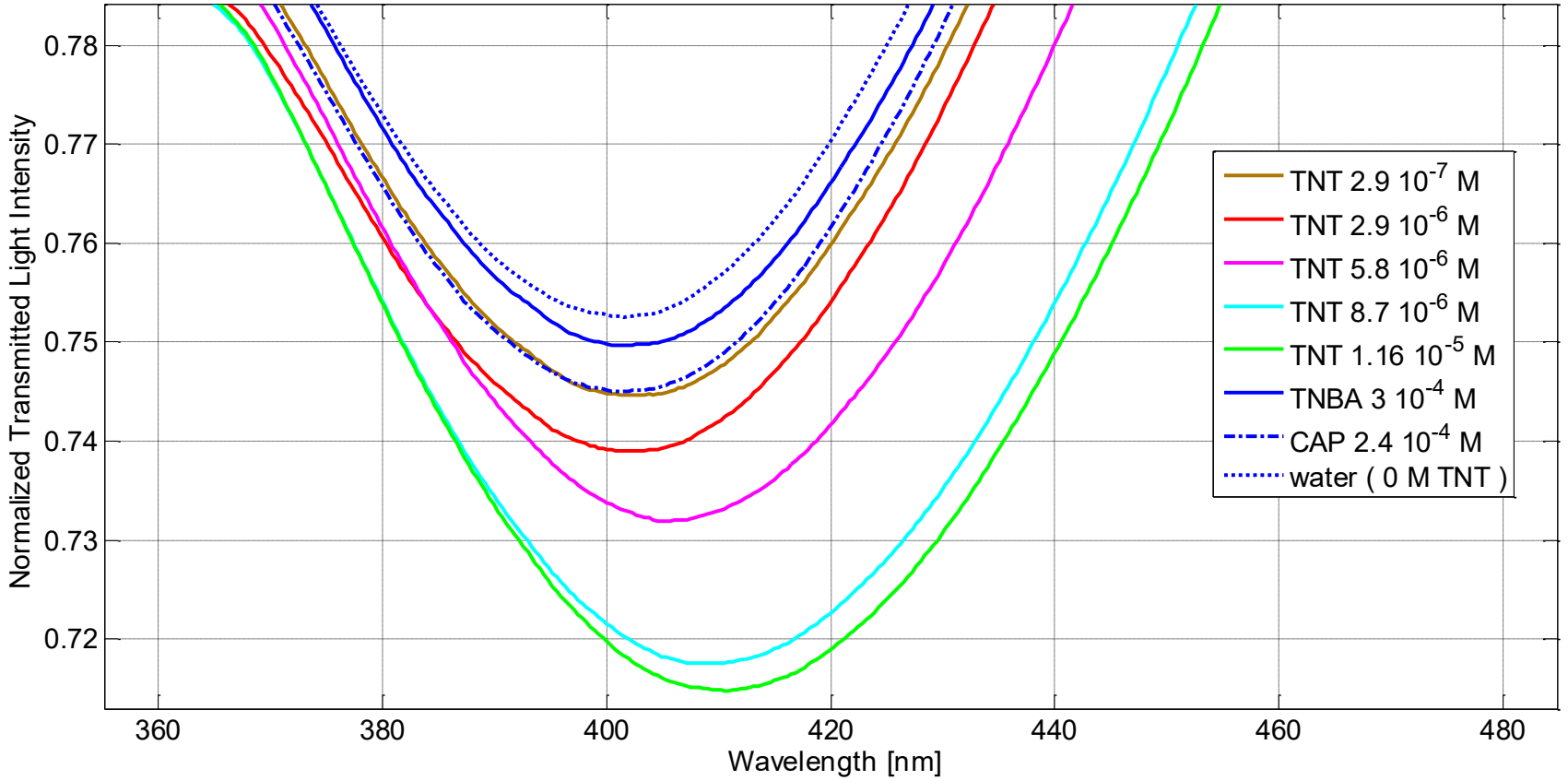

CAP: Chloramphenicol; TNBA: Trinitrobenzoicacid
(Molecules of similar chemical structure as TNT)

N. Cennamo, A. Donà, P. Pallavicini, G. D'Agostino, G. Dacarro, L. Zeni and M. Pesavento, Sensitive detection of 2,4,6-trinitrotoluene by tridimensional monitoring of molecularly imprinted polymer with optical fiber and five-branched gold nanostars, **Sensors and Actuators B**, 208, **2015**, Pages 291–298.

Selective Detection of TNT by MIPs and POFs

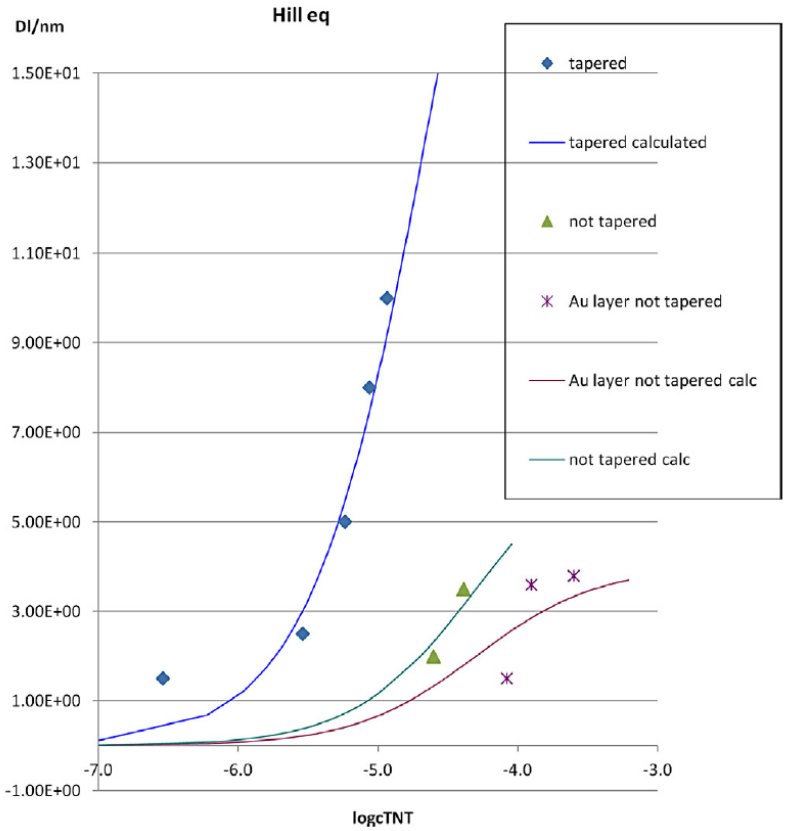

Fig. Plasmon resonance wavelength variation as a function of TNT concentration. Continuous curves: Hill fitting to the experimental data (parameters as in Table). ◊: GNS-MIP/tapered POF platform. ▲: GNS-MIP/POF platform. *: MIP on gold layer/POF platform.

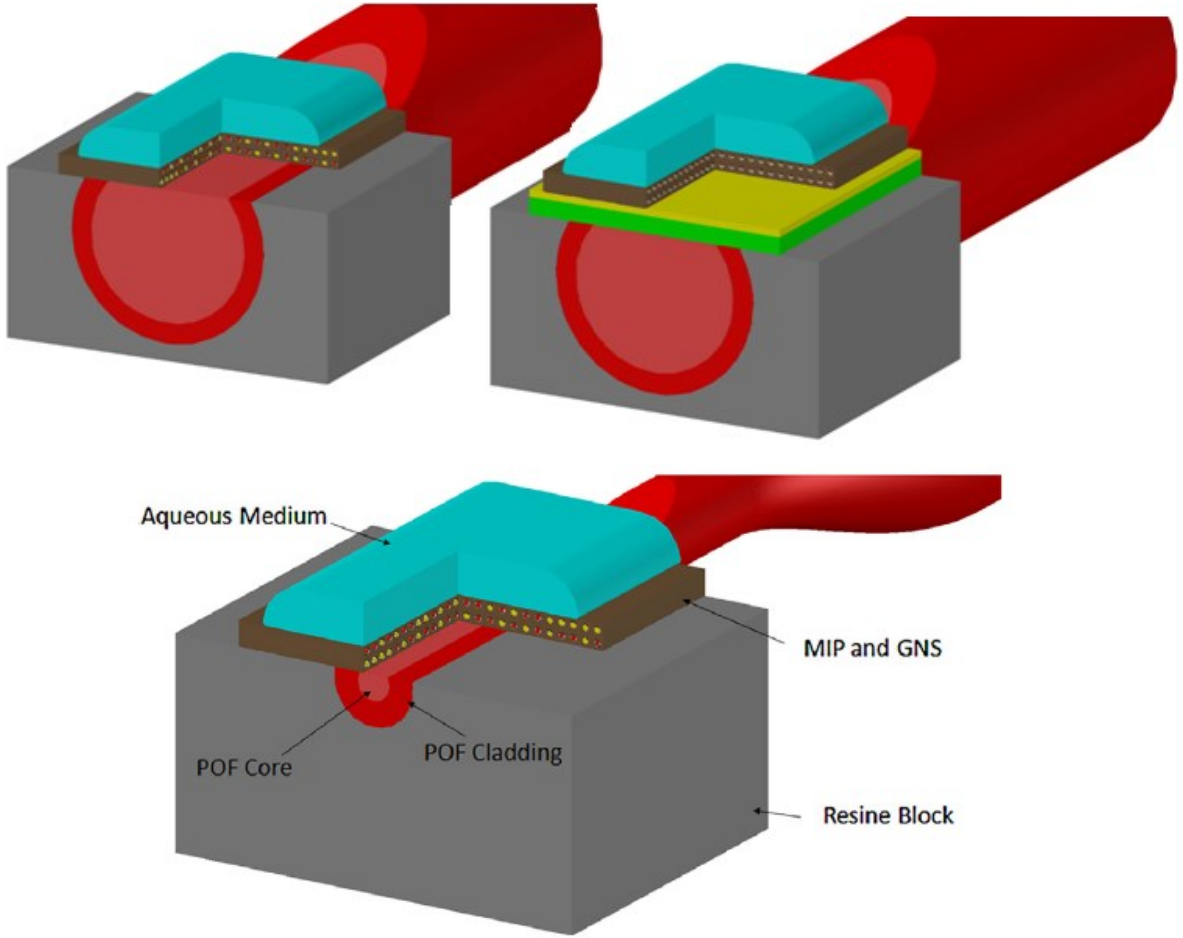

Table
Performance parameters for the GNS-MIP sensors with tapered (GNS-MIP/tapered POF) and not-tapered POF platform (GNS-MIP/POF), in the linear range. The parameters are compared with those for the same MIP for TNT, but with a gold layer interposed between the POF and the MIP layer previously obtained

Chemical sensor system in POF for TNT	Sensitivity [nm/M]	LOD	Hill equation parameters
MIP on gold layer/POF	2.7×10^4	5.1×10^{-5} M	$K_f = 4 \times 10^4$; $kc_{site} = 4$; $h = 1$
GNS-MIP/POF	8.5×10^4	2.4×10^{-6} M	$K_f = 2 \times 10^4$; $kc_{site} = 7$; $h = 1$
GNS-MIP/tapered POF	8.3×10^5	7.2×10^{-7} M	$K_f = 4 \times 10^4$; $kc_{site} = 29$; $h = 1$

Clinical applications based on bioreceptors. The case of transglutaminase/antitransglutaminase complex

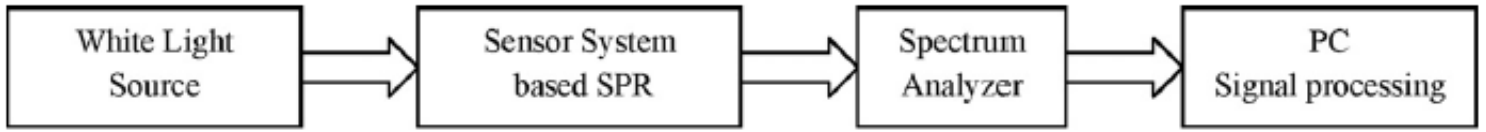

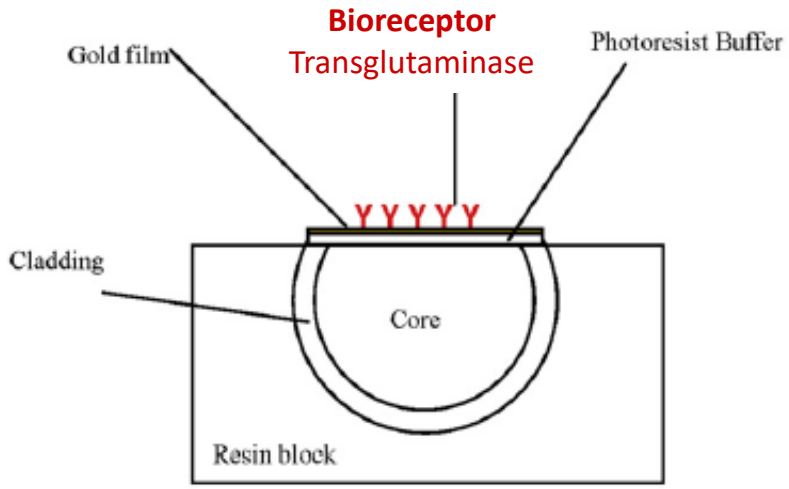

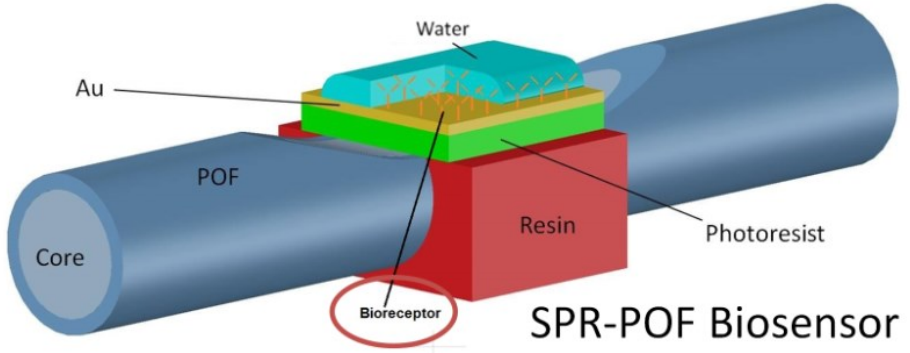

Current Research Partners

CNR-ISA
Avellino - Italy

N. Cennamo, A. Varriale, A. Pennacchio, M. Staiano, D. Massarotti, L. Zeni, S. D'Auria, "An Innovative Plastic Optical Fiber-based Biosensor for new Bio/applications. The Case of Celiac Disease", **Sensors and Actuators: B. Chemical**, 176, Pages 1008-1014, (**2013**)

Clinical applications: the transglutaminase/antitransglutaminase complex

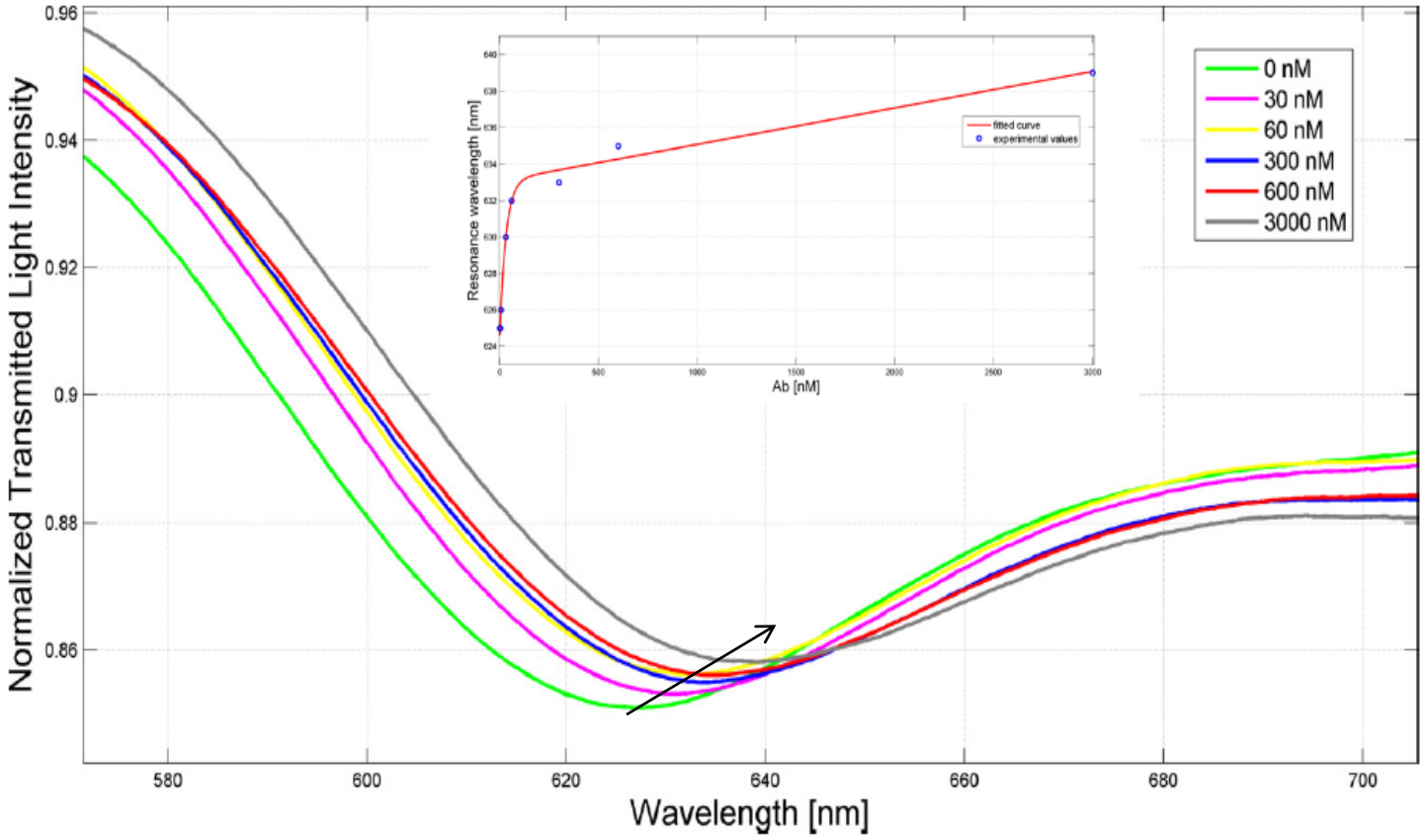

Fig. SPR transmission spectra, normalized to the air spectrum, for different analyte concentrations in the case of sensor with gold layer with tTG (bio-receptor).

This POF-biosensor is able to sense the transglutaminase/anti-transglutaminase complex in the range of concentrations between **30 nM and 3000 nM**. In celiac patients the specific antibodies concentration against tTG is in the range **0.4–3 mM**, about 1.0–10.0% of all IgA present in the serum of normal adults (4.4 and 31.2 mM). **The protein concentrations detected in our experiments is in the nanomolar range, indicating that our biosensor is a good candidate for the diagnosis and follow-up of CD**

Selectivity analysis

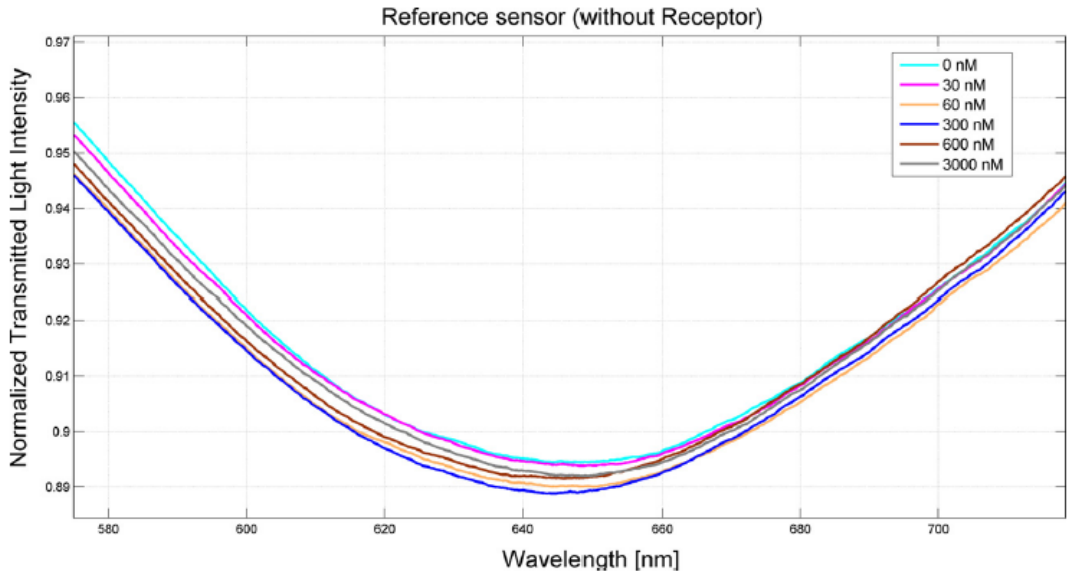

Fig. SPR transmission spectra, normalized to the air spectrum, for different analyte concentrations in the case of the reference sensor with gold layer without tTG (bio-receptor).

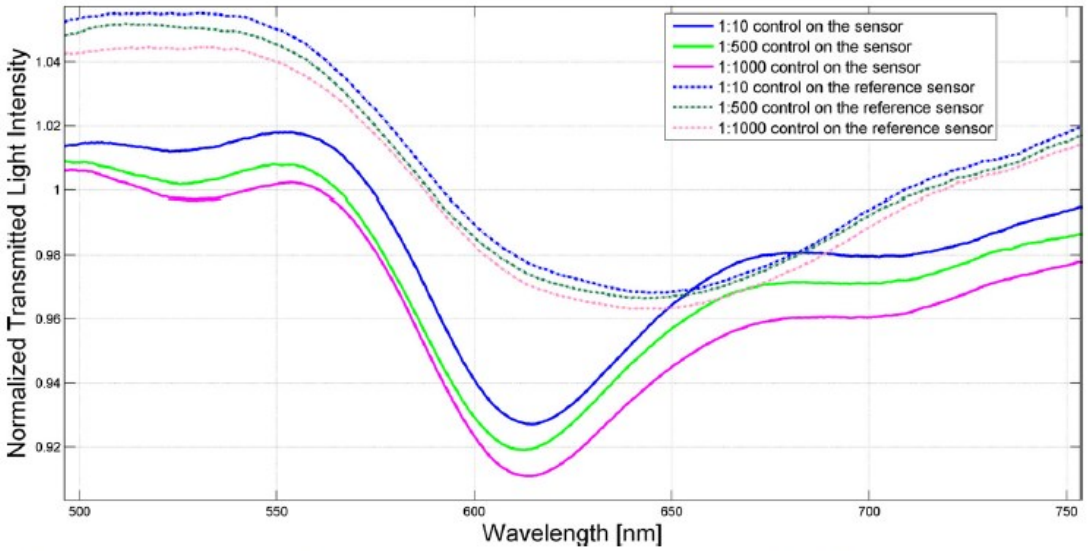

Fig. SPR transmission spectra, normalized to the air spectrum, for different control analyte concentrations for the both sensors (with and without tTG).

Clinical applications:

Aptasensor for the detection of Vascular endothelial growth factor (VEGF), selected as a circulating protein potentially associated with cancer

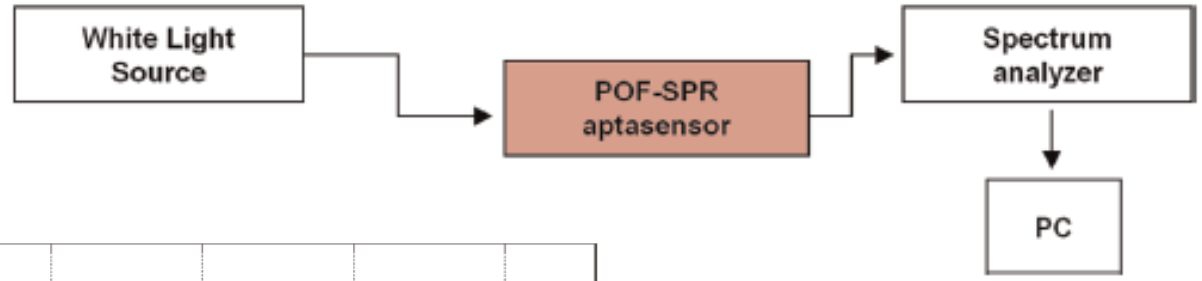

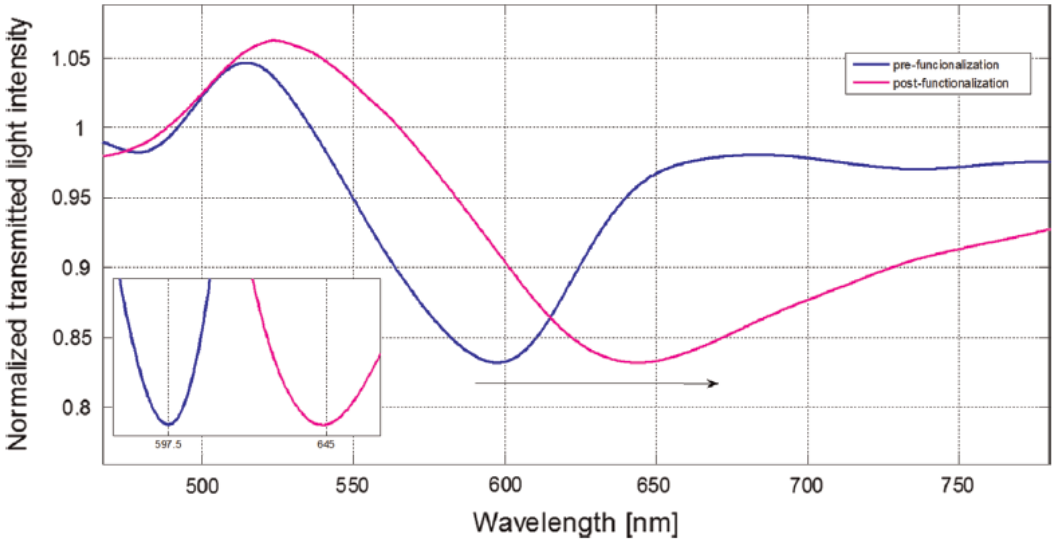

Wavelength resonance shift when the functionalization process is completed (functionalization with aptamers followed by passivation (mercaptoethanol (MPET))

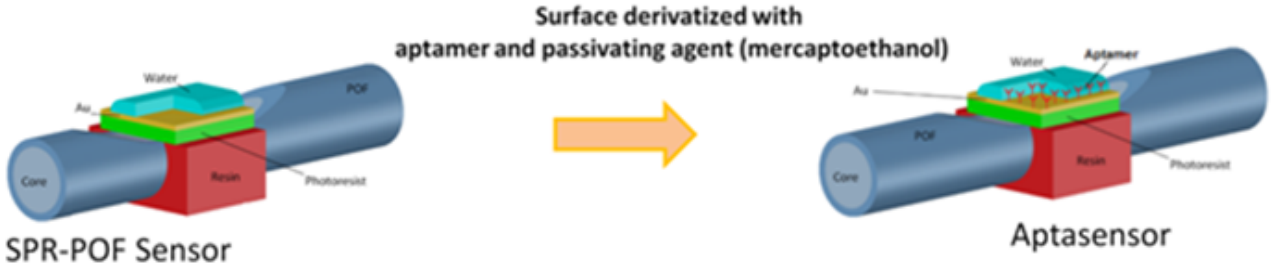

Current Research Partners

FBK
Trento - Italy

Nunzio Cennamo, Maria Pesavento, Lorenzo Lunelli, Lia Vanzetti, Cecilia Pederzolli, Luigi Zeni and Laura Pasquardini, An easy way to realize SPR aptasensors: a multimode plastic optical fiber platform for cancer biomarkers detection, **TALANTA**, 140 (**2015**), pages 88–95

Clinical applications:

Aptasensor for the detection of Vascular endothelial growth factor (VEGF), selected as a circulating protein potentially associated with cancer

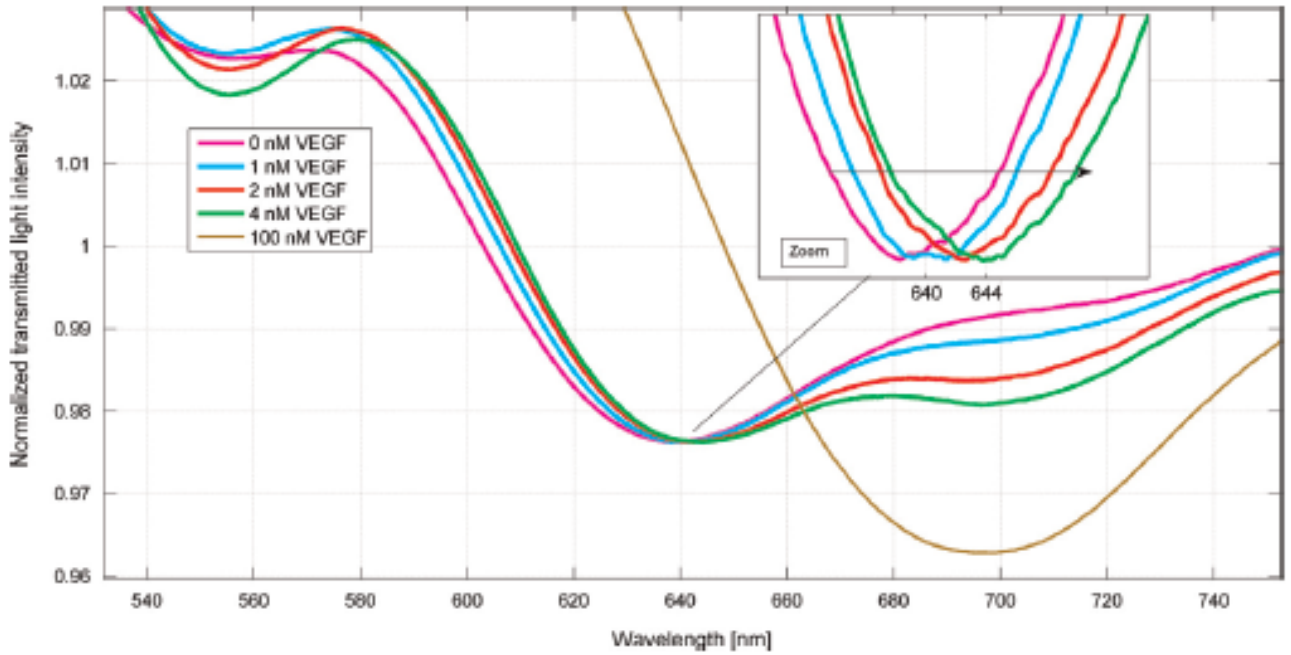

Limit of detection (LOD) is 0.8 nM

Aptasensor	Equilibrium parameters			Kinetical parameters	
	K_f (M^{-1})	$kc_{site}K_f$	kc_{site} (nm)	$k_{kinetical}$ ($M^{-1}s^{-1}$)	$K'c_{site}$
Apt–MPET	$2.1(9) \times 10^7$	$1.3(4) \times 10^9$	74.4	8.0×10^5	1.7

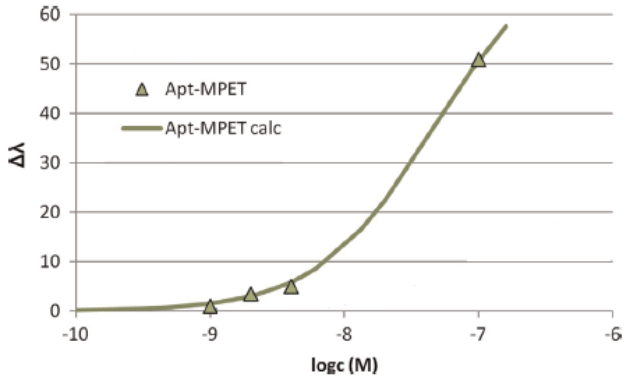

Nunzio Cennamo et al., An easy way to realize SPR aptasensors: a multimode plastic optical fiber platform for cancer biomarkers detection, **TALANTA**, 140 (**2015**), pages 88–95

Aptasensor for the thrombin detection in nanomolar range (Clinical applications)

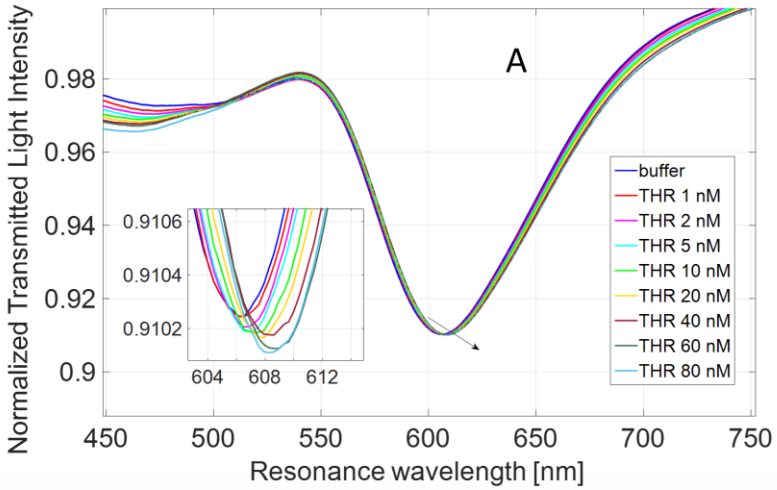

Aptasensor functionalized with a specific aptamer for THR

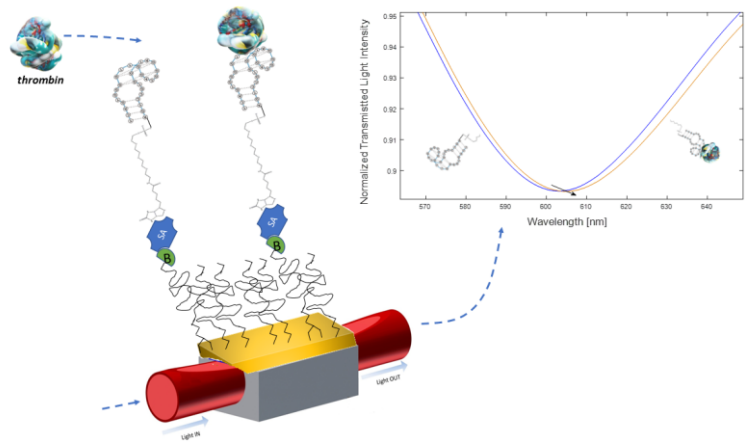

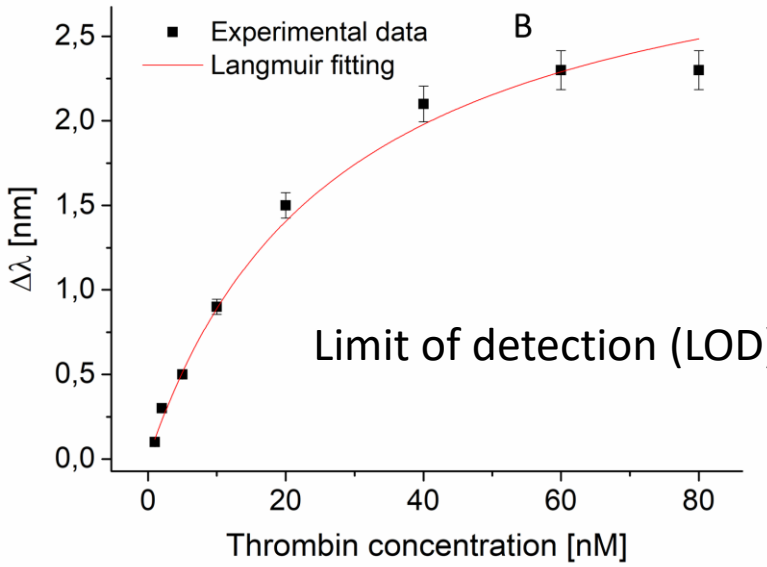

Limit of detection (LOD) is 1.6 nM

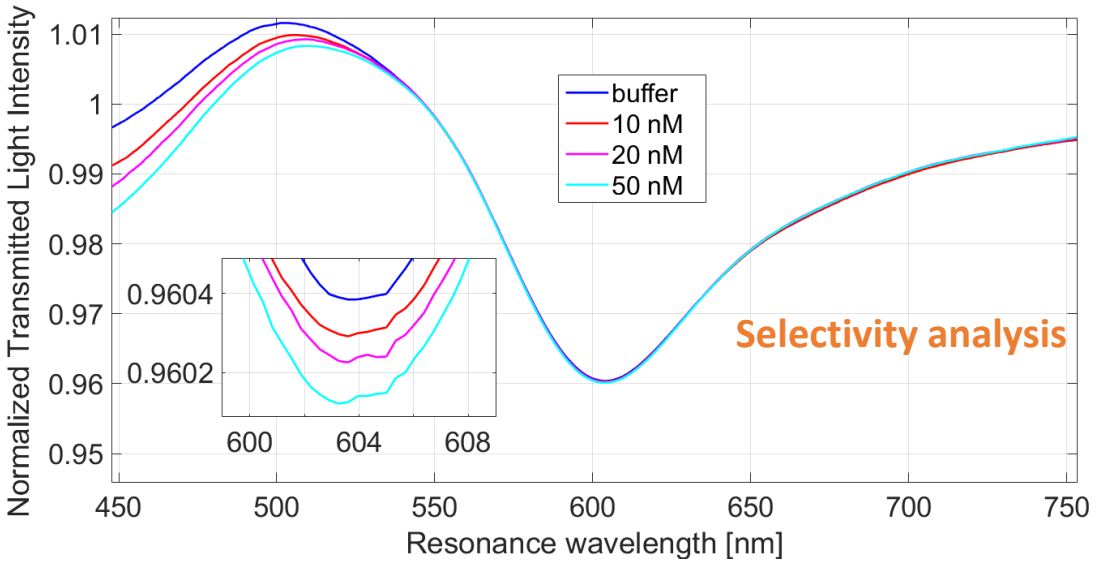

Reference sensor, functionalized with a non specific aptamer for THR

Nunzio Cennamo, Laura Pasquardini, Francesco Arcadio, Lia E. Vanzetti, Alessandra Bossi, Luigi Zeni, D-shaped plastic optical fibre aptasensor for fast thrombin detection in nanomolar range, Scientific Reports, 9, 18740, **2019**

Simultaneous detection of Fe(III) and Cu(II) by chemical receptors

Experimental Setup to measure the transmitted light spectrum

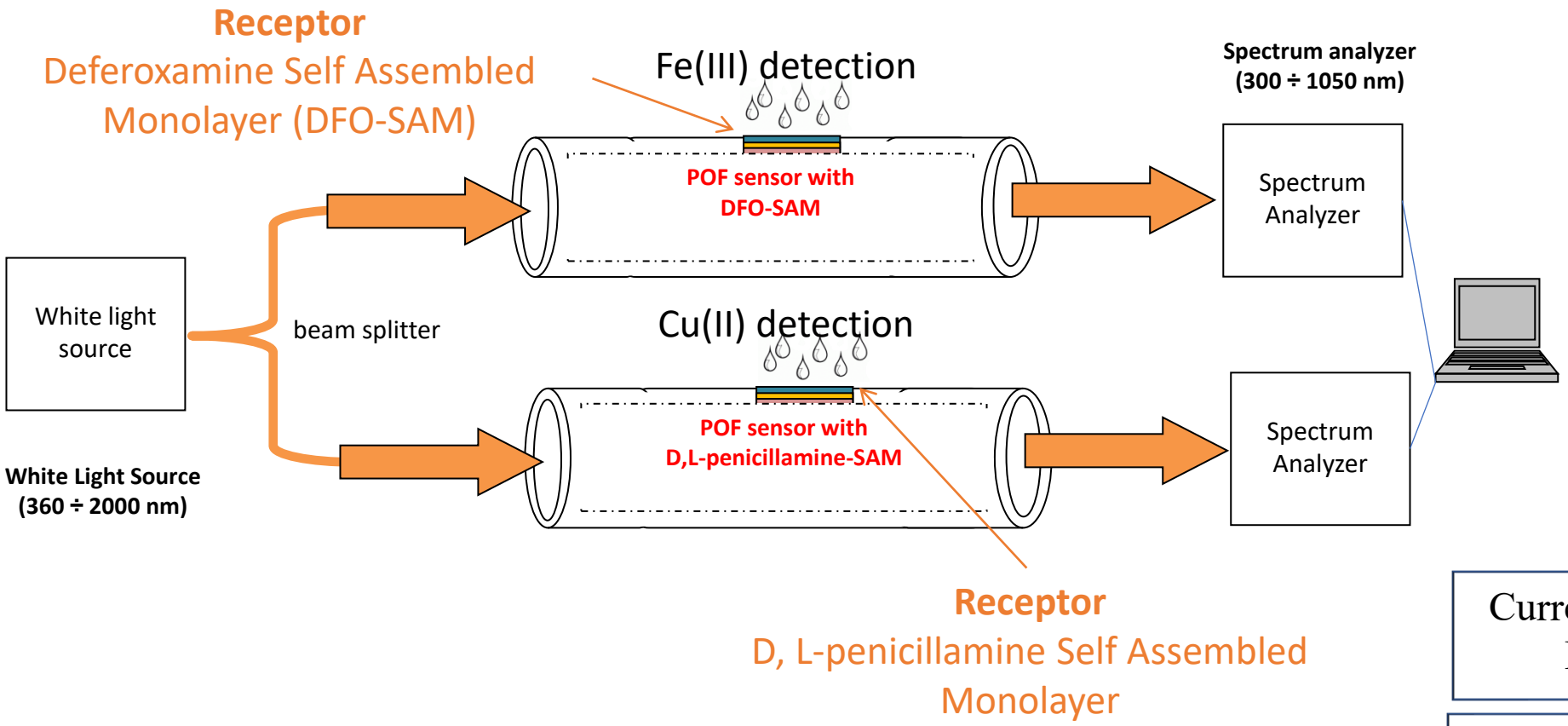

Measurements were carried out with an experimental setup arranged to measure the transmitted light spectra. It was characterized by a halogen lamp, a beam splitter, two optical chemical sensors and two spectrometers.

Current Research Partners

University of Pavia Italy

Experimental results D,L-PENICILLAMINE-SAM-POF

The detection limit, calculated as twice the standard deviation of the blank, is 1.39 x10^{-6}M

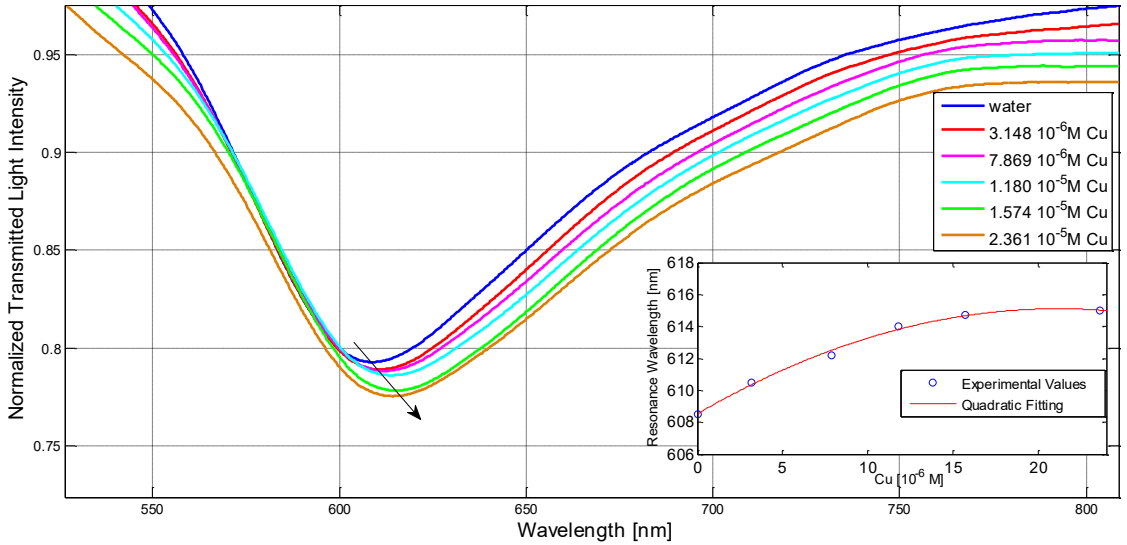

SPR transmission spectra, normalized to the air spectrum, for different analyte concentrations [Cu(II) 3.1x10^{-6} M ÷ 2.4x10^{-5} M].
Inset: Plasmon resonance wavelength as a function of analyte concentrations, with the corresponding fitting curve (red line).

SPR transmission spectra, normalized to the air spectrum, for different analytes: Ca and Fe. For comparison, the spectrum of pure water is reported.

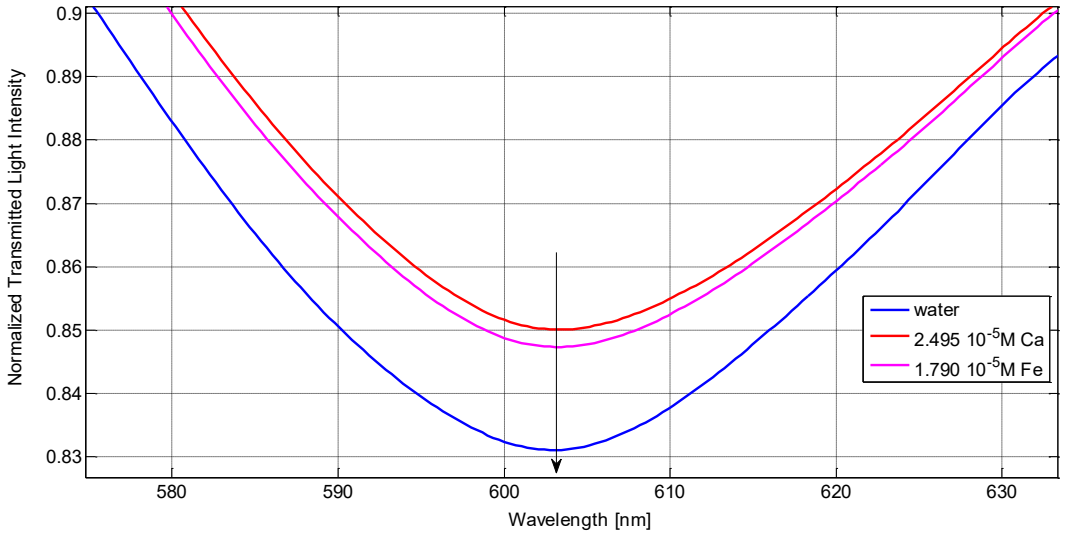

Selectivity analysis

Pesavento, M.; Profumo, A.; Merli, D.; Cucca, L.; Zeni, L.; Cennamo, N. An Optical Fiber Chemical Sensor for the Detection of Copper(II) in Drinking Water. Sensors **2019**, 19, 5246

Experimental results DFO-SAM-POF

Transmission spectra of DSO-SAM-POF sensor in 0.5% HNO_3 at increasing concentration of Fe(III). (**a**) measures with DFO-SAM modified gold layer (DFO-SAM sensor)

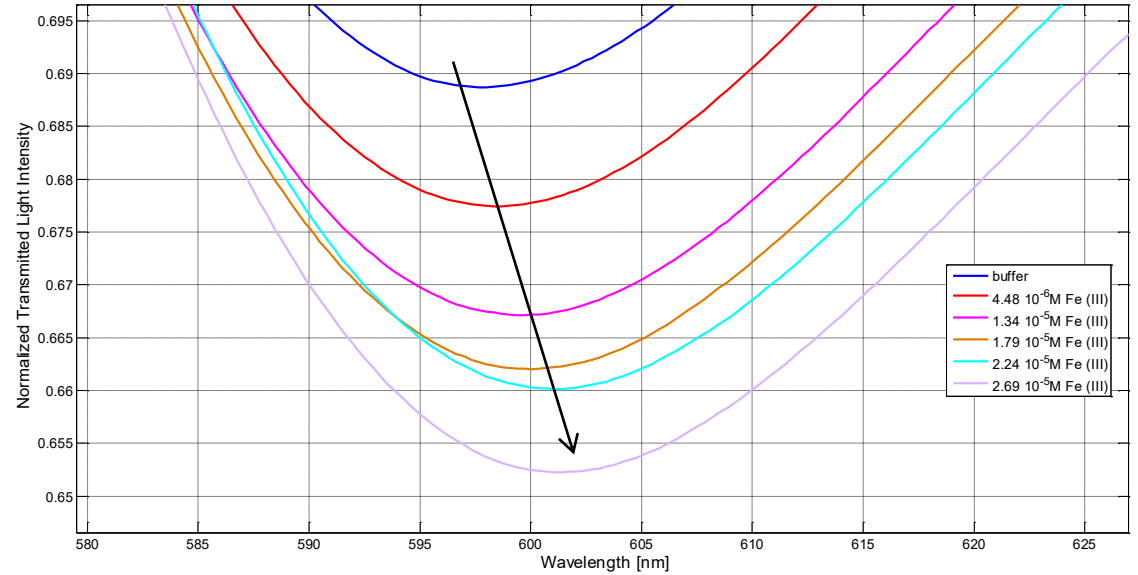

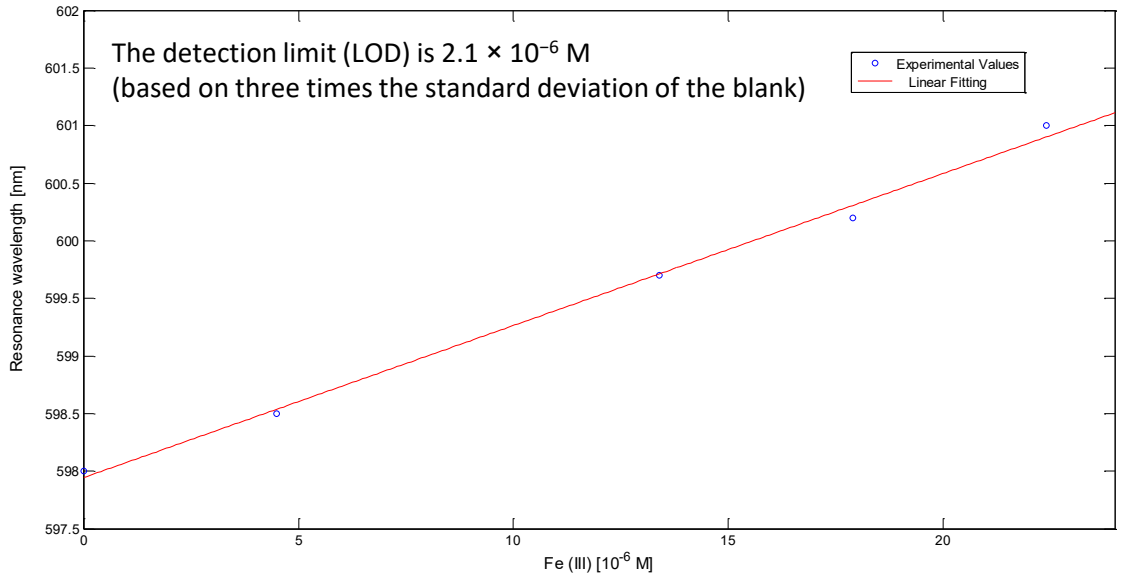

Plasmon resonance wavelength variation as a function of Fe (III) concentration in the range up to 2.24 10^{-5} M

Transmission spectra of bare sensor (without DFO-SAM) in 0.5% HNO_3 at increasing concentration of Fe(III). Inset: Zoom of the resonance wavelengths region.

Selectivity analysis

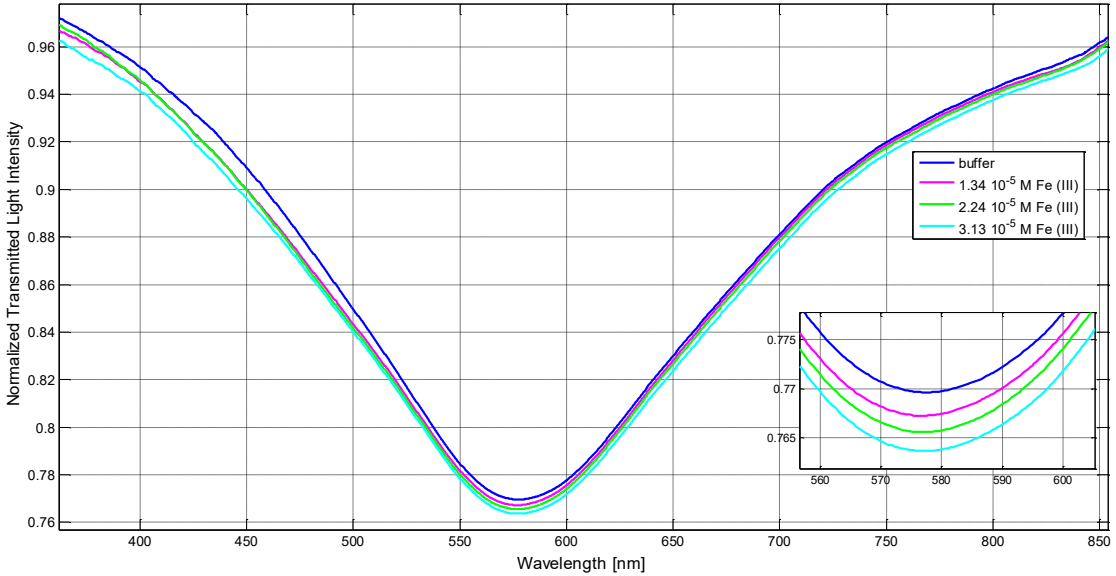

SPR transmission spectra obtained on DFO-SAM-POF sensor for two metal ions: Cu^{2+} and Ca^{2+}. For comparison, the spectrum of 0.5% HNO_3 ("buffer" solution) is reported. Inset: Zoom of the resonance wavelengths region.

Selectivity analysis

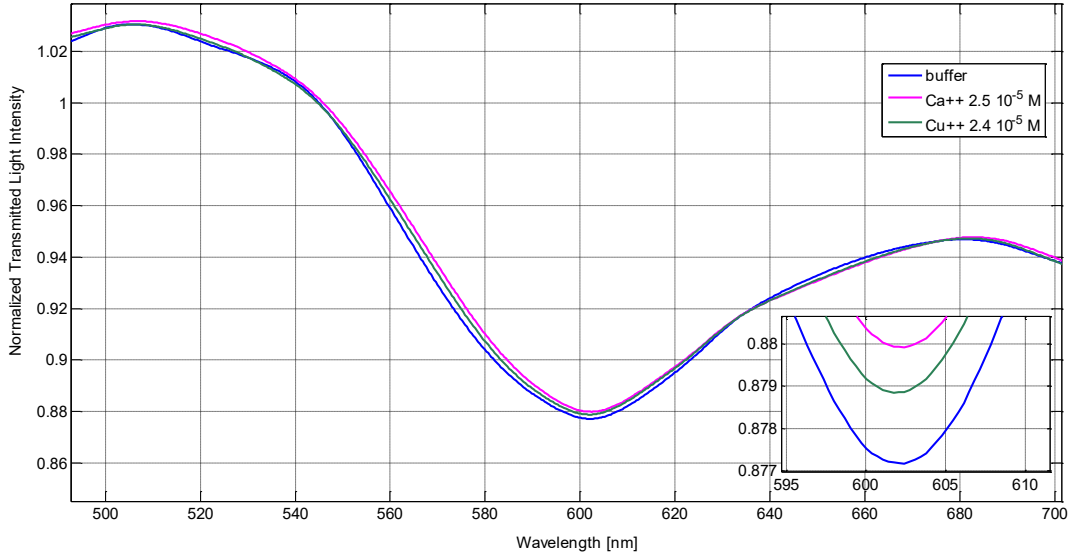

Nunzio Cennamo, et al., A simple small size and low cost sensor based on Surface Plasmon Resonance for selective detection of Fe(III), **Sensors,** 14**,** 4657-4671 (**2014**)

Environmental monitoring: detection of PFOA by MIP receptor

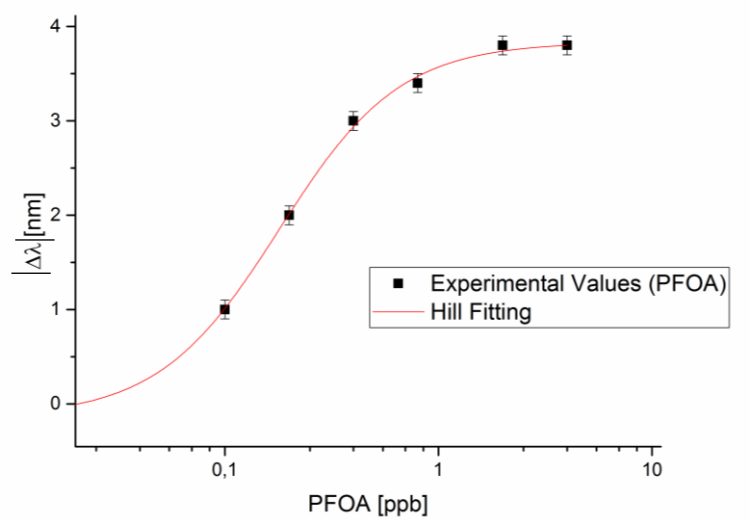

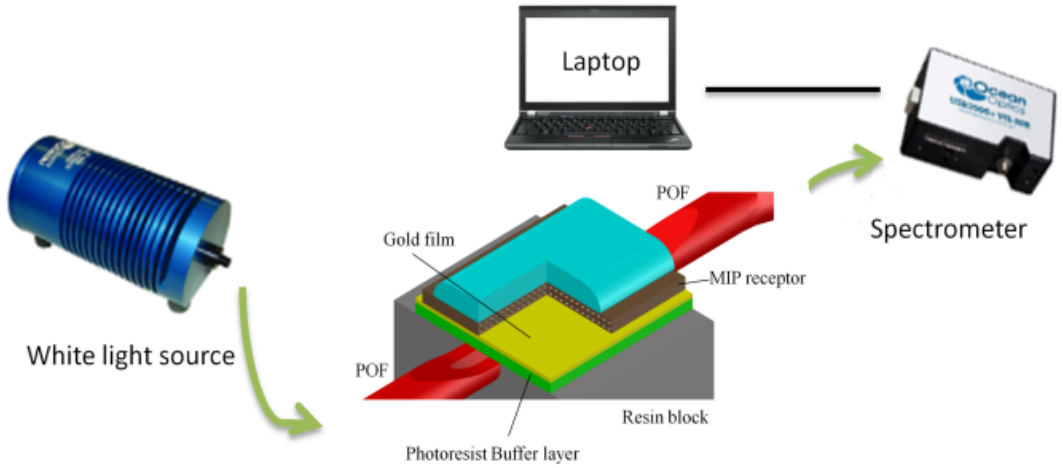

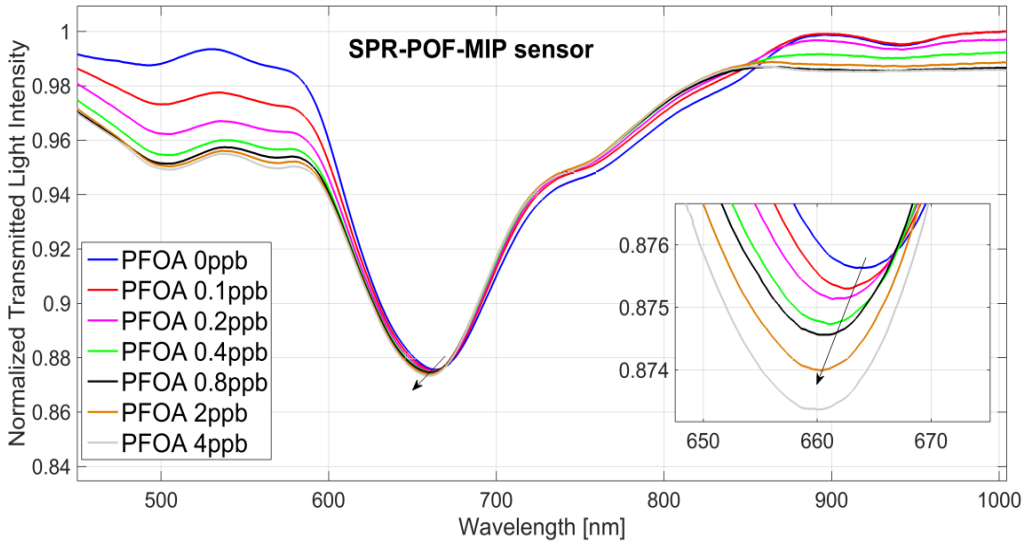

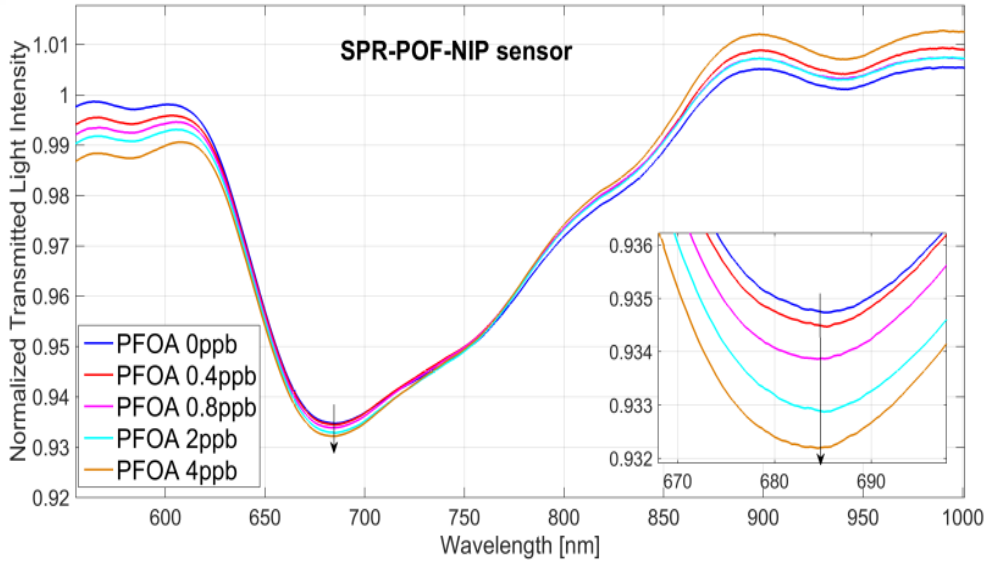

N. Cennamo, G. D'Agostino, G. Porto, A. Biasiolo, C. Perri, F. Arcadio, L. Zeni, A Molecularly Imprinted Polymer on a Plasmonic Plastic Optical Fiber to detect perfluorinated compounds in water, **Sensors, 18, 2018**

Environmental monitoring : detection of PFOA by Ab

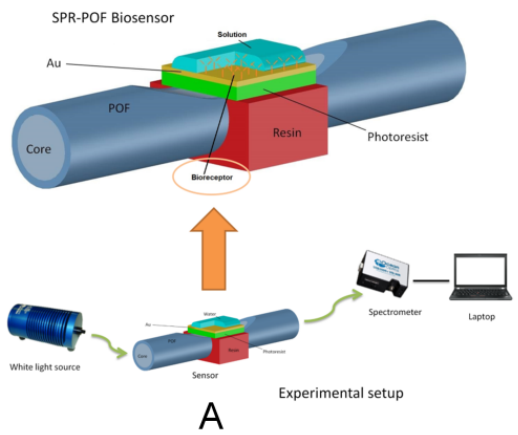

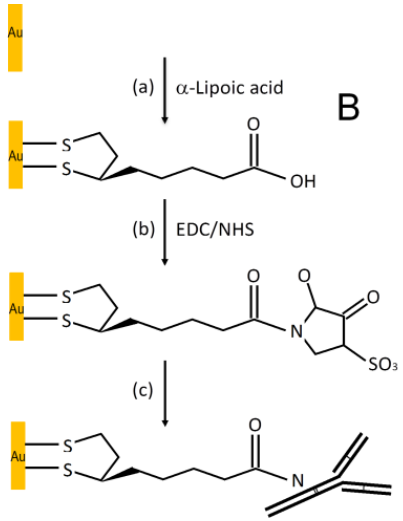

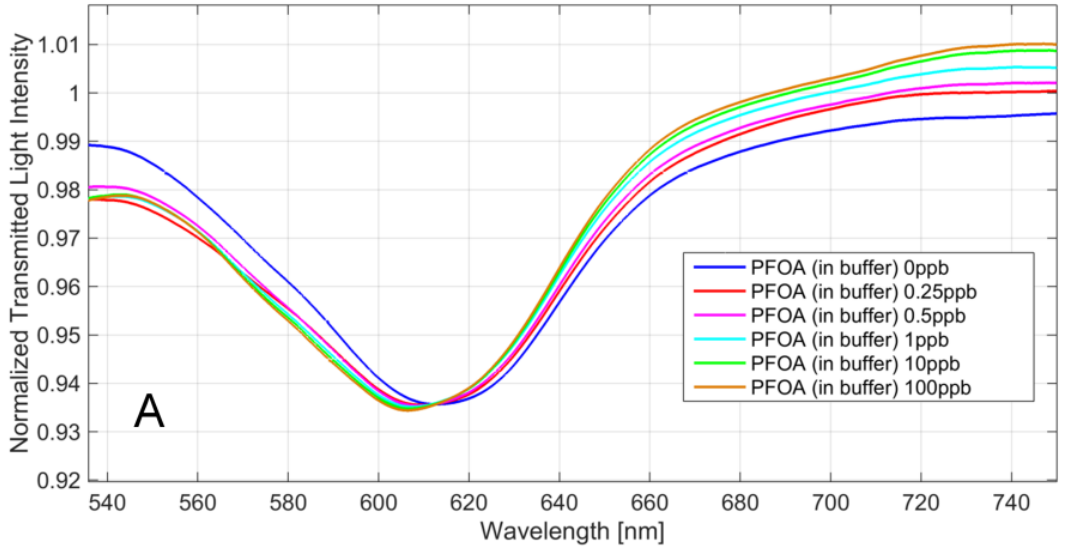

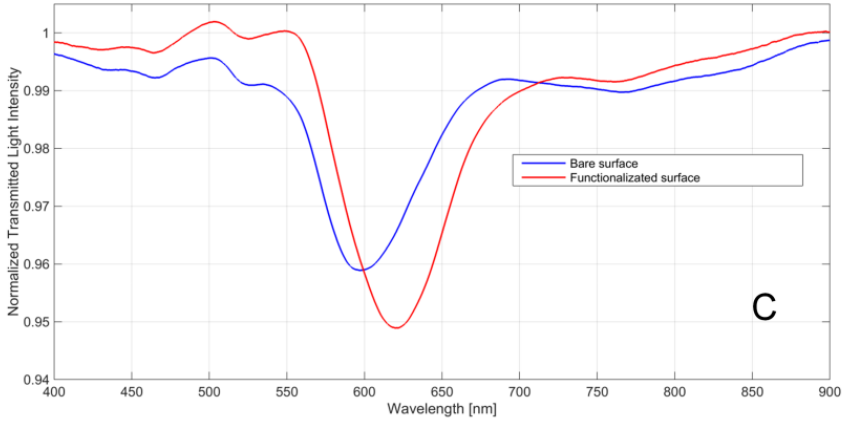

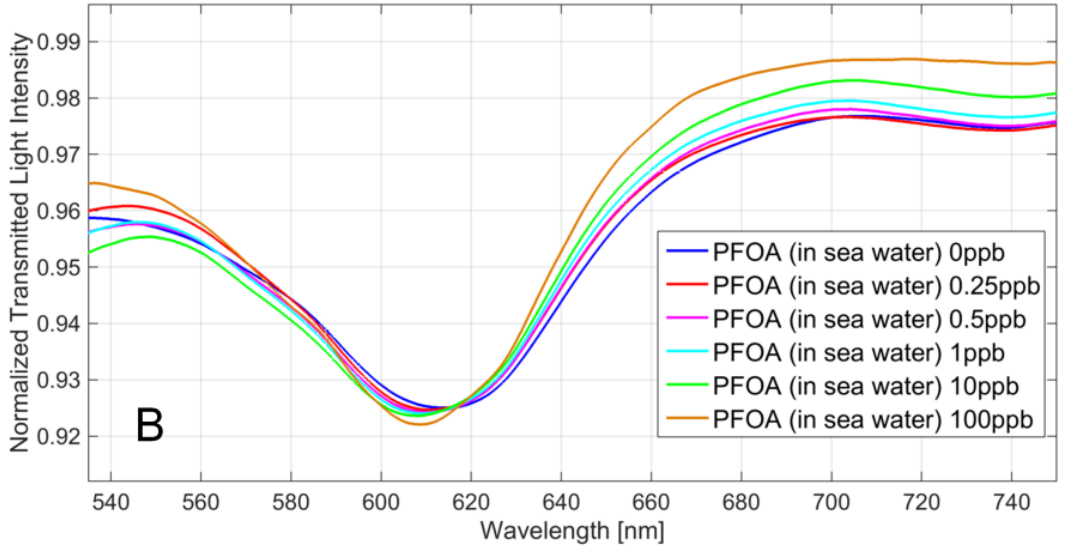

Current Research Partners

CNR-ISA
Avellino - Italy

N. Cennamo, L. Zeni, P.Tortora, M. E. Regonesi, A. Giusti, M. Staiano, S. D'Auria, A. Varriale, A High Sensitivity Biosensor to detect the presence of perfluorinated compounds in environment, **Talanta** 178 (**2018**) 955–961

Environmental monitoring : detection of PFOA by Ab

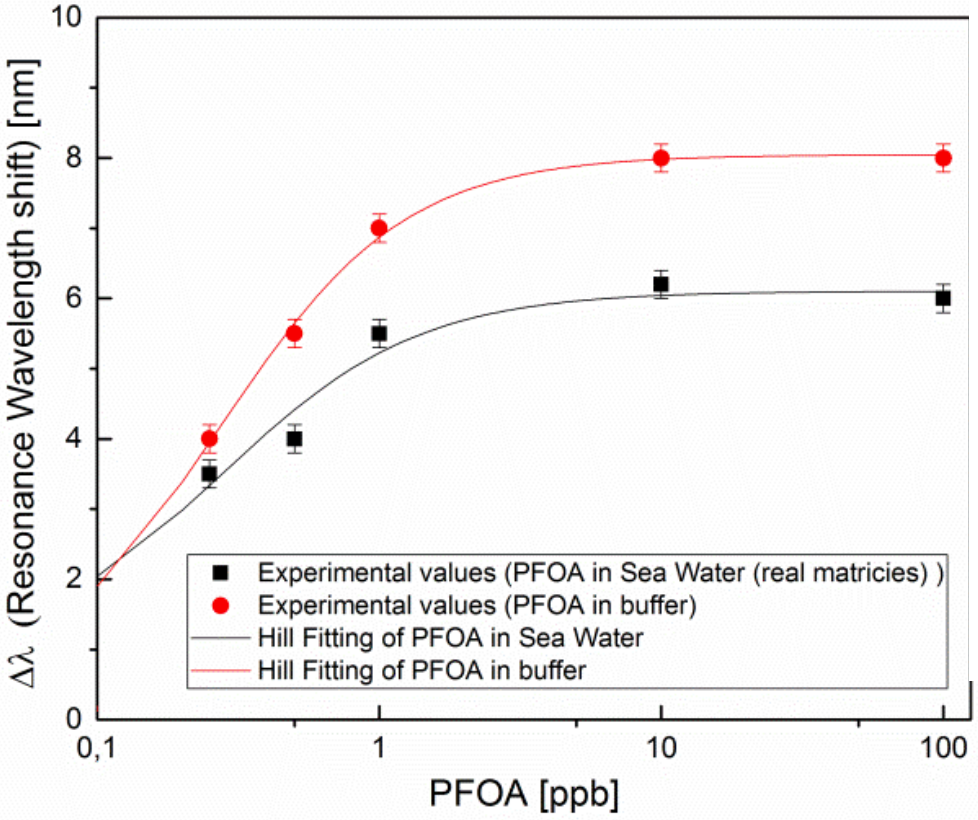

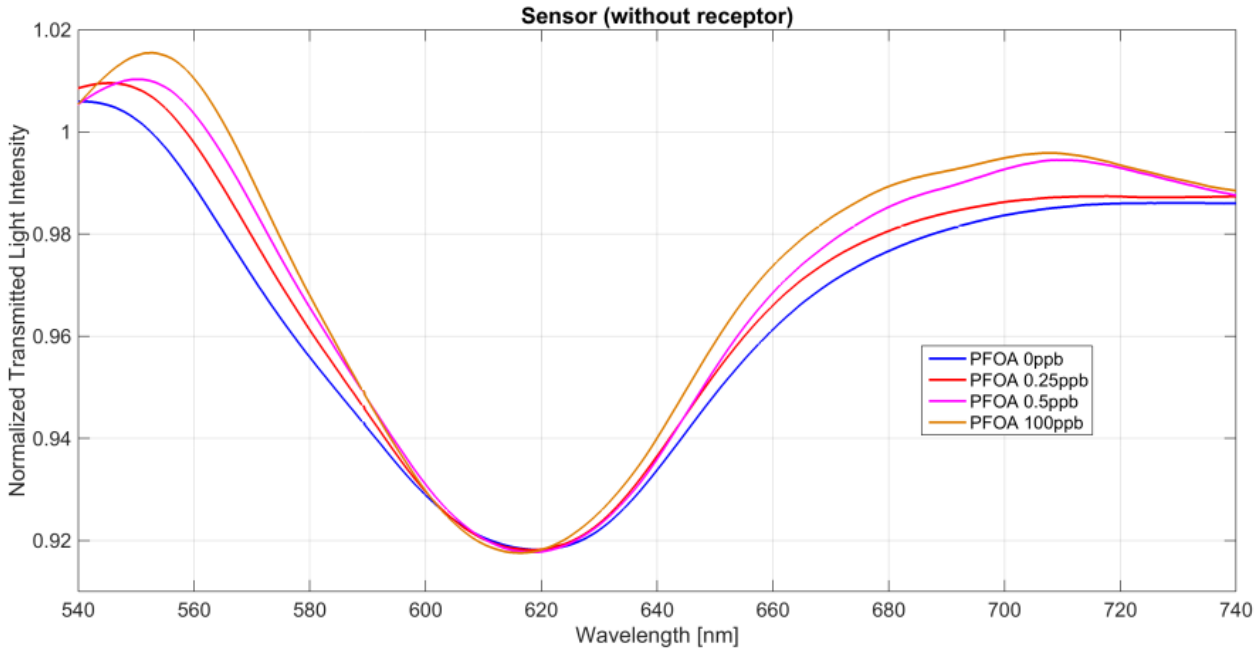

Selectivity analysis

Current Research Partners

CNR-ISA
Avellino - Italy

N. Cennamo, L. Zeni, P.Tortora, M. E. Regonesi, A. Giusti, M. Staiano, S. D'Auria, A. Varriale, A High Sensitivity Biosensor to detect the presence of perfluorinated compounds in environment, **Talanta** 178 (**2018**) 955–961

Detection of PFOA in water solution

Table. PFOA detection in water by an SPR-POF-MIP sensor and by an SPR-POF with a bio-receptor

Receptor	Parameters	Value
MIP Receptor [1]	Sensitivity at low c of PFOA [nm/ppb]	22.14
	LOD [ppb] (3 × standard deviation of blank/ sensitivity at low c of PFOA)	0.13
Antibody [2]	Sensitivity at low c of PFOA [nm/ppb]	29.82
	LOD [ppb] (3 × standard deviation of blank/sensitivity at low c of PFOA)	0.24

[1] N. Cennamo, G. D'Agostino, G. Porto, A. Biasiolo, C. Perri, F. Arcadio, L. Zeni, A Molecularly Imprinted Polymer on a Plasmonic Plastic Optical Fiber to detect perfluorinated compounds in water, **Sensors, 18, 2018**

[2] N. Cennamo, L. Zeni, P.Tortora, M. E. Regonesi, A. Giusti, M. Staiano, S. D'Auria, A. Varriale, A High Sensitivity Biosensor to detect the presence of perfluorinated compounds in environment, **Talanta** 178, 955–961, **2018**

SARS-CoV-2 sensor (MIP-based)

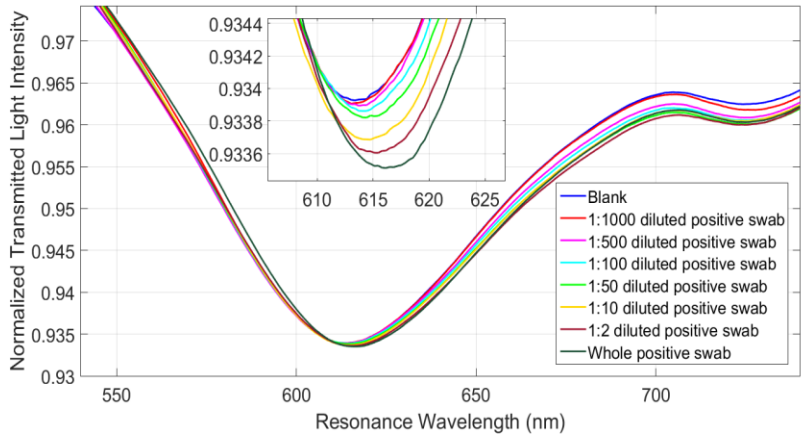

Response curves of **SARS-CoV-2 Positive swab (36th RT-PCR cycle) in physiological medium**, at different dilutions, tested with SARS-CoV-2 MIP-sensor. The samples were diluted with physiological solution.

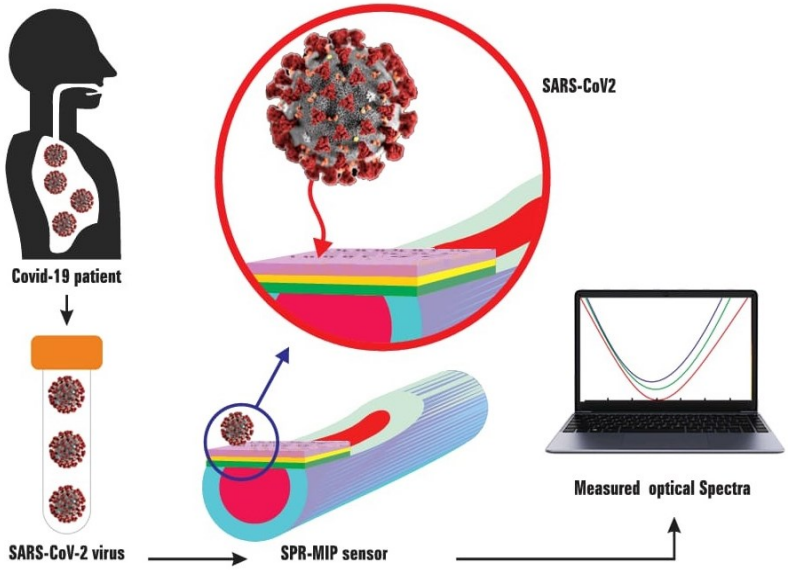

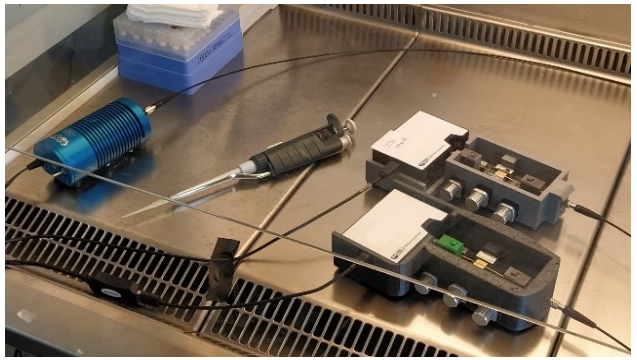

Cennamo, N.; D'Agostino, G.; Perri, C.; Arcadio, F.; Chiaretti, G.; Parisio, E.M.; Camarlinghi, G.; Vettori, C.; Di Marzo, F.; Cennamo, R.; Porto, G.; Zeni, L. *Proof of Concept for a Quick and Highly Sensitive On-Site Detection of SARS-CoV-2 by Plasmonic Optical Fibers and Molecularly Imprinted Polymers*. ***Sensors* 2021**, *21*, 1681

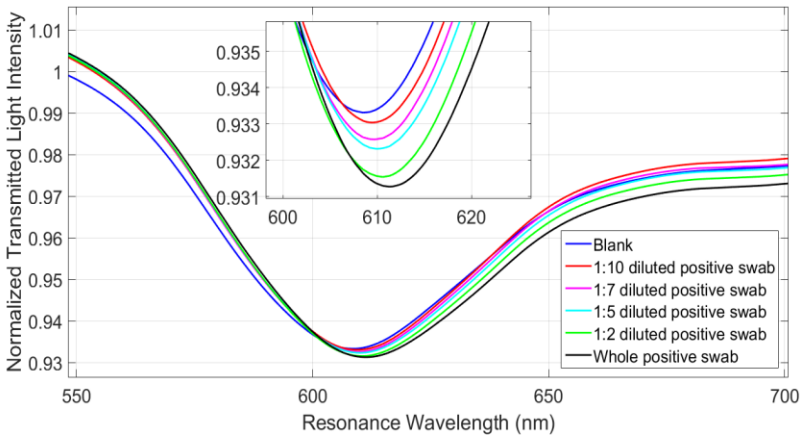

Response curves of **SARS-CoV-2 Positive UTM swab (36th RT-PCR cycle), at different dilutions**, tested with SARS-CoV-2 MIP-sensor. The samples were diluted with physiological solution.

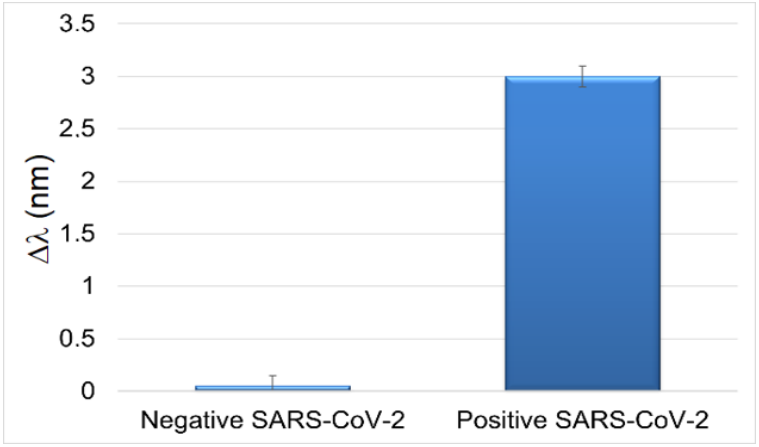

Comparison of the response obtained by the MIP-SPR sensor with a negative SARS-CoV-2 swab (Physiological medium) and a positive SARS-CoV-2 swab (Physiological medium) (confirmed by RT-PCR).

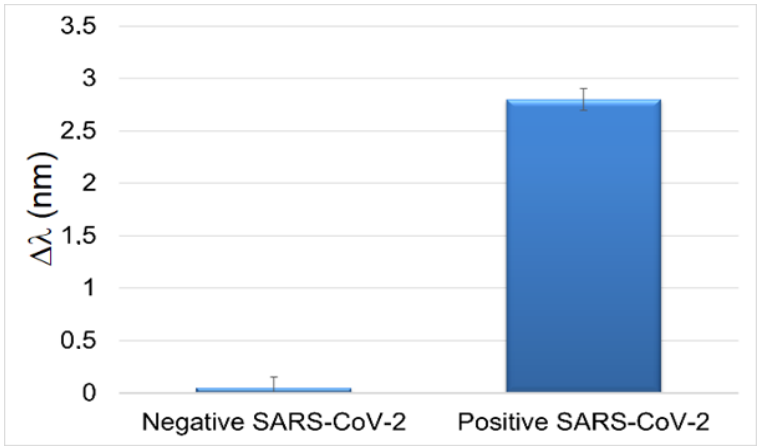

Comparison of the response obtained by the MIP-SPR sensor with a negative SARS-CoV-2 swab in UTM (universal transport medium) and a positive SARS-CoV-2 swab in UTM (confirmed by RT-PCR).

SARS-CoV-2 Aptasensor

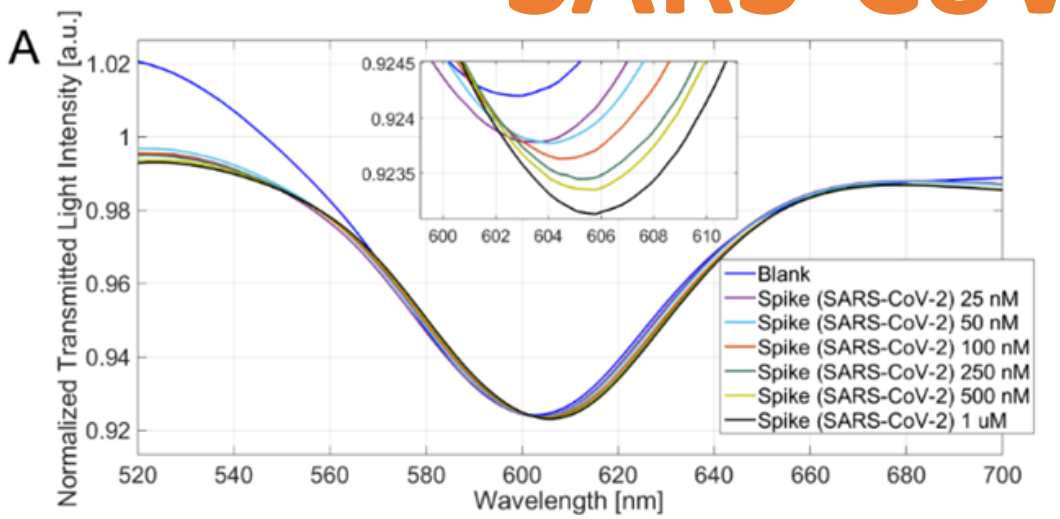

Current Research Partners

indivenire

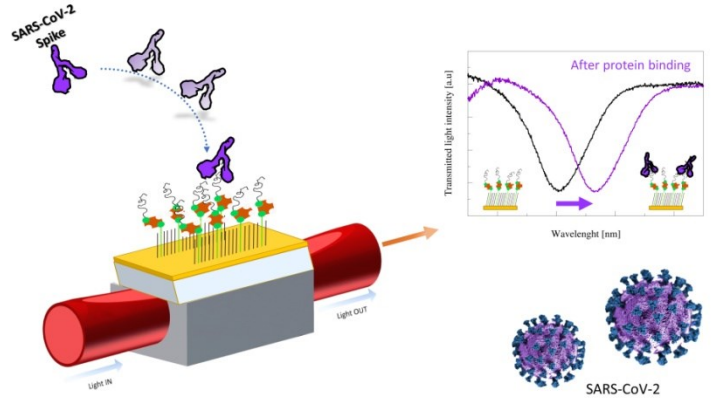

(A) Transmission spectra for different SARS-CoV-2 spike protein concentrations (25 ÷ 1000 nM) with a zoom of the resonance wavelengths region (inset).

(B) Resonance shift (Δλ) versus the spike protein concentrations (nM), measured on at least three sensors for each value. Data are reported as mean value with standard deviation. Langmuir and linear fitting are also reported.

(C) Resonance wavelength variation (Δλ), with respect to the blank, obtained incubating 250 nM of different proteins (BSA, AH1H1 hemagglutinin protein, MERS spike protein and SARS spike protein) on apt-1C- modified platform

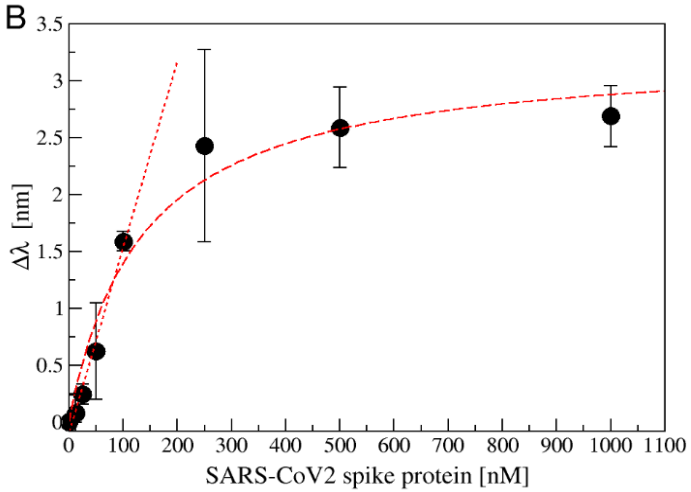

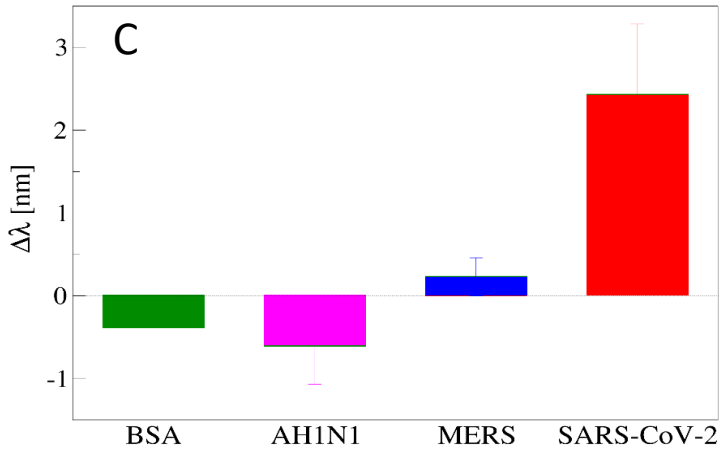

N. Cennamo, L. Pasquardini, F. Arcadio, L. Lunelli, L. Vanzetti, V. Carafa, L. Altucci, L. Zeni, *SARS-CoV-2 spike protein detection through a plasmonic D-shaped plastic optical fiber aptasensor*, **Talanta 2021**, 122532

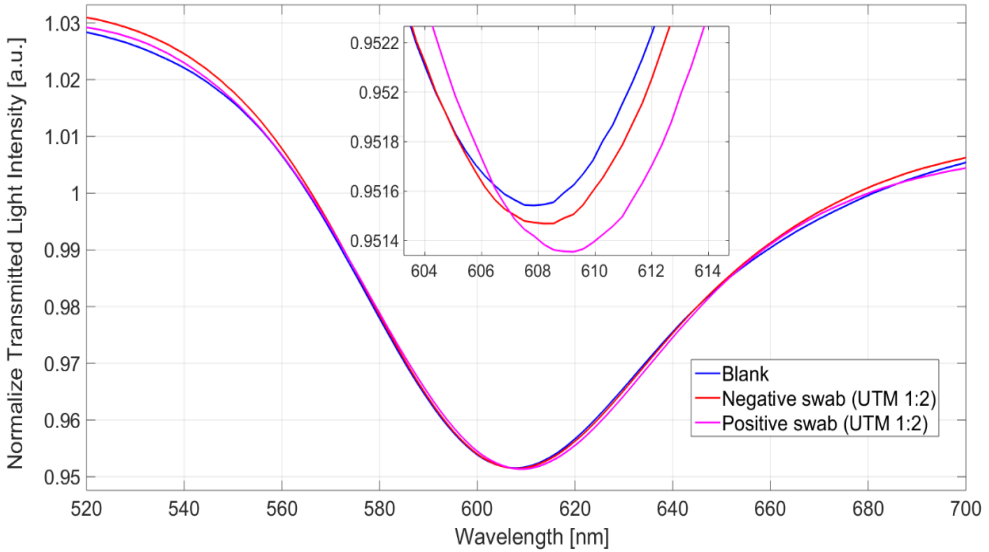

Comparison of the response obtained by the SPR Aptasensor with a negative SARS-CoV-2 swab in UTM (universal transport medium) and a positive SARS-CoV-2 swab in UTM (confirmed by RT-PCR), both diluted 1:2.

An SPR-Slab-POF Sensor (extrinsic POF sensor)

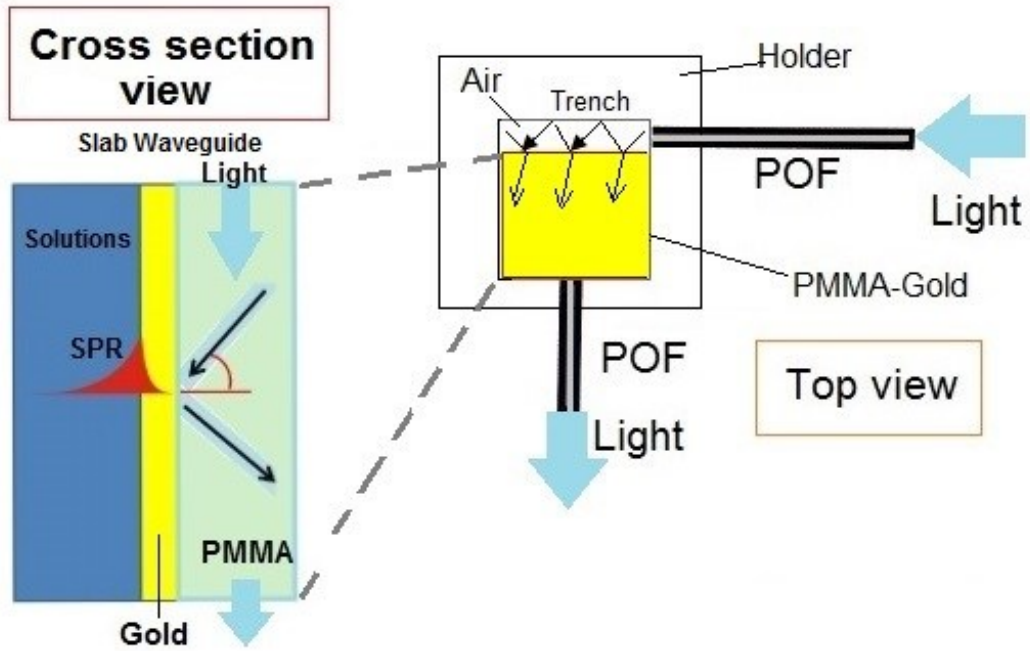

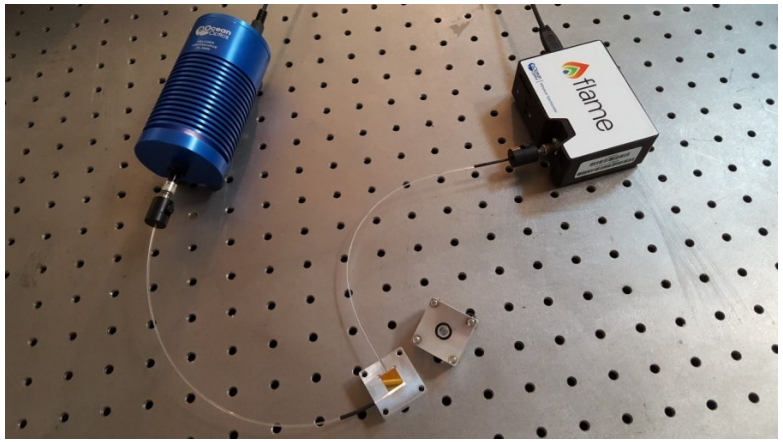

The **optical fiber sensors** can be classified as **intrinsic and extrinsic**, depending on whether the fiber is interacting with the analysed medium or it is used only as a waveguide that allows the propagation of the light to the sensing region and its collection, respectively.

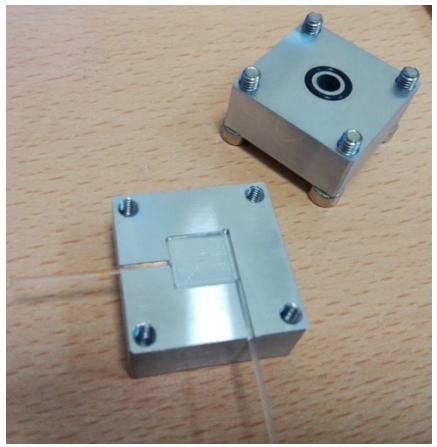

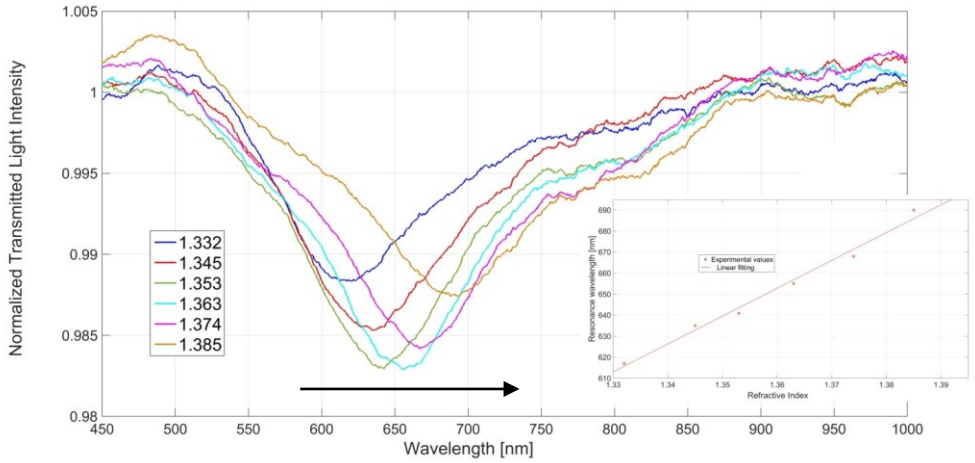

N. Cennamo, F. Mattiello, L. Zeni, Slab Waveguide and Optical Fibers for Novel Plasmonic Sensor Configurations, **Sensors**, vol. 17, pp. 1488, **2017**

Food application: SPR-Slab-POF Sensor with an MIP for 2-FAL detection in water

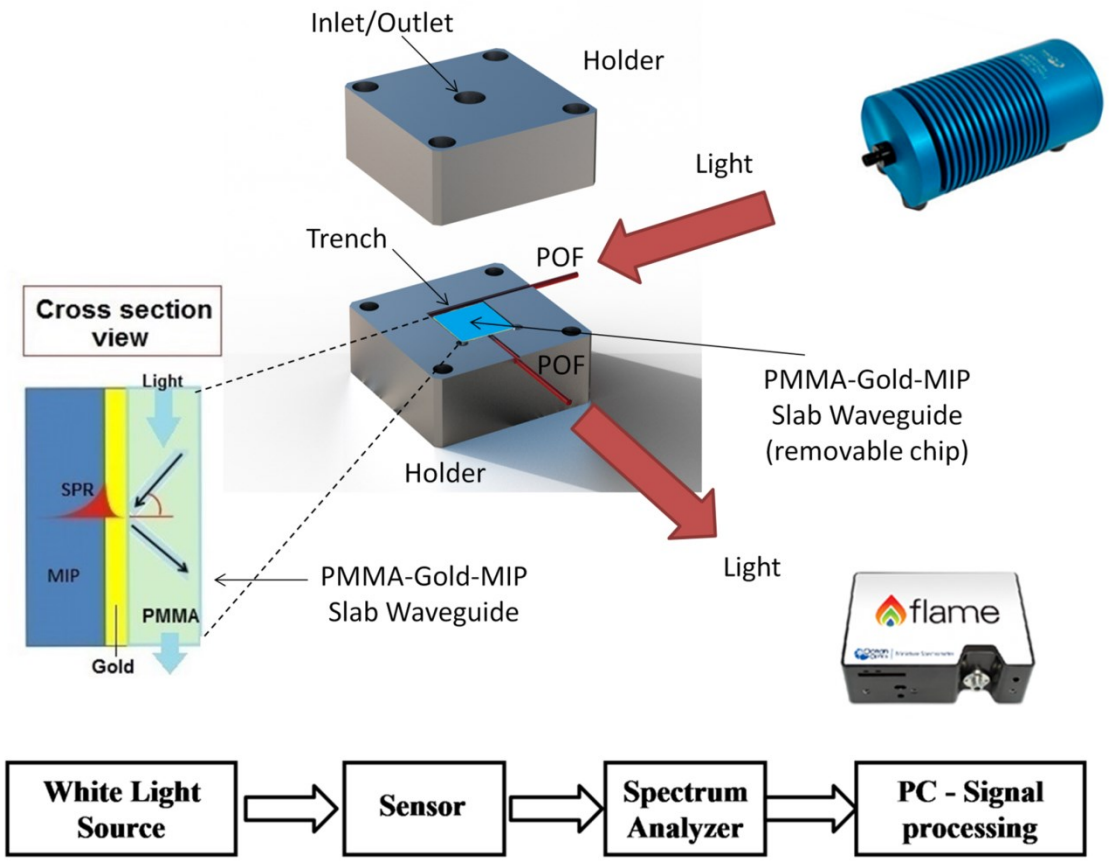

Current Research Partners

University of Pavia Italy

In the future, we will test this new SPR sensor system for specific applications in *real matrices*, as for example, **the determination of 2-FAL in beverages as wine and beer,** which can have a high practical interest on one hand for its toxic and carcinogenic effects on human beings and, on the other hand, for its impact on the aroma.

SPR-Slab-POF Sensor with MIP for 2-FAL detection in water

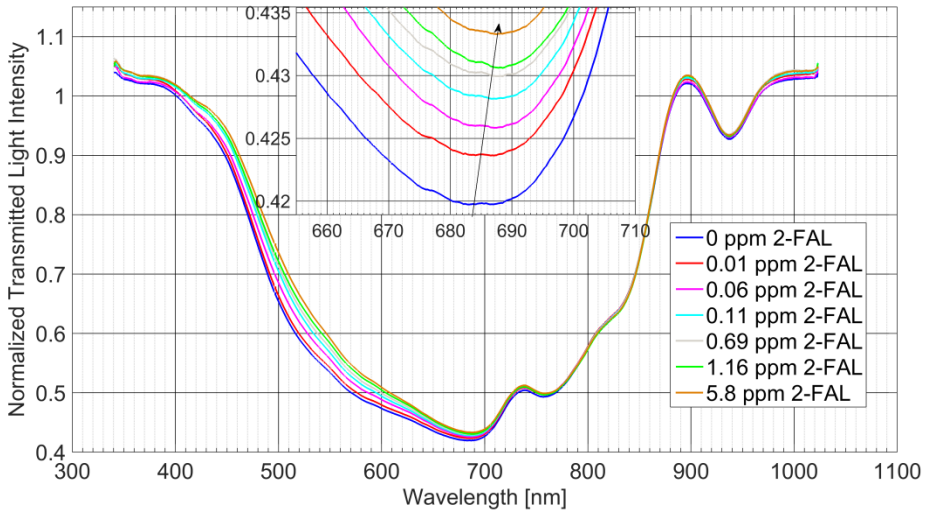

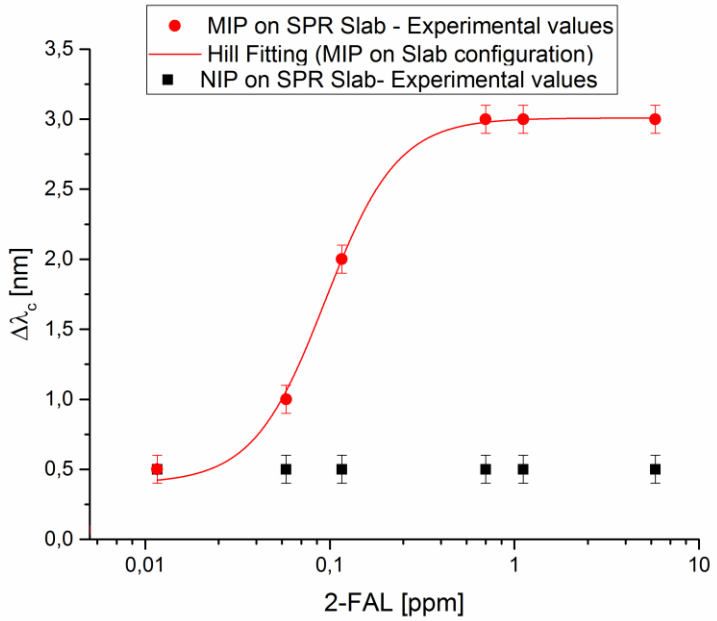

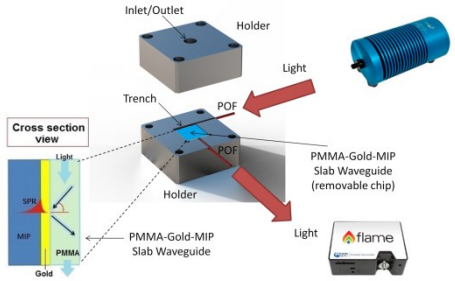

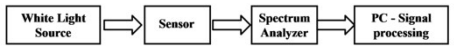

START ($\Delta\lambda_0$)		END ($\Delta\lambda_{max}$)		K		n		Statistics	
Value	Standard Error	Value	Standard Error	Value	Standard Error	Value	Standard Error	Reduced Chi-Sqr	Adj. R-Square
0.398	0.266	3.008	0.145	0.094	0.017	2.22	1.01	1.40	0.96

Table. Hill parameters of 2-FAL detection in water by SPR-Slab-MIP sensor

SPR-POF Sensor with MIP for 2-FAL detection in water

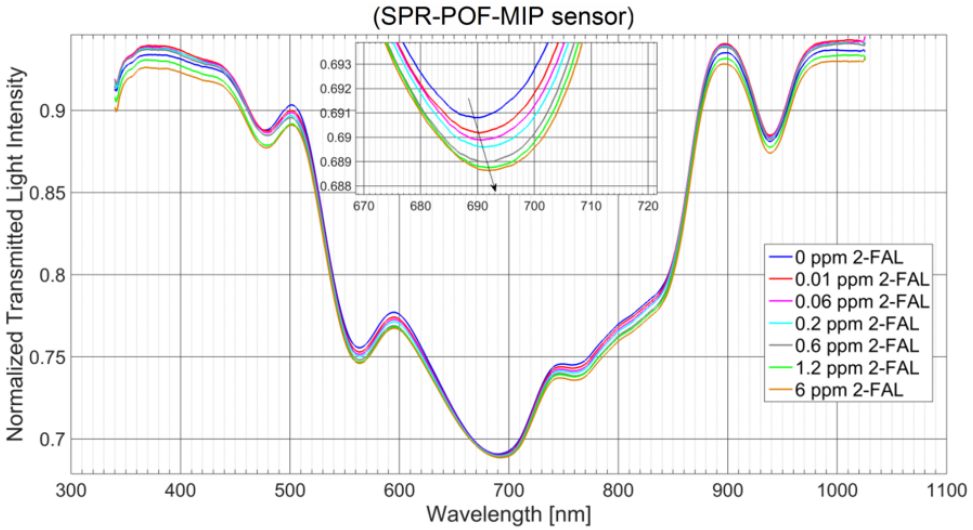

(a)

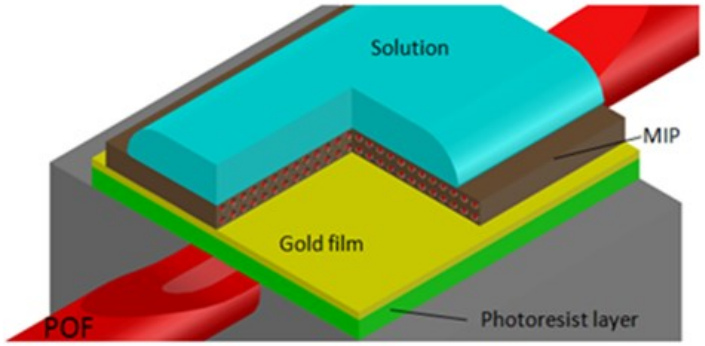

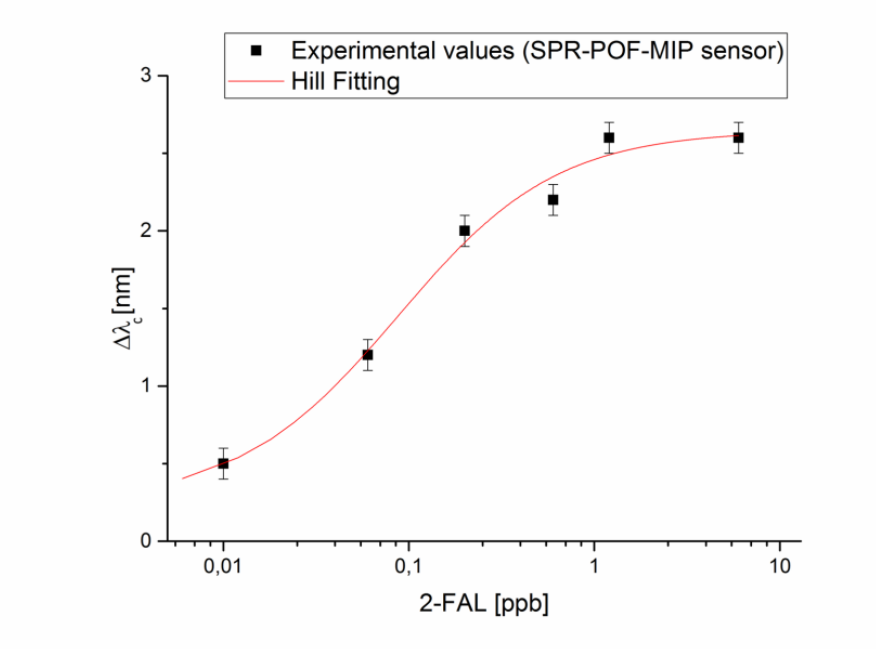

(b)

START ($\Delta\lambda_0$)		END ($\Delta\lambda_{max}$)		K		n		Statistics	
Value	Standard Error	Value	Standard Error	Value	Standard Error	Value	Standard Error	Reduced Chi-Sqr	Adj. R-Square
0.253	0.476	2.647	0.219	0.087	0.045	1.011	0.503	3.500	0.968

Table. Hill parameters of 2-FAL detection in water by SPR-POF-MIP sensor

L. Zeni, M. Pesavento, S. Marchetti, N. Cennamo, "Slab plasmonic platforms combined with Plastic Optical Fibers and Molecularly Imprinted Polymers for chemical sensing," **Optics and Laser Technology**, **2018**, doi.org/10.1016/j.optlastec.2018.06.028

SPR Sensors with MIP for 2-FAL detection in water

Sensor	Detection of 2-FAL in water solutions	
	Parameters	***Value***
SPR-slab-MIP	K_{aff} [ppm^{-1}]	10.59
	Sensitivity at low *c* [nm/ppm]	27.66
	LOD [ppm] (3*standard deviation of blank/ sensitivity at low *c*)	0.029
Sensor	**Detection of 2-FAL in water solutions**	
	Parameters	***Value***
SPR-POF-MIP	K_{aff} [ppm^{-1}]	11.49
	Sensitivity at low *c* [nm/ppm]	27.49
	LOD [ppm] (3*standard deviation of blank/ sensitivity at low *c*)	0.052

L. Zeni, M. Pesavento, S. Marchetti, N. Cennamo, "Slab plasmonic platforms combined with Plastic Optical Fibers and Molecularly Imprinted Polymers for chemical sensing," **Optics and Laser Technology**, **2018**, doi.org/10.1016/j.optlastec.2018.06.028

A simple chemical optical sensor based on MIP, optical fibers and InkJet printing technology (extrinsic POF sensor)

Top section view

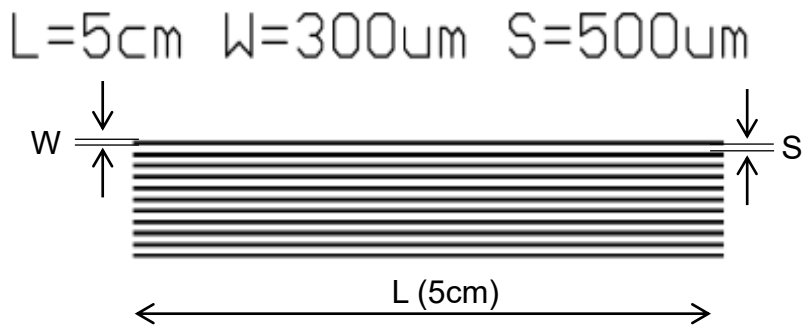

The printing process adopted to make the parallel lines on a PET (polyethylene terephthalate) substrate uses a low-cost WF-2010 piezo inkjet printer (Epson, Suwa, Japan) and a metal ink for the creation of conductive patterns.

The metal ink is the **silver nanoparticles** solution "Metalon® JS-B15P" by Novacentrix (Austin, TX, USA).

The adopted PET substrate is the Novele™ IJ-220 Printed Electronics Substrate by Novacentrix, suited to low-cost and low-temperature applications and specially designed for inkjet-compatible conductive inks.

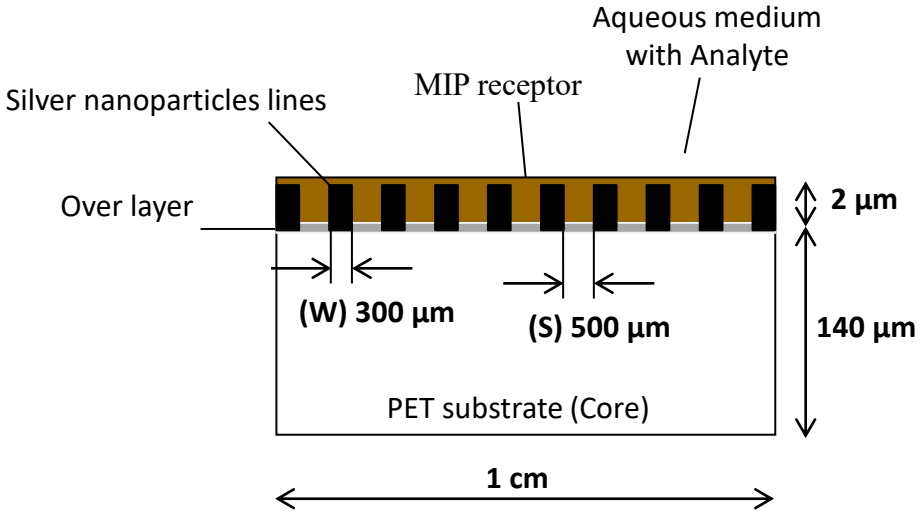

Cross section view

The MIP prepolymeric mixture (200µL) is dropped on the pattern of silver nanoparticles and spun for 2 min at 1000 rpm.
Thermal polymerization was then carried out for 16 h at 80 ° C.
The model was extracted by repeated washings with 96% ethanol.

Experimental Setup (extrinsic POF sensor)

MIP for 2-FAL detection in water

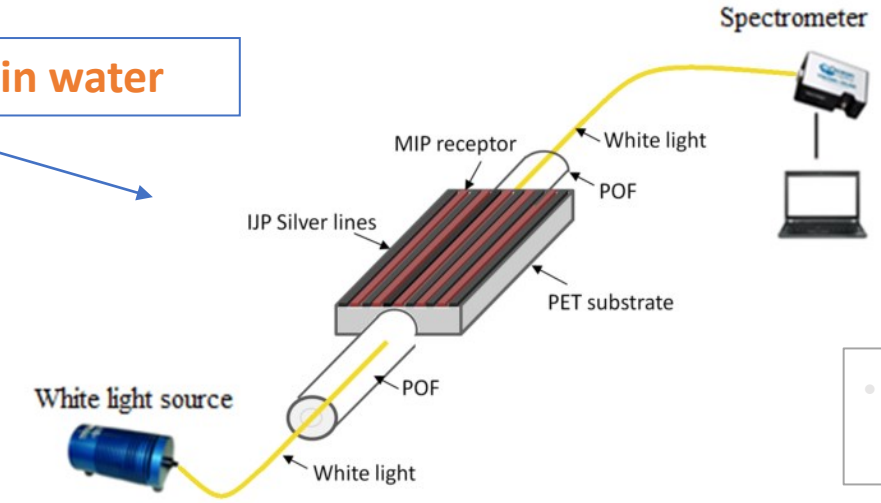

(360 ÷ 2000 nm)

(200 ÷ 850 nm or 300 ÷ 1050 nm)

- The proposed sensing device is low-cost and relatively easy to realize.

Two POFs (core of PMMA and cladding of fluorinated polymer, with 500µm of total diameter) connect the optical waveguide (PET layer covered with silver lines and MIP for 2-FAL) with a light source and with a spectrometer.

Experimental Procedure:

A small quantity of solution, about 200 µL, was dropped over the MIP layer (chemical receptor) and the spectrum checked in after only ten-minute incubation.

The transmission curves and the data values were displayed online on the computer screen and saved by an advanced software provided by Ocean Optics.

Each experimental value is the average of 5 subsequent measurements. The signal processing has been performed by Matlab and OriginPro 8.5 software

Experimental Results

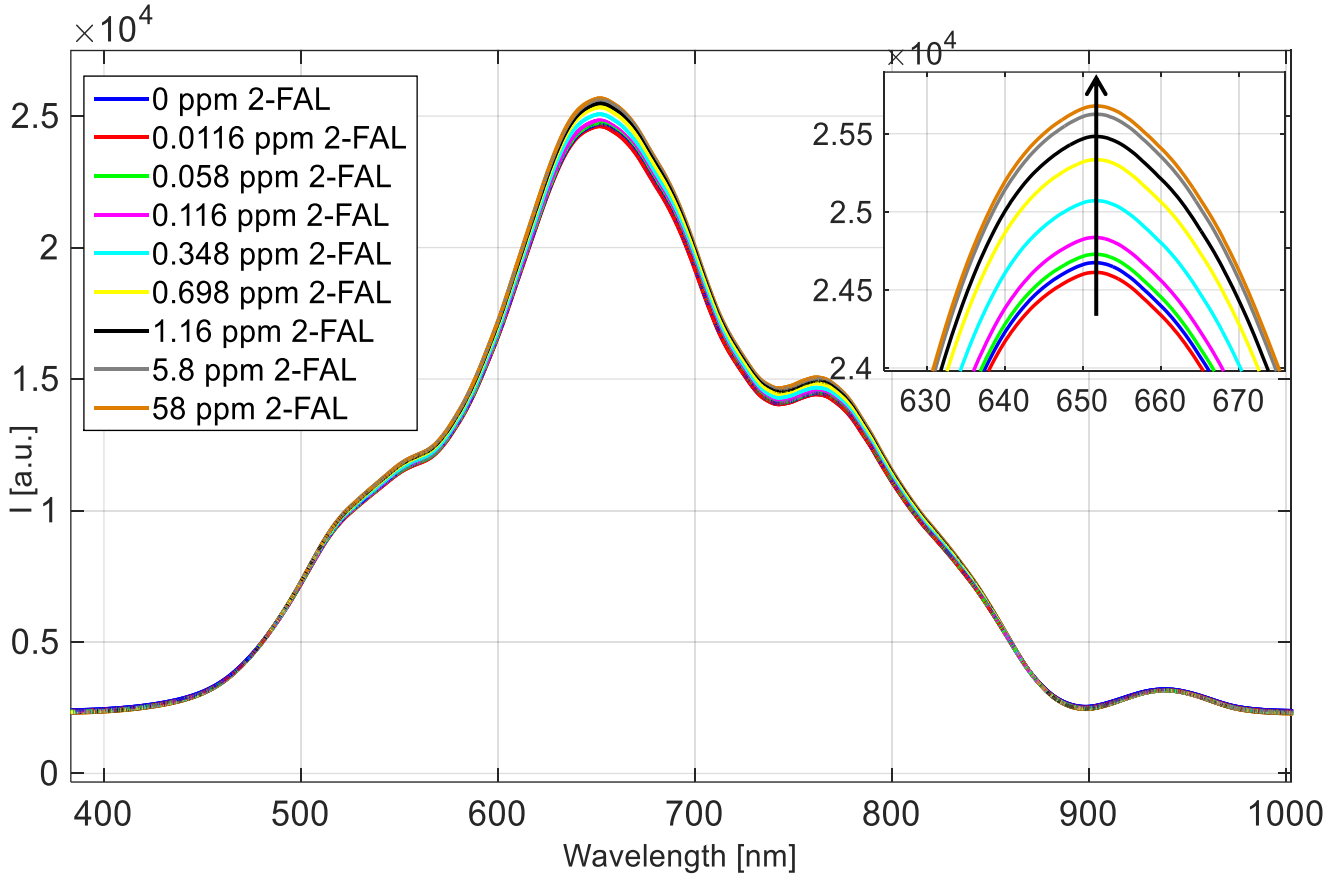

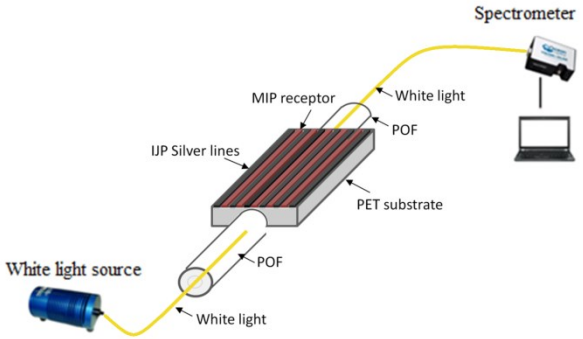

Current Research Partners

University of Catania - Italy

University of Pavia Italy

Transmission spectra obtained by the PET-Lines-MIP sensor for different furfural concentrations (in ppm) in water. Inset: zoom of the wavelengths around 650 nm.

N. Cennamo, L. Zeni, M. Pesavento, S. Marchetti, V. Marletta, S. Baglio, S. Graziani, A. Pistorio, B. Andò, A Novel Sensing Methodology to Detect Furfural in Water, Exploiting MIPs, and Inkjet-Printed Optical Waveguides**, IEEE Transactions on Instrumentation and Measurement** 68 (2019) 1582-1589

Data Analysis (Dose-Response curve at 652nm)

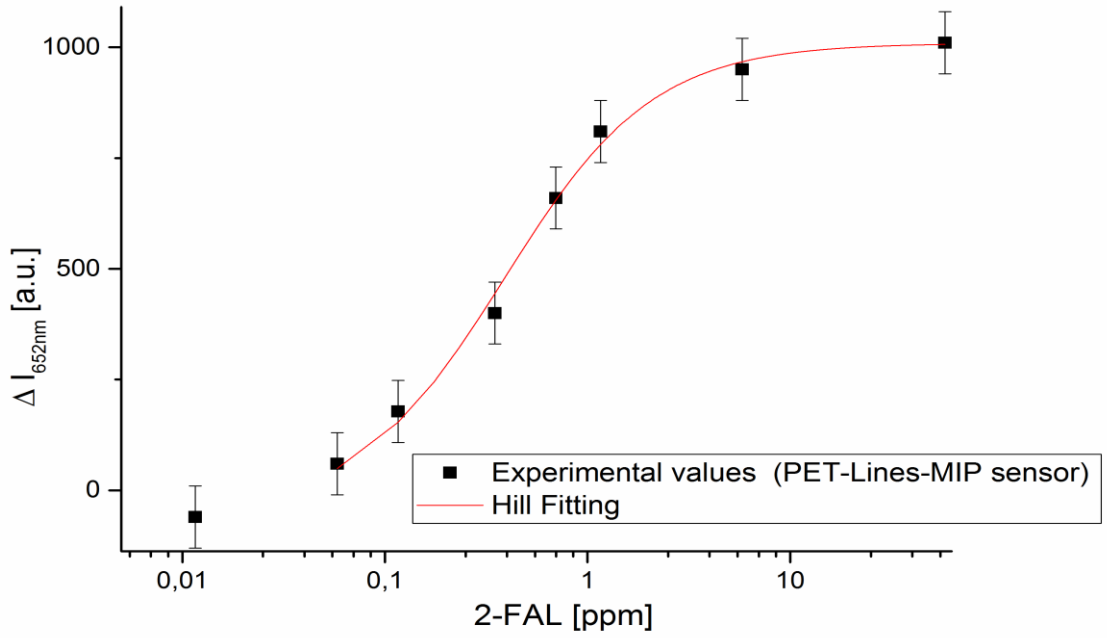

PET-Lines-MIP sensor	
Parameter	***Value***
K_{aff} [ppm^{-1}] (1/K)	2.58
Sensitivity at low *c* ($\Delta I_{max}/K$) [a.u./ppm]	2739.12
LOD [ppm] (2*standard deviation of blank (ΔI_0) / Sensitivity at low *c*)	0.031

Where: $\Delta I_{max} = I_{max} - I_0$

ΔI_0		ΔI_{max}		K		n		Statistics
Value	Std Error	Value	Std Error	Value	Std Error	Value	Std Error	Adj. R-Square
-52	42.40	1009.30	32.30	0.39	0.05	1.10	0.16	0.99

The LOD is the same of those obtained by other SPR-POF sensors.

From the table with Hill parameters, the affinity constant (K_{aff}), the sensitivity at low concentration and the limit of detection (LOD) of 2-FAL in water can be calculated.

Biochemical sensing exploiting plasmonic sensors based on gold nano-gratings and polymer optical fibers

(extrinsic POF sensor)

Sensor Chip

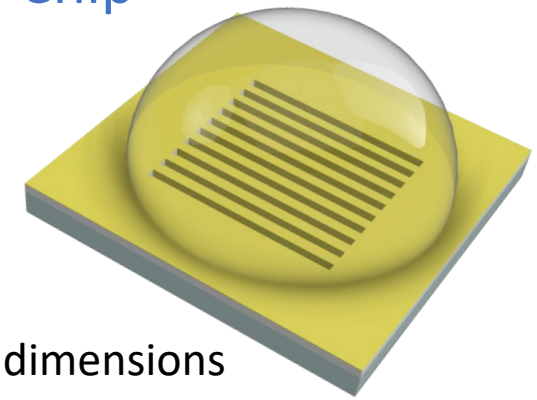

PMMA chip dimensions
10 mm x 10 mm x 0.5 mm

Setup 1

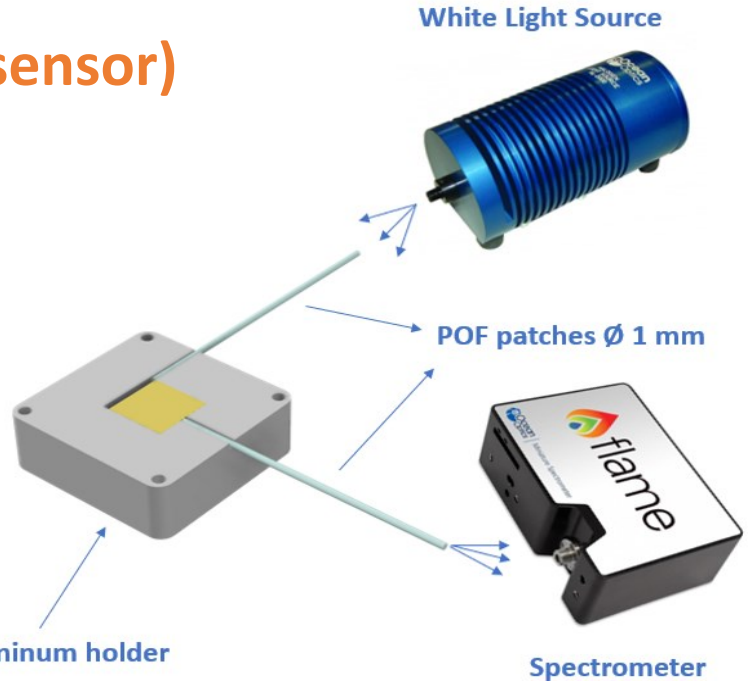

Setup 2

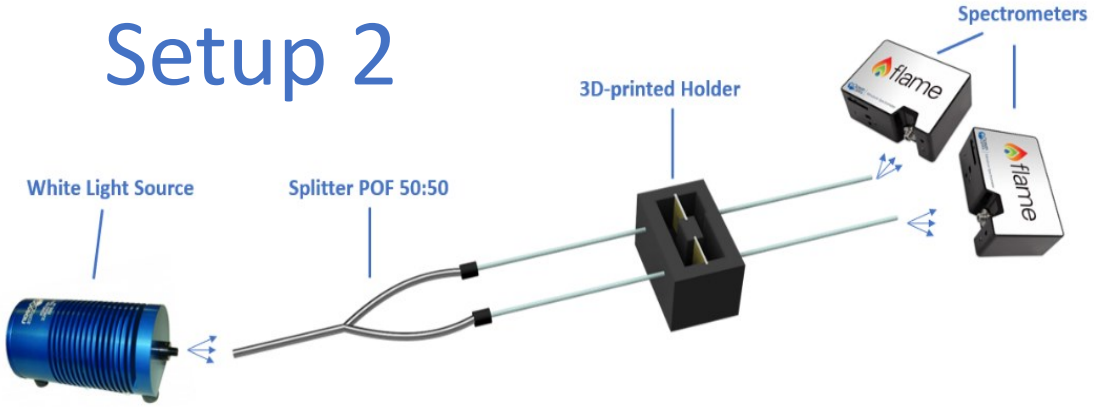

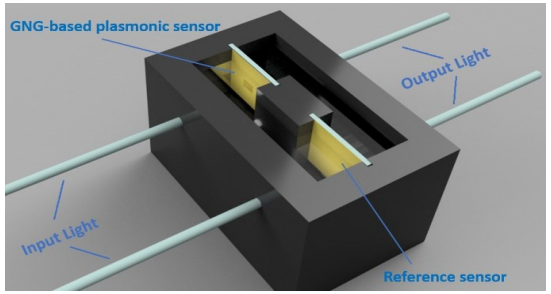

Biochemical sensing exploiting plasmonic sensors based on gold nano-gratings and polymer optical fibers

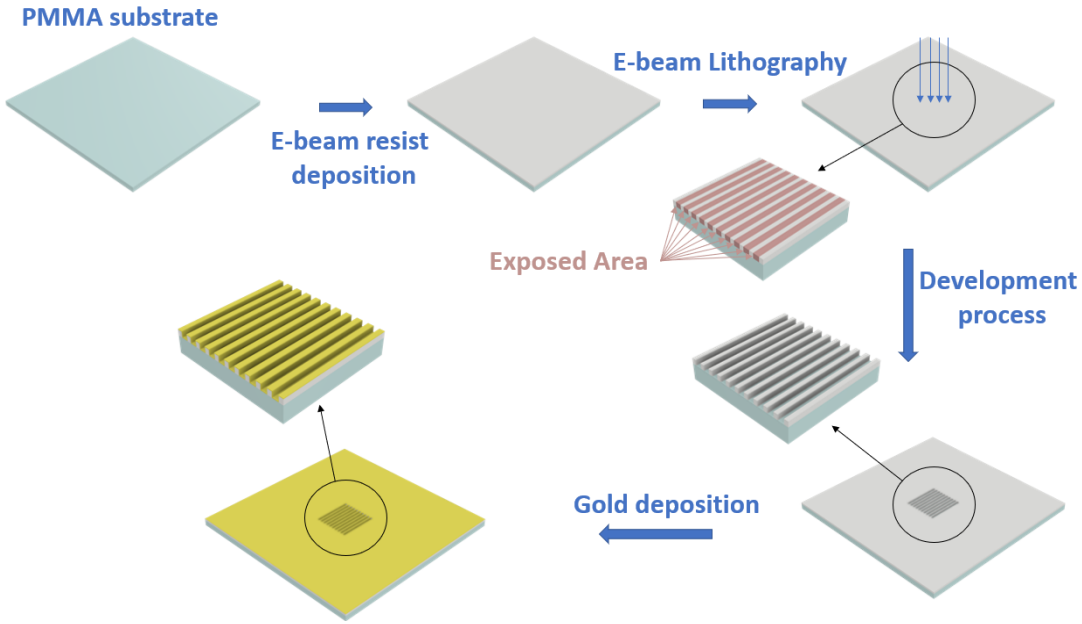

Outline of the plasmonic sensor fabrication

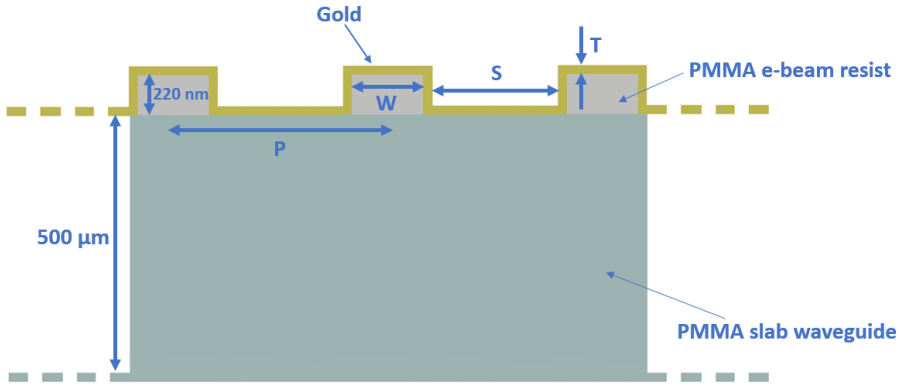

Schematic cross section of the studied plasmonic GNG-based sensors.

In the case of SPR-POF sensor the sensing area is 10 mm^2 instead of an area of 1 mm^2 for the proposed GNG sensor

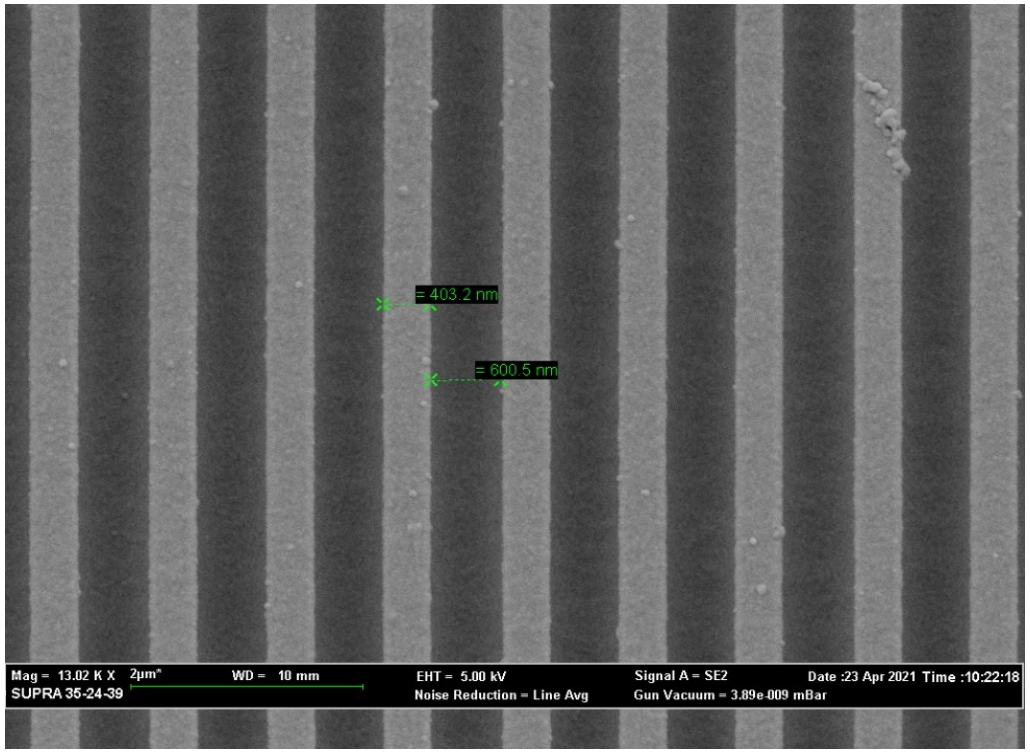

SEM image of the fabricated gold nanograting

F. Arcadio, L. Zeni, D. Montemurro, C. ERAMO, S. DI RONZA, C. Perri, G. D Agostino, G. Chiaretti, G. Porto, N. Cennamo, Biochemical sensing exploiting plasmonic sensors based on gold nanogratings and polymer optical fibers, **Photonics Research 2021**, DOI 10.1364/PRJ.424006

A binding test: the BSA detection by MIP receptor

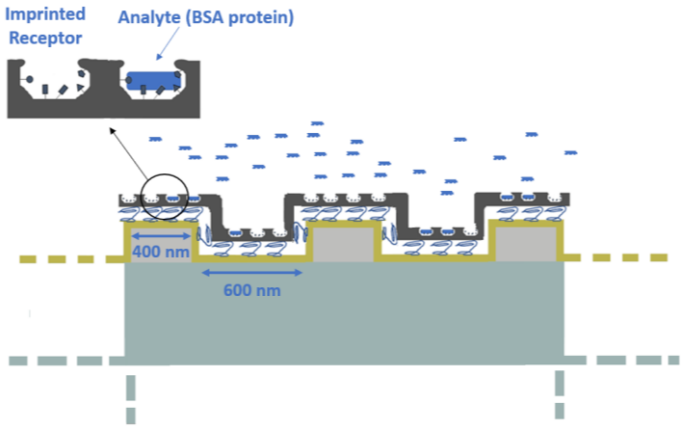

Outline of the functionalized surface

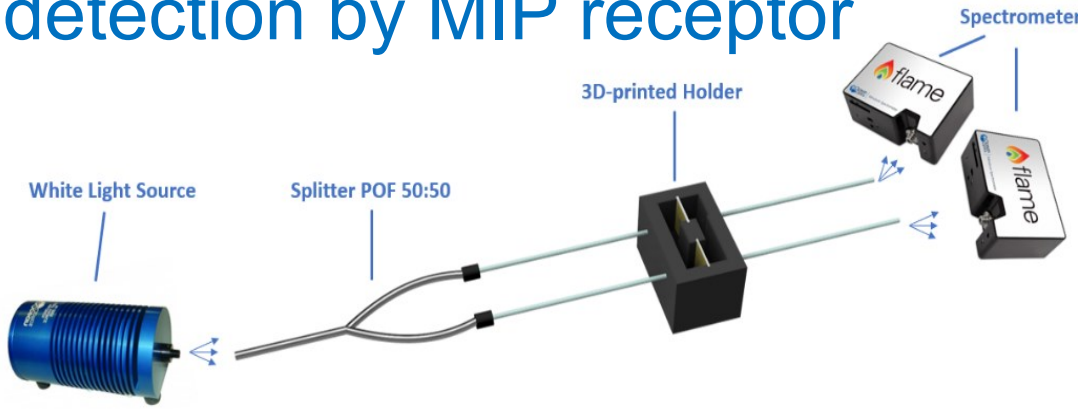

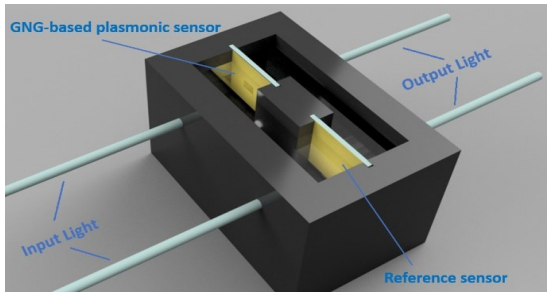

Outline of the specially designed transmission-based experimental setup. Zoom on the specially designed 3D-printed metallic (AISI 316 steel) holder with the PMMA chips and POFs

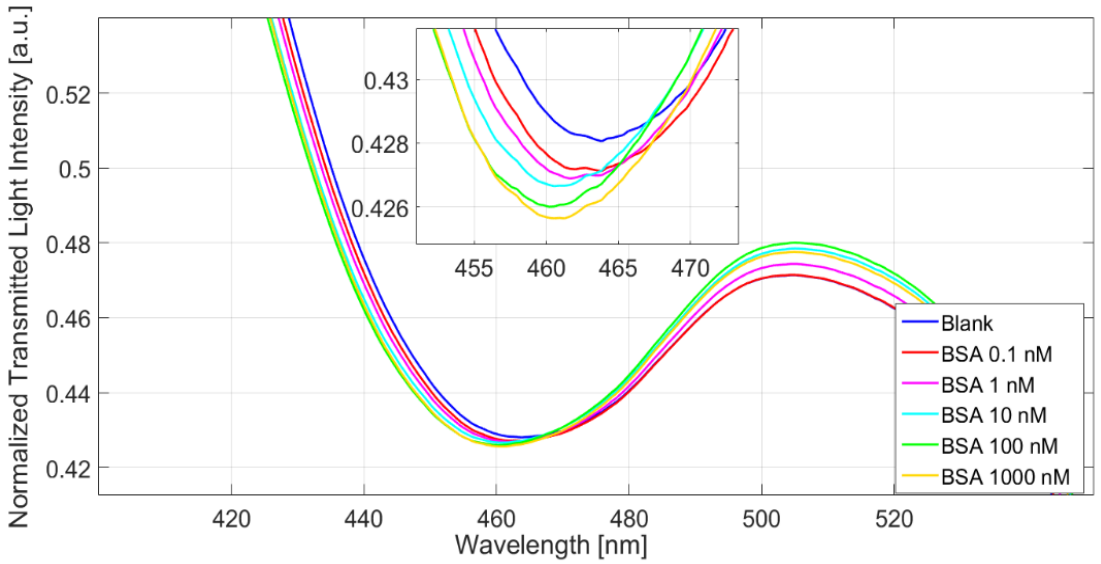

Plasmonic spectra obtained at different Bovine Serum Albumin (BSA) protein concentrations. Inset: zoom of the resonance region.

F. Arcadio, L. Zeni, D. Montemurro, C. ERAMO, S. DI RONZA, C. Perri, G. D Agostino, G. Chiaretti, G. Porto, N. Cennamo, Biochemical sensing exploiting plasmonic sensors based on gold nanogratings and polymer optical fibers, **Photonics Research 2021**, DOI 10.1364/PRJ.424006

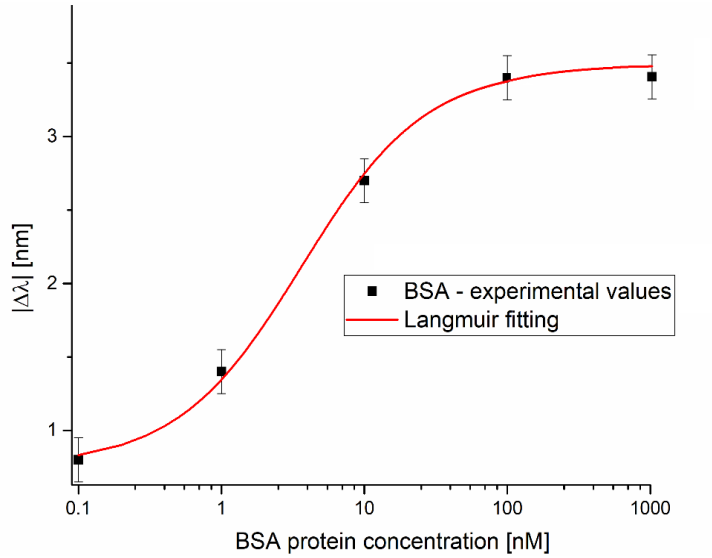

Absolute value of resonance wavelength variation (|Δλ|), with respect to the blank, versus the concentration of BSA protein (nM), with the Langmuir fitting of the experimental values and the error bars, in semi-log scale.

Bovine serum albumin (BSA) detection

Comparative analysis between several sensors' configurations for selective BSA detection

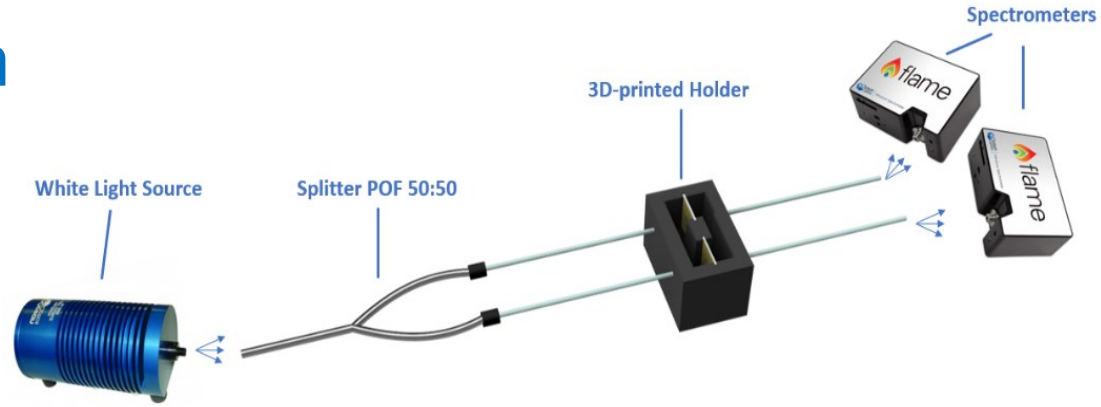

Configuration	LOD	BSA detection range	Reference
SPR-POF-MIP	0.37 µM	0.37-6.5 [µM]	N. Cennamo, et al., Proof of concept for quick and on-site highly sensitive detection of SARS-CoV-2 by plasmonic optical fibers and molecularly imprinted polymers, **Sensors** 21, 1681 (2021).
Fluorescence sensor	10 nM	0.01-2 [µM]	M. Cui, et al., Fluorescence sensor for bovine serum albumin detection based on the aggregation and release of CdS QDs within CMC, **Cellulose** 27, 1621-1633 (2020).
Aggregation-induced emission biosensor coupled with graphene-oxide	0.4 µM	0.4-1.5 [µM]	X. J. Xu, et al., A graphene oxide-based AIE biosensor with high selectivity toward bovine serum albumin, **Chem. Commun**. 47, 12385-12387 (2011).
SPR-MoS_2 optical fiber	4.36 nM	4.36-750 [nM]	S. Kaushik, et al., Two-dimensional transition metal dichalcogenides assisted biofunctionalized optical fiber SPR biosensor for efficient and rapid detection of bovine serum albumin, **Sci. Rep.** 9, 6987 (2019).
LSPR based on bimetallic nanoparticles	0.15 pM	$0.15\text{-}15\cdot10^3$ [pM)	K. Jia, et al., Strong Improvements of Localized Surface Plasmon Resonance Sensitivity by Using Au/Ag Bimetallic Nanostructures Modified with Polydopamine Films, **ACS Appl. Mater. Interfaces** 6, 219-227 (2014).
GNG-MIP-based	37 pM	0.037-100 [nM]	F. Arcadio, et al., Biochemical sensing exploiting plasmonic sensors based on gold nanogratings and polymer optical fibers, **Photonics Research** 2021, DOI 10.1364/PRJ.424006

F. Arcadio, L. Zeni, D. Montemurro, C. ERAMO, S. DI RONZA, C. Perri, G. D Agostino, G. Chiaretti, G. Porto, and N. Cennamo, Biochemical sensing exploiting plasmonic sensors based on gold nanogratings and polymer optical fibers, **Photonics Research 2021**, DOI 10.1364/PRJ.424006

Green Plasmonic Sensors based on Bacterial Cellulose Waveguides & POFs for Disposable Biosensor Implementations

(extrinsic POF sensor)

Picture of BC samples with (above) and without Ionic Liquids (ILs) (below)

The LSPR-BC sensor is simply obtained by sputtering gold on the slab waveguide of the previously described BC, with dimensions of 1 cm x 2 cm. The BC used in this study was provided by BioFaber s.r.l. and produced by bacteria.

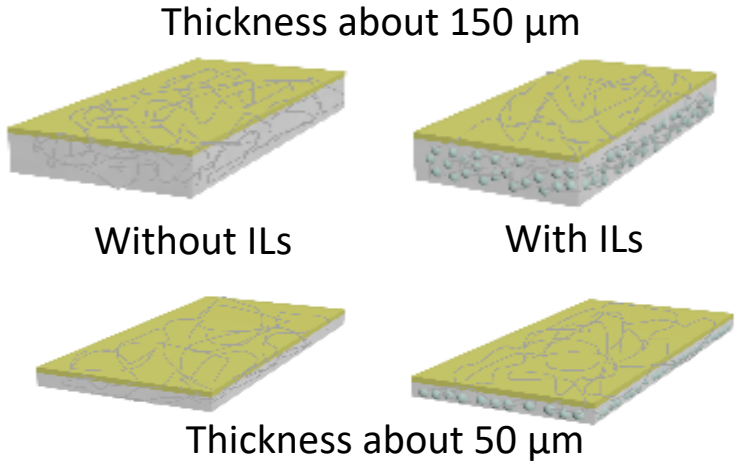

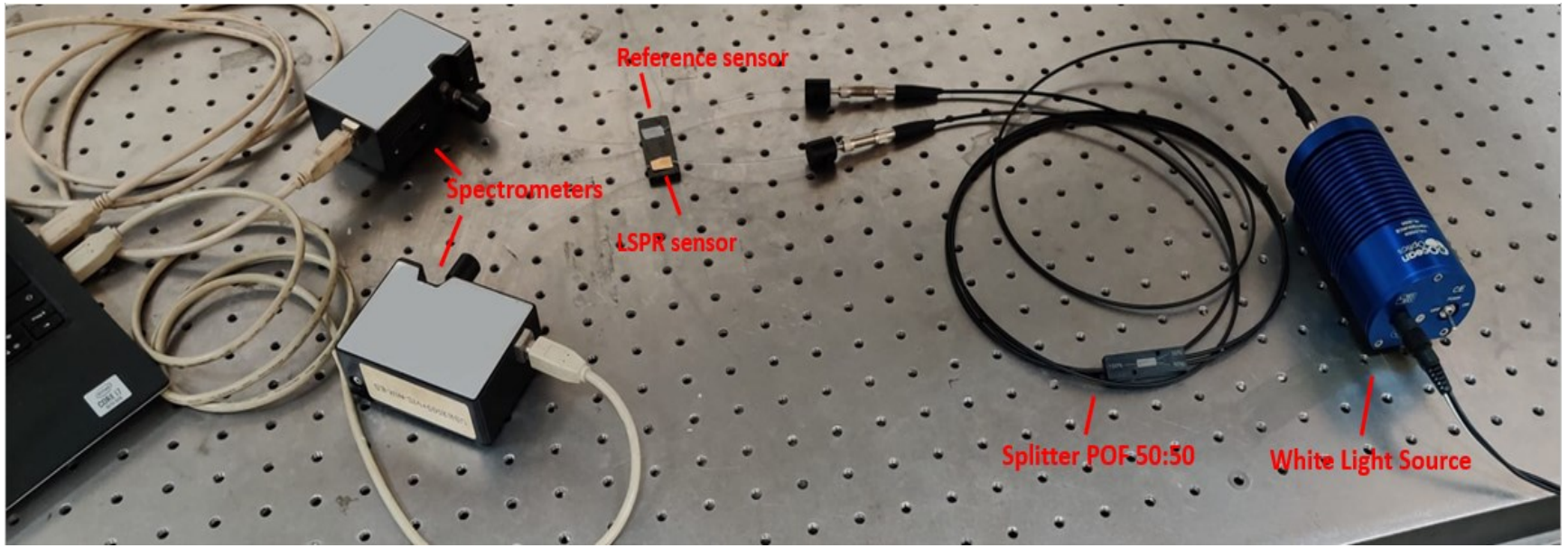

BC chip dimensions
1 cm x 2 cm

Current Research Partners

University of Catania - Italy

Green Plasmonic Sensors based on Bacterial Cellulose Waveguides

Without ILs

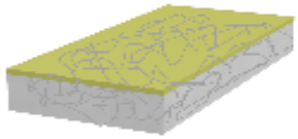

Thick (thickness about 150 µm)

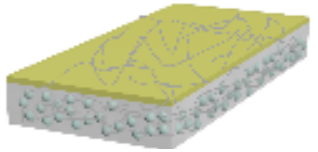

With ILs

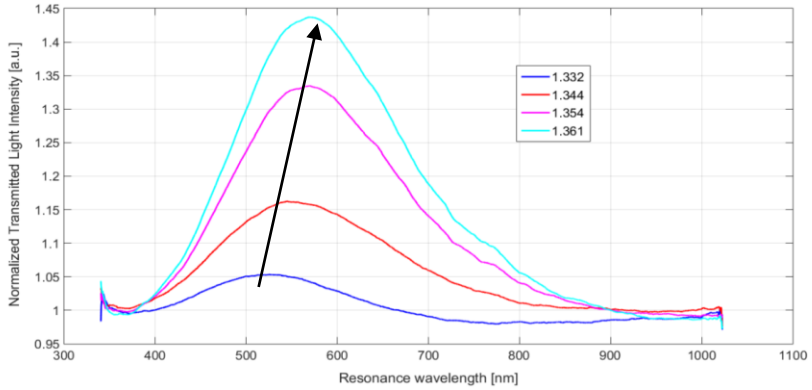

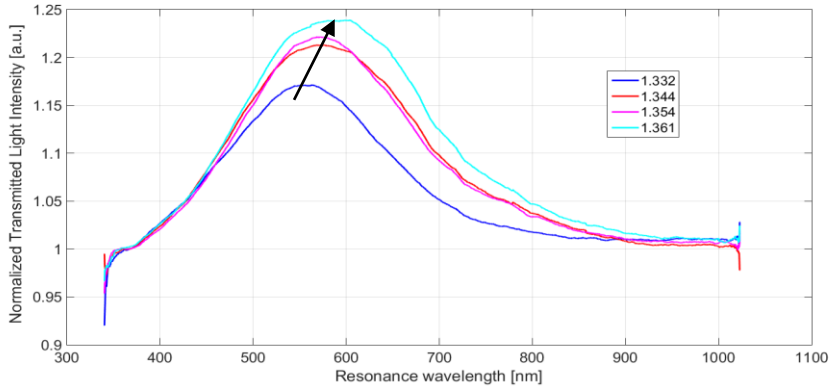

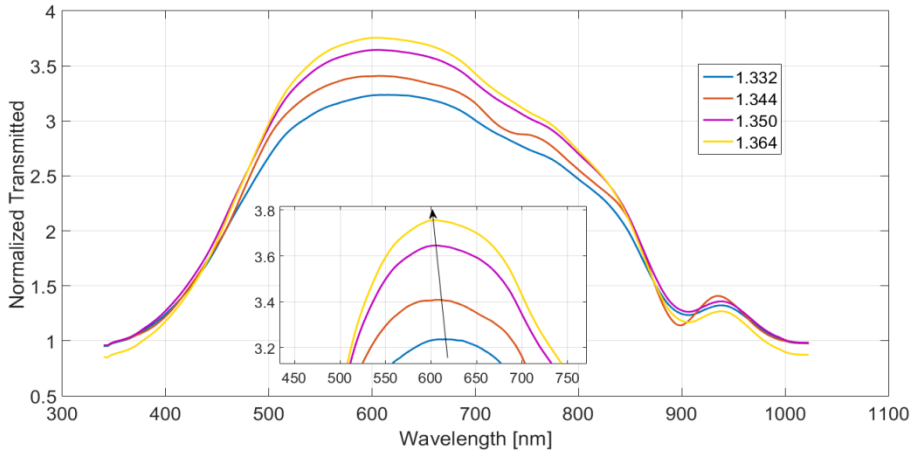

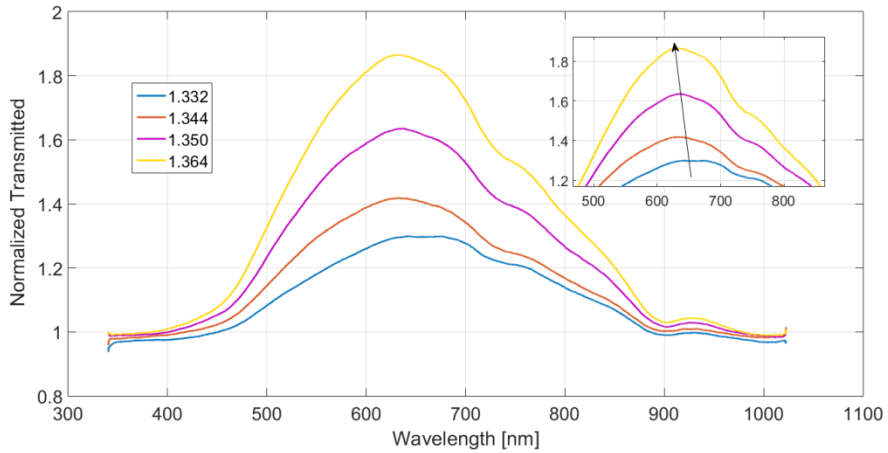

Without ILs

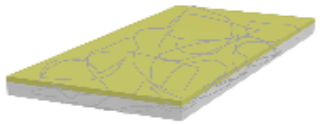

Thin (thickness about 50 µm)

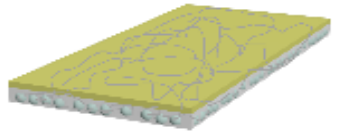

With ILs

Green Plasmonic Sensors based on Bacterial Cellulose Waveguides & POFs

Sensor Configuration	Measured Value				
	Normalized Intensity (I) [a.u.]		Resonance Wavelength (λ) [nm]		
	S_I [a.u./RIU]	Δn_I [RIU]	S_λ [nm/RIU]	Δn_λ [RIU]	Resonance type
Thin BC slab waveguide with ILs [1]	18.44	2.7×10^{-4}	725	2×10^{-3}	blue-shift
Thin BC slab waveguide without ILs [1]	13.75	3.6×10^{-4}	350	4.3×10^{-3}	blue-shift
Thick BC slab waveguide with ILs [2]	2.23	1.79×10^{-3}	980	1.5×10^{-3}	red-shift
Thick BC slab waveguide without ILs [2]	13.54	7.4×10^{-5}	1600	9.4×10^{-4}	red-shift

[1] N. Cennamo et al., Green LSPR Sensors Based on Thin Bacterial Cellulose Waveguides for Disposable Biosensor Implementation, IEEE Transactions on Instrumentation and Measurement, 70,1-8, **2021**, 9507908

[2] N. Cennamo, C. Trigona, S. Graziani, L. Zeni, F. Arcadio, G. Di Pasquale, and A. Pollicino, An Eco-Friendly Disposable Plasmonic Sensor Based on Bacterial Cellulose and Gold, Sensors, 19(22), **2019**, 4894

Conclusions

- Low-cost and small size optical biosensors have been presented for high-sensitivity and high-selectivity detection of several substances.
- Its potential ranges from detecting and treating diseases or measuring components in biological fluids, security, industry, to environmental monitoring and prevention of contamination and bioterrorism.
- All the presented sensor configurations have been produced by simple and low-cost technology and innovative materials.

N. Cennamo, M. Pesavento, and L. Zeni, “A review on simple and highly sensitive plastic optical fiber probes for bio-chemical sensing”, Sensors & Actuators: B. Chemical, Volume 331, **2021**, 129393